INFORMATION TO USERS

This material was produced from a microfilm copy of the original document. While the most advanced technological means to photograph and reproduce this document have been used, the quality is heavily dependent upon the quality of the original submitted.

The following explanation of techniques is provided to help you understand markings or patterns which may appear on this reproduction.

1. The sign or "target" for pages apparently lacking from the document photographed is "Missing Page(s)". If it was possible to obtain the missing page(s) or section, they are spliced into the film along with adjacent pages. This may have necessitated cutting thru an image and duplicating adjacent pages to insure you complete continuity.

2. When an image on the film is obliterated with a large round black mark, it is an indication that the photographer suspected that the copy may have moved during exposure and thus cause a blurred image. You will find a good image of the page in the adjacent frame.

3. When a map, drawing or chart, etc., was part of the material being photographed the photographer followed a definite method in "sectioning" the material. It is customary to begin photoing at the upper left hand corner of a large sheet and to continue photoing from left to right in equal sections with a small overlap. If necessary, sectioning is continued again — beginning below the first row and continuing on until complete.

4. The majority of users indicate that the textual content is of greatest value, however, a somewhat higher quality reproduction could be made from "photographs" if essential to the understanding of the dissertation. Silver prints of "photographs" may be ordered at additional charge by writing the Order Department, giving the catalog number, title, author and specific pages you wish reproduced.

5. PLEASE NOTE: Some pages may have indistinct print. Filmed as received.

University Microfilms International
300 North Zeeb Road
Ann Arbor, Michigan 48106 USA
St John's Road, Tyler's Green
High Wycombe, Bucks, England HP10 8HR

7820945

GOODBRAKE, CHRIS JOE
REACTION OF BETA DICALCIUM-SILICATE AND TRICALCIUM-SILICATE WITH CARBON-DIOXIDE AND WATER.

UNIVERSITY OF ILLINOIS AT URBANA-CHAMPAIGN, PH.D., 1978

REACTION OF BETA DICALCIUM SILICATE AND TRICALCIUM SILICATE WITH CARBON DIOXIDE AND WATER

BY

CHRIS JOE GOODBRAKE

B.S., University of Illinois, 1970
M.S., University of Illinois, 1975

THESIS

Submitted in partial fulfillment of the requirements
for the degree of Doctor of Philosophy in Ceramic Engineering
in the Graduate College of the
University of Illinois at Urbana-Champaign, 1978

Urbana, Illinois

UNIVERSITY OF ILLINOIS AT URBANA-CHAMPAIGN

THE GRADUATE COLLEGE

April, 1978

WE HEREBY RECOMMEND THAT THE THESIS BY

CHRIS JOE GOODBRAKE

ENTITLED REACTION OF BETA DICALCIUM SILICATE AND TRICALCIUM SILICATE WITH CARBON DIOXIDE AND WATER

BE ACCEPTED IN PARTIAL FULFILLMENT OF THE REQUIREMENTS FOR THE DEGREE OF DOCTOR OF PHILOSOPHY

Director of Thesis Research

Head of Department

Committee on Final Examination†

Chairman

† Required for doctor's degree but not for master's

D517

REACTION OF BETA DICALCIUM SILICATE AND TRICALCIUM SILICATE WITH CARBON DIOXIDE AND WATER

Chris Joe Goodbrake, Ph.D.
Department of Ceramic Engineering
University of Illinois at Urbana-Champaign, 1978

Anhydrous β-C_2S and C_3S powders were reacted with CO_2 and H_2O and the reaction kinetics determined. The carbonation reaction was best described by a decreasing volume, diffusion controlled kinetic model. The activation energies for anhydrous β-C_2S and C_3S powders were experimentally determined to be 16.4 and 9.8 Kcal/mole, respectively. An equation was developed to predict the degree of carbonation of anhydrous silicate powders using selected reaction parameters.

The anhydrous carbonated calcium silicates formed only aragonite while the wetted samples formed calcite initially, then formed aragonite as the exothermic carbonation reaction dried the samples. The size of the carbonate crystallites depended on the reaction conditions. Rapid carbonation formed many small crystals while slow carbonation formed a few large crytals.

Wetted β-C_2S and C_3S powders (0.05-0.30 w/s) fitted a logarithmic kinetic model which consisted of two straight line segments for the initial and long-term carbonation periods. Wetted powders reacted more rapidly and the degree of reaction was more erratic than the anhydrous samples because the degree of wetness was difficult to control.

The strength of pelletized β-C_2S, C_3S and a 50:50 molar mixture increased exponentially with decreased porosity. The pore space in the pellets eventually filled with carbonates and the decrease in porosity was linear with respect to the degree of carbonation. The highest tensile and

compressive strengths recorded during this study were 47 MPa (7.5 Ksi) and 330 MPa (49 Ksi), respectively, which was lower than theoretical compressive strength calculated for β-C_2S or C_3S pastes 750-900 MPa (109-131 Ksi). The tensile and compressive strength was much higher than normally hydrated β-C_2S or C_3S which have significant porosity, and the rate of hardening was 500-4000 times more rapid than normally hydrated calcium silicates.

ACKNOWLEDGMENT

The author gratefully acknowledges his advisors Dr. R. L. Berger and Dr. J. F. Young for their suggestions and insights on the research topic and Dr. J. A. Nelson and Dr. S. D. Brown for their timely discussion of research problems.

A special thanks goes to A. Bentur, J. M. Ghinazzi, L. W. Herron, M. K. Ferber, J. H. Kung and E. A. Richards for their advice and friendship during this research project.

This research was supported by the U. S. Army Research Office under Grant No. DAAG29-76-G-0116, entitled, "Reaction of Calcium Silicates with Carbon Dioxide."

TABLE OF CONTENTS

Page

Page

LIST OF FIGURES

Figure | Page

LIST OF TABLES

I. LITERATURE SURVEY

A. History of Carbonation

The process of carbonation is not a recent discovery. Atmospheric carbon dioxide ($\overline{C}$)* and water (H) can form dilute carbonic acid which causes weathering of rocks and minerals.[1] Materials containing alkali and alkaline earth elements are quite susceptible to carbonation. Natural forms of cement have been formed by the action of $\overline{C}$ and H. Ground water percolating into limestone formations leaches out Ca^{2+}, HCO_3^- and CO_3^{2-} ions which combine with leached silica to form calcareous cement. Many agglomerated materials are bonded by a microcrystalline matrix of carbonaceous material and hydrous silica. The history of building materials indicates that many materials which have been used successfully are based on the calcareous bonding principle.

1. Ancient Civilizations

The Egyptians formed crude cements by calcining impure gypsum ($\overline{CS}\cdot H_x$) and mixing the material with sand, gravel and water to form concrete.[2,3] Strength was developed by the hydration of $\overline{CS}$ and by slow carbonation of free calcia by atmospheric $\overline{C}$. Egyptian concretes were not always reliable with respect to final properties or working time. In some instances calcined gypsum was mixed with reactive sand to form mortars.

Both the Greeks and the early Romans used calcined limestone and gypsum which relied in part on slow atmospheric carbonation. However, large

---

*Standard cement nomenclature used throughout the text: C = CaO, S = SiO_2, H = H_2O, $\overline{C}$ = CO_2, $\overline{S}$ = SO_3.

Other standard abbreviations used routinely are: w/s = water/solids ratio, C/S = CaO/SiO_2 ratio, H/S = H_2O/SiO_2 ratio.

structures could not be routinely produced with this type of material. The Greeks also used reactive sands with calcined limestone or gypsum and this type of concrete or mortar was superior to the carbonated gypsum. The reactive sands, which were high surface area hydrous silica, reacted with calcium and magnesium in the calcined limestone or gypsum to form hydrated alkaline earth silicates (C-S-H gels) in addition to the carbonated alkaline earths.[4]

2. Hydraulic Limes

The Romans eventually perfected hydraulic lime mortars which would harden under water and which displayed consistent curing properties and higher final strength than carbonated gypsum or limestone. The Romans used calcined limestone as a starting material but heated the rock at higher temperatures than the Greeks and carefully selected the mineral deposits to assure uniformity. The reactive sands (pozzulana) used by the Romans were also mined from selected areas. Roman concrete was formed by mixing the calcined limestone with water and allowing the mass to hydrate into a thick paste. Pozzulana and building rubble was mixed into a stiff plastic mass which was usually tamped into place accounting for low porosity, moderate strength and long life (2000 years). Until the 18th century the Roman cements, which were hydraulic limes, were regarded as secret compositions or processes lost to history. Actually, the success of Roman cement was due to a good formula (determined by trial and error) and strictly followed processing steps.[3]

Equation 1 shows the reaction for the formation of slaked lime used in the Egyptian, Greek and Roman cements by the action of water on dry calcia.

The early cements which relied on carbonation follow equation 2, while reaction of slaked lime with pozzulana materials follow equation 3.[4] Equation 2 pertains to early cements which hardened by the carbonation process while equation 3 pertains to the Roman hydraulic limes which hardened by the formation of C-S-H gels.

$$C + H \text{ -------- } CH \qquad (1)$$

$$CH + \overline{C} \text{ -------- } C\overline{C} + H \qquad (2)$$

$$CH + SH \text{ -------- } C_xS_yH \qquad (3)$$

The development of hydraulic limes and the use of carbonation have cycled throughout history. The knowledge of hydraulic limes was lost during the Middle Ages and the older carbonation technology was used. In 1756 Smeaton rediscovered hydraulic limes.[2] The final strength of Smeaton's cement was better than the commercial cements of the time, the setting properties and the final strength being more predictable. Thus, carbonation was not extensively used during this period because the setting time was slower and the strength lower than the hydraulic limes. In 1824 Aspidin[3] first patented portland cement which is characterized as an intimate mixture of hydraulic calcium silicates which react when mixed with water. The reaction products are similar to the hydraulic limes. Carbonation of both portland cement and lime was developed throughout the period of 1820 until the present in a cyclic manner depending on the economics of the process and the advantages derived from carbonation.

3. Commercial Uses of Carbonation

In 1870 Roland patented gaseous methods of hardening cement to produce "artificial stone." The literature on the carbonation process is quite

extensive and the term cement encompasses quick-lime, hydraulic lime, calcia or magnesia minerals or hydrates, and hydraulic calcium silicate cements. Normally, the material which is to be carbonated must contain a cation which will form a stable carbonate precipitate. The cations Ca^{2+}, Mg^{2+}, Sr^{2+} and Ba^{2+} form insoluble carbonates when present in the portland cement system. Roland's processes used a combination of $\overline{C}$ and steam to rapidly produce articles from Ca or Mg silicates or cements. Roland[5-9] determined that fine particle size, low w/s ratio, and low porosity were critical to consistent products. He also developed the concept of wrapping formed shapes with impermeable materials to hold the $\overline{C}$ and H near the reacting surface. Von Pittler[10] had similar ideas for the carbonation of calcia and magnesia rocks to form fine grained lithographic stone. Neither Roland nor Von Pittler controlled the reaction conditions rigorously and the early lithographic stone was usually inferior to natural products due to high porosity, low strength and higher cost.[11,12] Hienzerling[13] modified the processing of artificial stone to include de-airing of the pressed compact and backfilling the shape with steam and $\overline{C}$. This process yielded a more uniform product by rapidly filling the pores through the mass.

From 1900-1940 hydrated and hydrating calcium and magnesium silicates were processed under varying carbonation conditions. The majority of the patents issued were improvements on existing patents or slight modifications for specialty products.[14-23]

Research was conducted on a very low level from 1940-1946 and much of the research data was destroyed in Germany during World War II. In 1949 Meyers[24] revived interest in the hydration-carbonation reaction for portland cement. Consequently, extensive research was conducted in the 1950's on

both wet and dry calcium silicates.[25-30] Carbonation was studied from the view that it could cause excessive shrinkage and cracking of concrete and mortar. After the researchers had determined that special sealants could inhibit destructive carbonation, they began investigating the actual reaction mechanisms and the beneficial uses for carbonation. The patent literature in this period on carbonation processes is characterized by references 31, 32.

During the 1960's commercial uses of carbonation included rapid curing of cinder blocks[33-35] and waste materials.[36] Optimum processing conditions were determined for specific material systems; in 1963, Bierlich[37] used high pressure $\overline{C}$ to accelerate the hardening of portland cement. Several other studies on the carbonation mechanism were completed[38-41] but the emphasis during this period was on carbonation shrinkage. The effect of $\overline{C}$ on the dimensional stability of concretes, pastes and mortars was extensively evaluated.[42-53]

In the 1970's specialized research continued. Commercial carbonation techniques were developed for pelletized batch feed for portland cement production.[54] Matsuda and Yamada[55] investigated the reaction parameters of carbonated slaked lime construction materials and a series of carbonate bonded slaked lime materials were also developed by Uschmann.[56] Sakaeda, Fujihara and Imai[57] investigated the durability of carbonated building materials and determined that carbonated materials can degrade with time. Moorehead and Morand[58] studied the reaction of single crystals of CH when exposed to $\overline{C}$ and found that the reaction was similar to carbonation in portland cement. Additional research was directed toward understanding the basic carbonation reaction and optimizing the processing parameters.[59-68]

4. Recent Research

From 1972-1978 Berger and co-workers studied the carbonation of both hydraulic and nonhydraulic calcium silicates in detail.[69-74] The mechanism proposed for carbonation[71] was similar to the models for hydration as described by equations (1-3). The carbonation of nonhydraulic silicates such as gamma dicalcium silicates (γ-C_2S) and wollastonite (CS) were investigated by Bukowski.[75] It appears that any of the calcium silicates can be carbonated if the reaction parameters are controlled. Elevated pressure and temperature and controlled w/s ratio increase the reactivity of the calcium silicates. Generally, the silicates lose water and gain $\overline{C}$ during the exothermic reaction. Compacted silicates gain strength 500-4000 times more rapidly during carbonation than during normal hydration.[73]

B. Composition of Portland Cement

1. Compound Compositions

Portland cement is manufactured by heating the finely ground materials (limestone with clay or shale) in a rotary kiln fired at approximately 1500°C to produce a partial fusion of the raw materials into a cement clinker.[3,4] A portland cement clinker contains four main phases: tricalcium silicate (C_3S), beta dicalcium silicate (β-C_2S), tricalcium aluminate (C_3A) and calcium aluminoferrite (C_4AF). Regular portland cement is ground to a surface area of 3500-4000 cm^2/g. Several types of portland cement are commercially available but the important item is that β-C_2S and C_3S constitute 70-75 wt.% of all portland cements.

β-C_2S can exist in at least five polymorphic states.[2] The beta phase

is not stable at room temperature without the addition of MgO or B_2O_3. β-C_2S, when stabilized, has a monoclinic crystal structure and the irregular arrangement of calcium atoms in the lattice makes β-C_2S hydraulic. γ-C_2S is the stable phase at room temperature, has an orthorhombic structure and is nonhydraulic.

C_3S is also metastable at room temperature but is usually stabilized by additions of MgO and Al_2O_3. At least five polymorphs have been observed for C_3S and all appear to be hydraulic.[2] The pure C_3S used in this study was triclinic and again, the nonuniform calcium coordination causes the hydraulic activity. C_3S has one mole of calcia which is very reactive and the reaction of C_3S with respect to hydration or carbonation is more rapid than β-C_2S.

2. Hydrated Portland Cement

The hydration products for portland cement are similar to those formed in the hydraulic limes and in the pure calcium silicates (see Section C). During hydration C-S-H gel and CH are formed but the relative amounts depend on the exact compounding of portland cement and the reaction conditions. The gel is the major strength producing component formed during hydration. The rate at which portland cement hardens depends on the porosity of the cement which decreases with the degree of hydration. As hydration proceeds, the C-S-H gel slowly develops and forms an intricate morphology which determines the volume stability and the strength of the cement. Hydration is a slow process which may continue up to 1 year.

3. Carbonation of Portland Cement

Both hydrated and hydrating portland cement and cement compounds have

been carbonated and the reaction rates and products evaluated. Rapid carbonation requires the presence of water and a threshold value of $\overline{C}$. In unhydrated portland cement the rate of carbonation depends on the initial w/s ratio and the most rapid reaction occurs at w/s = 0.15 wt.%. The threshold partial pressure for $\overline{C}$ was approximately 0.1 atm. Samples which were hydrated for 28 days and then carbonated showed surface shrinkage and cracking, while samples which were wetted, mixed and carbonated immediately showed little shrinkage. The hydrating-carbonated samples showed good strength gains because the carbonate filled the pore space and formed a bonding matrix. On the other hand, the hydrated-carbonated samples showed lower strength gains initially because the carbonation reaction destroyed some of the hydration reaction products (C-S-H gel and CH). As carbonation proceeded, the pore space was filled and a carbonate matrix supported the applied loads.

C. Hydration of Calcium Silicates

Some discussion of hydration of calcium silicates is necessary for comparison of curing and strength mechanisms with carbonated specimens.

1. Stoichiometry

The hydration reaction of the calcium silicates is usually studied by quantitative x-ray diffraction analysis (QXDA) but the method suffers from experimental difficulties. Reliable values for the degree of hydration are attained by repetition of the experiment. Approximate hydration reactions[4] are shown in equations 4 and 5.

$$2C_2S + 4H \text{ -------- } C_3S_2H_3 + CH \qquad (4)$$

$$2C_3S + 6H \text{ -------- } C_3S_2H_3 + 3CH \qquad (5)$$

C_3S requires more water to react and forms more CH than β-C_2S. The CH phase contributes to strength because it fills space but the gel phase forms the bonding matrix. Gel is quite variable in composition because such factors as reaction time, temperature, w/s ratio and fineness influence the rate at which the gel forms. The C/S ratio stabilizes at approximately 1.65, as determined by Brunauer and Kantro.[4] The H/S ratio is also variable but depends on the C/S ratio at all degrees of hydration. The H/S ratio is generally more variable because β-C_2S and C_3S are hydraulic and may incorporate different amounts of water in the gel depending on the relative humidity surrounding the specimen.

2. Hydration Kinetics

The reaction products of normal hydration control the kinetics of hydration at all but the earliest stages because they form a barrier to diffusion of water and soluble ions into and away from the reacting layer of the calcium silicate. The rate of hydration is dependent on the temperature and the grain size of the silicate. There are several stages in the hydration process:[76]

1. Initial hydrolysis of the cement grain. Soluble ions (Ca^{2+}, OH^-, SiO_4^{-4}) build up at the reaction interface and in the capillary water.
2. The Ca^{2+} and OH^- levels saturate with respect to CH during the induction period.
3. Calcium hydroxide (CH) precipitates and a gel layer forms around the grain.
4. Water diffuses into and through the gel while Ca^{2+} and soluble SiO_2

diffuse outward; more Ca^{2+} leaches from the grain and the gel layer grows thicker; CH crystals grow in size both interdispersed in the gel and in the pore space; water and $\overline{C}$ continue counterdiffusion.

5. The C/S ratio of the gel stabilizes and the gel on adjacent grains grows together to form the final structure.

All of the steps listed for the hydration sequence may vary in duration or may overlap for different cement components or reaction conditions.

3. Heat of Hydration

The heat of hydration is usually determined using calorimetry. Calorimetry, like QXDA, presents experimental difficulties such as the effects of initial temperature, particle size and the initial w/s ratio. β-C_2S reacts more slowly than C_3S but the ratio of gel to CH is greater than C_3S and the β-C_2S is as strong as the faster reacting C_3S. Table 1 shows the relative rate of hydration and the heat liberated during the hydration of β-C_2S and C_3S.[3]

Table 1

Rate of Hydration and Heat of Hydration for β-C_2S and C_3S

Time (days)	0.5	1	10	30	100	300	(100% Hyd.)
β-C_2S	0.10	0.13	0.30	0.57	0.72	0.81	1.00 (100% Hyd.)
C_3S	0.23	0.33	0.59	0.81	0.94	0.995	1.00
β-C_2S	0.42	0.55	1.26	2.49	2.92	3.40	4.20 (Kcal/mole)
C_3S	5.06	7.26	12.98	17.82	20.68	21.89	22.00

4. Morphology of Hydration Products

The initial hydration products are observable only by transmission electron microscopy (TEM) since the gel and CH particles may be 30-200 Å in size. The most common shapes for the gel are long needles which radiate from the surface of the hydrating calcium silicate grain and a second gel morphology which occurs as thin crumpled foils. Many intermediate morphologies have been reported by De Carvalho,[77] Tiegs,[78] and Grudemo[79] which may be caused by the variability of the C-S-H gel stoichiometry either during formation of the hydrate or during TEM observation by the high intensity electron beam. TEM has also been used to determine the identity of the reaction products with selected area electron diffraction (SAED). TEM studies have indicated that gels and freshly hydrated calcium silicate can be accidently carbonated and the carbonates have the same appearance as the gel or microcrystalline CH. The high reactivity of the gel and the CH may be attributed to their high surface areas (100-450 m^2/g).

Even though the carbonates and the hydrates cannot be easily distinguished by TEM micrographs and are initially too small to study by SAED, some information can be determined indirectly by observing the reacted microstructures before and after HCl acid etching. HCl will dissolve the calcia rich phases but does not attack the polymerized silica in the gel structure. β-C_2S tends to form a continuous gel matrix while C_3S forms silica shells around each grain and exhibits much less connectivity of the gel phase.

Additional information on the placement of the gel and CH from normally hydrated calcium silicate was obtained through scanning electron microscope (SEM) studies. The morphology of C-S-H gel in C_3S paste and the relationship of the hydration products within the microstructure was determined by

Lawrence and Young.[80] The relative stoichiometry of the gel was also evaluated using an energy dispersive x-ray detector with the SEM.

D. Hydration Models

The parameters controlling the hydration of calcium silicates are quite complex but certain simplifying assumptions can be made to develop theoretical models of hydration. Zur Strassen[76] made two assumptions. The first was that diffusion through the coating of the reaction products is so rapid that the rate is controlled by the solid-water reaction. This is expressed mathematically by equation 6 where x is the thickness of the reaction zone and k is the rate constant and t the reaction time.

$$x = kt \tag{6}$$

The second assumption is that the solid-liquid reaction is so fast that the rate is controlled by diffusion of water through the hydrated layer. If it is also assumed that the diffusion rate is inversely proportional to the thickness of the reacted layer, the model can be expressed by equation 7 where x, k and t are defined similarly to equation 6.

$$x^2 = 2kt \qquad \text{or}$$

$$x = Kt^{1/2} \tag{7}$$

This simple model fits the hydration data for β-C_2S and C_3S up to approximately 30 and 120 days respectively, but is not especially accurate immediately after water is added and is not accurate for long times.

Berovitch[76] fitted the hydration data to equation 8 where $(1-\alpha)$ is the amount of unreacted material. Other symbols were previously defined.

$$d(1 - \alpha)/dt = -k(1 - \alpha)$$

$$-\log_{10}(1 - \alpha) = \frac{kt}{2.303} + \text{const.} \tag{8}$$

Equation 8 was first order when the experimental data was plotted log $(1 - \alpha)$ versus time and formed two straight line segments.[76] The first straight line was due to the induction period for hydration and the second line which intersected the initial curve at 3-5 days was the hydration rate equation for later stages of hydration (5-180 days). The intersection of the two lines is indicative of the termination of the induction period for hydration.

Thus, two hydration models, one parabolic (eq. 7) and one logarithmic (eq. 8), have been suggested for the same reaction. Unless the reaction is repeated a number of times, the exact kinetic mechanism is difficult to determine. The largest experimental error arises from the QXDA method for determining the degree of reaction. There are other models which fit the hydration data better than the models previously discussed. A model proposed by Jander[81] was based on the following considerations:

1. Diffusion through the interface was the controlling step.

$$x^2 = kDt \tag{9}$$

where x = diffusion layer thickness

k = rate constant

D = diffusion coefficient

t = time

2. If an irregularly shaped particle (radius r) is reacted to a depth x, the unreacted volume is given by equation 10.

$$V = 4/3\pi \quad (r - x)^3 \tag{10}$$

3. The unreacted volume is also given by equation 11.

$$V = 4/3\pi r^3(1 - \alpha) \quad \text{where } \alpha = \text{fraction reacted} \tag{11}$$

Thus, combining eqs. 9-11, equation 12 is obtained.[81]

$$(1 - (1 - \alpha)^{1/3})^2 = \frac{kD}{r^2} t \tag{12}$$

This equation works quite well except for very short or very long hydration periods when the mechanism seems to deviate from simple diffusion. If the diffusional effect is deleted from eq. 12, the hydration model describes a reaction controlled by a decreasing volume and the rate of reaction at the interface of the particle can be expressed by:

$$(1 - (1 - \alpha)^{1/2})^n = k_T' t \qquad \text{where } n = 1 \qquad (13)$$

Campbell[82] also developed a kinetic model from studies of water-suspended calcium silicates and the data fit eq. 13.

If n = 2, the diffusional case arises, but if n > 2, complex combinations of diffusion and other processes are acting simultaneously. Jander's basic assumptions were:

(i) The sectional area of diffusion was the original surface.

(ii) The thickness of the reaction zone increased with time.

(iii) Mass transfer depended only on the inward diffusion of reactant.

(iv) Volume of the products was the same as that of the reactant.

(v) Diffusion of the reactant was the slow controlling step.

Ginstling and Brounstein[76] modified eq. 12 to include the thickness of the reaction layer since for hydration the gel has lower density than the unreacted silicate.

$$(1 - (1 - \alpha)^{1/3})^2 - 2/3(1 - (1 - \alpha)^{1/3})^3 = 2DCt \cdot \frac{1}{ar_o^2} \qquad (14)$$

where C = concentration difference of the reactant across the gel layer

a = portion of the reactant which diffuses outward during the reaction

Other symbols were listed previously.

The first term in eq. 14 is the same as eq. 12 and both equations fit very well for intermediate hydration times. The second term in eq. 14 is a cubic term which dominates the hydration rate at long times and fits the hydration data better than eq. 12. The basic problem in applying either eq. 12 or 14 is that both models assume that the hydration products have the same density as the unreacted calcium silicate, which is not true. Another problem is the fact that hydration occurs in the pore spaces and not just at the reaction zone on the silicate grains. Finally, the reacted layer is not smooth but has highly textured morphologies and the effects of surface area are not addressed in these simple models.

Taplin[76] formed a hydration model which considered an inner and outer diffusion layer of different permeability and thickness and allowed for counterdiffusion of water into the reaction zone and calcium away from the reactive layers. The hydration model is given by:

$$1/D_i[1 - (1 - \alpha)^{2/3} - 2/3\ \alpha) \ + \ 1/D_o\ (z-1)\{1 + 2/3\ (z-1)\alpha - [1 + (z-1)\alpha]^{2/3}\} = \frac{2Ct}{ar_o^2} \qquad (15)$$

where D_i and D_o are the diffusion coefficients for the inner and outer hydration product layers

z = (vol. prod.)/(vol. react.)

$a = (z-1)/z$ and is the fraction of material which diffuses outward.

If one can derive or measure all of the pertinent data for Taplin's equation (eq. 15), it gives a good fit for the portion of the hydration reaction which is diffusion controlled.

The equations which have been developed for mass transfer controlled by

diffusion have been subdivided into models for small segments of the hydration curve. The mass transfer models are complicated and accurate for very short or long hydration periods.[76]

E. Carbonation of Calcium Silicates

1. Stoichiometry

β-C_2S and C_3S are the main components of portland cement and are readily carbonated. If the carbonation process is controlled, reduced shrinkage and improved hardness and strength can be attained. However, if concretes or mortars are improperly protected, the effects of carbonation can be damaging. A simplistic view of the action of carbon dioxide on hydraulic calcium silicates includes eq. 16-19.

$$H + \overline{C} = H\overline{C} \tag{16}$$

The ionic species coexisting with $H\overline{C}$ are H^+, HCO_3^- and CO_3^{2-} depending on the local pH. Carbonation of β-C_2S, C_3S and gel are shown in equations 17-19, respectively,[71]

$$C_2S + (2-x)\overline{C} + yH \text{ ------ } C_xSH_y + (2-x)C\overline{C} \tag{17}$$

$$C_3S + (3-x)\overline{C} + yH \text{ ------ } C_xSH_y + (3-x)C\overline{C} \tag{18}$$

$$C_xSH_y + (x-x')\overline{C} \text{ ------ } C_{x'}SH_{y'} + (x-x')C\overline{C} + (y-y')H \tag{19}$$

Equation 16 indicates the formation of carbonic acid which attacks unreacted calcium silicate grains. Calcium ions which are dissolved by $H\overline{C}$ react with $\overline{C}$ according to eq. 17 and 18, and carbonate is precipitated. After the initial reaction in wetted samples, the gel may also be carbonated as in eq. 19. Initially, the stoichiometry of the gel is approximately that of fully hydrated gel, i.e., it has C/S ratio of 1.5-1.6 and H/S ratio

of 3-4, but as carbonation proceeds the C/S ratio and H/S ratio drop to approximately 0.4.[71,73]

Three polymorphic forms of carbonate are possible: calcite, aragonite, and vaterite. Calcite and aragonite are generally formed in concretes and pastes of calcium silicates. The pH of the carbonating silicate determines which polymorph forms. A pH<8 favors the formation of vaterite and calcite while a pH>8 tends to favor the formation of aragonite. The w/s ratio of the calcium silicate also affects the type of carbonate formed. High w/s ratio promotes the formation of calcite while a low w/s ratio promotes aragonite formation. Additionally, carbonated gel can be formed during the early stages of carbonation of wetted calcium silicates and at any time on previously hydrated calcium silicates.[64,77-79] Normally, the first carbonate observed with a TEM is vaterite which gradually converts to aragonite then calcite as long as water is present. Without water the calcite-aragonite transformation does not occur until 400°C. Vaterite has been detected in large quantities in well hydrated concretes and mortars.

The formation of stable carbonates depends on the reaction conditions. Two types of calcium silicates have been studied with respect to carbonation. The first silicate is termed hydrating, meaning that the silicate was wetted and immediately carbonated. The second type of silicate is termed hydrated, meaning that the silicate has been hydrated and has formed hydration products prior to carbonation. The hydrating samples tend to carbonate faster than the hydrated samples since the initial porosity is greater and there are no hydration products to form diffusion barriers. Both hydrating and hydrated calcium silicates require water to carbonate and the amount of liquid water controls the type and amount of carbonate formed.

2. Carbonation Kinetics

Early studies of carbonation of hydrated portland cement assumed that the CH formed during hydration was attacked by $\overline{C}$, thereby forming the carbonate. Calculation of the volume fraction for both hydration and carbonation indicated that if CH was converted to $C\overline{C}$ there should be a 0.005% expansion of portland cement samples. Direct observation showed that there was a 0.05-2.0% permanent shrinkage of the samples.[27-30,59-63] The shrinkage indicated that all of the hydration products were being carbonated, not just the CH. Experiments also indicated that the porosity of the hydrated portland cement first increased and then decreased as the samples were carbonated.[41] The loss of strength was due to degradation of the gel structure which increased the porosity since the carbonate has higher density and lower volume requirements than the gel. As carbonation of hydrated samples continues, a carbonate matrix forms and fills pore space. Strength gains of 900 MPa (131 Ksi) are possible if the carbonation reaction of densely packed portland cement goes to completion.[83] One possible mechanism proposed for the carbonation of hydrated calcium silicates is rapid carbonation of the nearly amorphous CH in the gel structure followed by the reaction of high surface area calcia in the gel and the well crystallized CH in the pore space. Finally, the unreacted cores of calcium silicate, which are the most inaccessible calcia compounds, react. The exact rate at which carbonation of the silicate occurs depends on the degree of hydration, the water content and the reaction temperature. Pastes, mortars and concretes carbonate at different rates and to differing extents. Secondary reaction parameters are: particle size, pressure of $\overline{C}$, relative humidity, sample porosity and reaction time.

If β-C_2S, C_3S or portland cement is dry-pressed or allowed to hydrate for a few hours, the rate of strength development is more rapid than for hydrated samples. Anhydrous silicates carbonate faster than hydrated samples because there is no hydration morphology to hinder diffusion of $\overline{C}$ or H.

Several important items should be noted for carbonation of calcium silicates:[69-75]

1. Water must be present for the carbonation reaction to proceed. Humidity from the air is sufficient if it is present for long periods of time.
2. Excessive water drastically limits the rate of carbonation because $\overline{C}$ cannot diffuse in the gaseous phase, but must first diffuse into a liquid filled pore system.
3. The carbonation reaction of calcium silicate requires diffusion of $\overline{C}$ and water to the reaction zone and some Ca^{2+} ions outward into the pore space.
4. The carbonation reaction is exothermic and heat can cause water to vaporize and the reaction to speed up due to the temperature rise.
5. The carbonation exotherm causes self-desiccation of the calcium silicate sample and can cause the reaction to slow significantly.

3. Heat of Carbonation

One mole of β-C_2S or C_3S releases 44 or 83 Kcal, respectively, if carbonation goes to completion.[84] Rapid flashing of liquid water can be

observed in powdered and pelletized calcium silicates when rapid carbonation occurs. Water is driven from the material during the initial stages of carbonation and a lack of water may limit the degree of carbonation.

4. Carbonate Morphology

Three polymorphic carbonates form from the calcium silicates.[85] The first form is calcite which typically forms hexagonal or rhombohedral crystallites with sharp facets. Calcite is thermodynamically stable at room temperature and is usually formed between 0-35°C.[85] The second form of carbonate is aragonite which is orthorhombic but exists in crystallites which are poorly shaped rhombohedrals, poorly shaped prisms and lath-like crystals radiating from the surface of the silicate. Aragonite is generally formed from 25-100°C and is metastable at room temperature.[86-88] The third form of carbonate is vaterite which is found extensively in concretes and mortars as amorphous areas or poorly shaped laths and is stable from 30-60°C.

Impurities may determine the polymorph which develops or the morphology of a particular polymorph. Cations such as K^+, Pb^{2+}, Ba^{2+} and Sr^{2+} tend to form aragonite while pure water or small amounts of Mg^{2+} form calcite.[88] Vaterite tends to form in the presence of low pH or silica.[88,89] The difference in the thermodynamic stability of calcite and aragonite is only 40 cal/mole which is quite easily overcome by thermal fluctuations during carbonation. Calcite forms predominantly in wetted silicates and aragonite forms when the silicates are reacted relatively dry but both polymorphs may coexist at room temperature. Whichever polymorph forms first tends to grow during carbonation.[86]

F. Carbonation Models

When calcium silicates are compounded with low w/s ratios (0.05-0.2), equations 16-18 apply and the reaction proceeds until the heat of carbonation drives off the free water. The rate of carbonation also depends on the porosity and the shape of the silicate compact or particle. When calcium silicates are carbonated as dispersed powders or mortars, the rate of migration of the interface is the rate of the reaction. McKewan[90] studied the effect of particle shape and described the model by equation 20.

$$rdf = kt \tag{20}$$

where r = av. radius of a particle

d = density of the particle

f = fractional penetration of the interface into the particle

k = rate constant

t = time

The fraction of material reacted is described by:

$$\alpha = 1 - \left\{\frac{(1-f)\ (a-f)\ (b-f)}{(ab)}\right\} \tag{21}$$

where a and b are the ratio of any two sides of a particle to the third side.

If a particle or a dense compact of particles is cubic, spherical or cylindrical with an aspect ratio of 1.0, eq. 21 reduces to:

$$\alpha = 1 - (1-f)^3 \tag{22}$$

By combining eq. 20 and 22 yields:

$$rd\ (1 - (1-\alpha)^{1/3}) = kt \tag{23}$$

If one divides through by d (density) and incorporates d in the rate constant, k, the equation reduces to eq. 13 with n = 1, which is a model for contracting volume without diffusion. The rate constant can be determined by plotting $(1 - (1-\alpha)^{1/3})$ versus log t and calculating the slope. If the slope is approximately 1.0 the model is contracting volume while if the slope is 2.0 the model is contracting volume with diffusion.

Generally, kinetic models for carbonation of hydrated portland cement,[43] pastes and concretes have been determined to follow equation 24.

$$t = ax^2 \tag{24}$$

where t = time

a = constant

x = depth of carbonation

Occasionally, an induction period is observed for carbonation and is modeled by:[43]

$$t = t_o + ax^2 \tag{25}$$

where t_o = induction period

Most concretes and mortars are subjected to a concentration of $\overline{C}$ which is 0.03% by volume. An induction period has been reported for carbonation of calcium silicates at low partial pressures of $\overline{C}$.

The depth of carbonation is usually determined by staining the reacted mortars or concretes with phenolphthalein which is colorless below a pH of 8.5, where the majority of the carbonate is sited, and pink at pH values above 8.5, which is common in the areas where the calcium silicates have not reacted. This testing method indicates a zone of carbonate reaction where the average pH is below 8.5. The actual depth of carbonation is greater

than the value obtained with phenolphthalein, therefore the models derived using this method are not completely accurate.[27] Carbonation for infinite slabs of concrete or mortar did exhibit parabolic dependency (eq. 24, 25) but the reaction constant (a) varied substantially depending on the porosity of the sample. QXDA and wet chemical methods are more accurate means of determining the depth or degree of carbonation.

The data obtained by carbonating cubes and spheres is quite different than that obtained on flat concrete walls. The model for a flat surface reduces to:[46]

$$rdx = kt \tag{26}$$

where r = radius or length of a side

x = reaction depth

d = density

k = rate constant

t = time

This is the form of eq. 21 when a and b are small, i.e., 1/20 or less. The effects of diffusion can be introduced into the model by squaring the left side of eq. 26.

$$(rdx)^2 = kt \qquad \text{or}$$

$$x^2 = \frac{kt}{(rd)^2} \tag{27}$$

Equation 27 is similar to eq. 9 and 24 but now the effect of particle size is obvious.

Finally, the rate of carbonation of a pressed calcium silicate pellet is different from a dispersed powder because the diffusion and permeability

are very different. The final carbonation model is based on diffusion of $\overline{C}$ or water being the controlling step.[46]

The diffusional reaction of $\overline{C}$ is given by:

$$x^2 = k_e t \tag{28}$$

2. The rate of $\overline{C}$ diffusion is:

$$N_o = \frac{D\Delta C}{x} \tag{29}$$

3. Rate of reaction then is:

$$\frac{dx}{dt} = \frac{N_o}{C_o d} = \frac{D\Delta C}{C_o dx} \tag{30}$$

4. From eq. 1 and 3

$$k = \frac{2D\Delta C}{C_o d} \tag{31}$$

where carbonation is assumed to occur at the reaction boundary and the diffusion and counterdiffusion or ionic species is an operative mechanism.

5. Diffusion coefficient for $\overline{C}$ is given by:

$$D_T = (D_o) \cdot (T/T_o)^{1.75} \tag{32}$$

6. Definitions for eq. 28-33

D_o = diffusion coefficient

ΔP = pressure difference

C_o = maximum fixed $\overline{C}$ or H

d = density of specimen

T = temperature

R = gas constant

ε = porosity

k_t = carbonation rate (theoretical)

k = rate constant

7. $k = k_t/f$ where f = tortuosity = $\varepsilon\Delta P$ (33)

8. The final equation for carbonation of a porous body is given by:[46]

$$k_t = \frac{2D_o \varepsilon \Delta P T^{0.75}}{273^{1.75} R C_o d} \qquad (34)$$

This carbonation model assumes linear concentration gradients for $\overline{C}$ and water which holds only for low concentrations of water or $\overline{C}$ (0.1 by volume). Equation 34 predicts the reaction depth of carbonate of concretes or mortars when exposed to atmospheric $\overline{C}$.

G. Objectives

The carbonation of well hydrated portland cement, pastes, mortars, and concretes has been thoroughly studied and is reasonably well understood. The carbonation of hydrating portland cement or its constituents is not yet fully characterized.

A systematic study of the factors which control the reaction kinetics during the carbonation of β-C_2S and C_3S was the main goal of this research. The study of the effect of $\overline{C}$ on β-C_2S and C_3S, which are hydraulic, is part of a larger project which includes the investigation of nonhydraulic γ-C_2S and CS.

The specific objectives of this study were to:

1. Determine the reaction kinetics of the carbonation of hydrating β-C_2S and C_3S.
2. Characterize the reaction products for the carbonation reaction of hydrated or hydrating β-C_2S, C_3S and an equimolar mixture of β-C_2S and C_3S.

3. Characterize the effects of the reaction parameters on the reaction product morphology and stoichiometry for the appropriate calcium silicate systems.
4. Determine the effects of the reaction parameters on the compressive strength and tensile strength of the reacted calcium silicates, initially pressed as pellets.

II. EXPERIMENTAL PROCEDURE

A. Preparation of Calcium Silicates

β-C_2S is not stable at room temperature without the incorporation of special trace oxides such as Al_2O_3, MgO, and B_2O_3. Malinckrodt analytical reagent grade CaO, silicic acid and stabilizing oxides were batched and placed in a Lucite (E.I. DuPont) plastic ball mill with 5-6 dense alumina balls and 2 liters of distilled water. The slurry was mixed for 12 hours, poured into plastic trays and dried at 60°C for 48 hours. The dried slurry was forced through a 100 mesh nylon screen and formed into 12.7 x 25.4 mm x 152.4 mm bars at a pressure of 5.5 MPa (0.8 Ksi) on a 50 ton Denison press (Denison Eng. Div. American Brake Shoe Co., Columbus, Ohio). The bars were placed on thin bars of pressed β-C_2S to prevent refractory contamination, sintered in a gas-fired Remmey kiln (Richard C. Remmey & Sons Co., Philadelphia, PA) at 1500°C for 12 hours, and then immediately air quenched.

The fired bars were then passed sequentially through a jaw crusher (Braun Chipmunk, BICO Inc., Burbank, CA) and a disk pulverizer (BICO, Inc.) which reduced the material to -100 mesh. Further grinding of the β-C_2S to 3850 cm^2/g was achieved by ball milling in porcelain mills. A Spex vibratory mixer (Spex Inc., Scotch Plains, NJ) was used to reduce the fineness of the β-C_2S still further from 3850 cm^2/g to 5300 and 6300 cm^2/g. The C_3S, which was supplied by the Portland Cement Association (PCA) in Skokie, IL, was similarly reduced from -100 mesh to 3900 cm^2/g by ball milling and to 5400 and 6280 cm^2/g by vibratory milling. All of the calcium silicates with surface areas greater than 4000 cm^2/g were stored in glass jars which were purged with dry nitrogen.

The β-C_2S and C_3S used in this study were analyzed for crystalline phase and possible impurities by x-ray diffraction. No unreacted material was detected and the diffraction patterns for β-C_2S and C_3S matched the ASTM Powder Diffraction File[85] cards 9-351a, 9-352. The phase identification was conducted on a Norelco Philips diffractometer (Philips Electronic Instruments, Mount Vernon, NY) using Cu K_α radiation. The batch composition of the β-C_2S and the theoretical and final composition of β-C_2S and C_3S are listed in Table 2. The chemical analyses were performed by the Canada Cement Lafarge Research Laboratories in Belleville, Ontario, by the courtesy of Mr. P. S. Grinrod.

Table 2

Oxide Composition of β-C_2S and C_3S

	β-C_2S batch	β-C_2S fired	β-C_2S theoretical	C_3S purchased	C_3S theoretical
CaO	65.91	64.06	65.1	72.05	73.7
SiO_2	33.44	33.28	34.9	25.70	26.3
Al_2O_3	0.11	0.12	----	-----	----
MgO	0.04	0.48	----	0.64	----
B_2O_3	0.50	0.44	----	-----	----
Ignition loss plus miscellaneous oxides		1.14	----	1.04	----
				(Fe_2O_3) 0.14	
Total	100.00	99.52	100.0	99.57	100.0

B. Preparation and Carbonation of Samples

1. Dry Powders

The β-C_2S and C_3S were weighed into clean glass petri dishes and set into one of two reactors. One reactor consisted of a set of five, 11 liter vacuum desiccators, while the second was a double-walled polyethylene glove bag having a volume of approximately 45 liters. The general setup is shown in Figure 1a. The glove bag was used for short term testing and the glass desiccators for long term testing. All of the carbonation reactions were stopped on removal from the reactor by adding 5 ml of acetone and flash drying at 105°C. The dried samples were stored in 20 ml glass vials.

2. Wet Powders

Dry calcium silicate powder was weighed into a petri dish and water was added to form pastes with w/s ratios of 0.025-0.4 wt.% and 10% excess water was added to compensate for evaporative losses. Each sample was hand-mixed for 3 minutes and the samples weighed to assure proper water content. The sample was then placed into one of the carbonation reactors. As before, most of the samples were removed from the reactor and treated with acetone. Some of the samples were not flash dried so that the noncombined water content (W_n) could be determined. The amount of noncombined water is determined by the equation below:

$$W_n = \frac{\text{Wt. after reaction - Wt. at 105°C}}{\text{Wt. at 105°C}} \qquad (35)$$

3. Dry Pellets

Dry calcium silicate powder was milled to the proper fineness, 3850 and 3900 cm^2/g as determined by the Blaine Method (ASTM C-204-55), and compacted

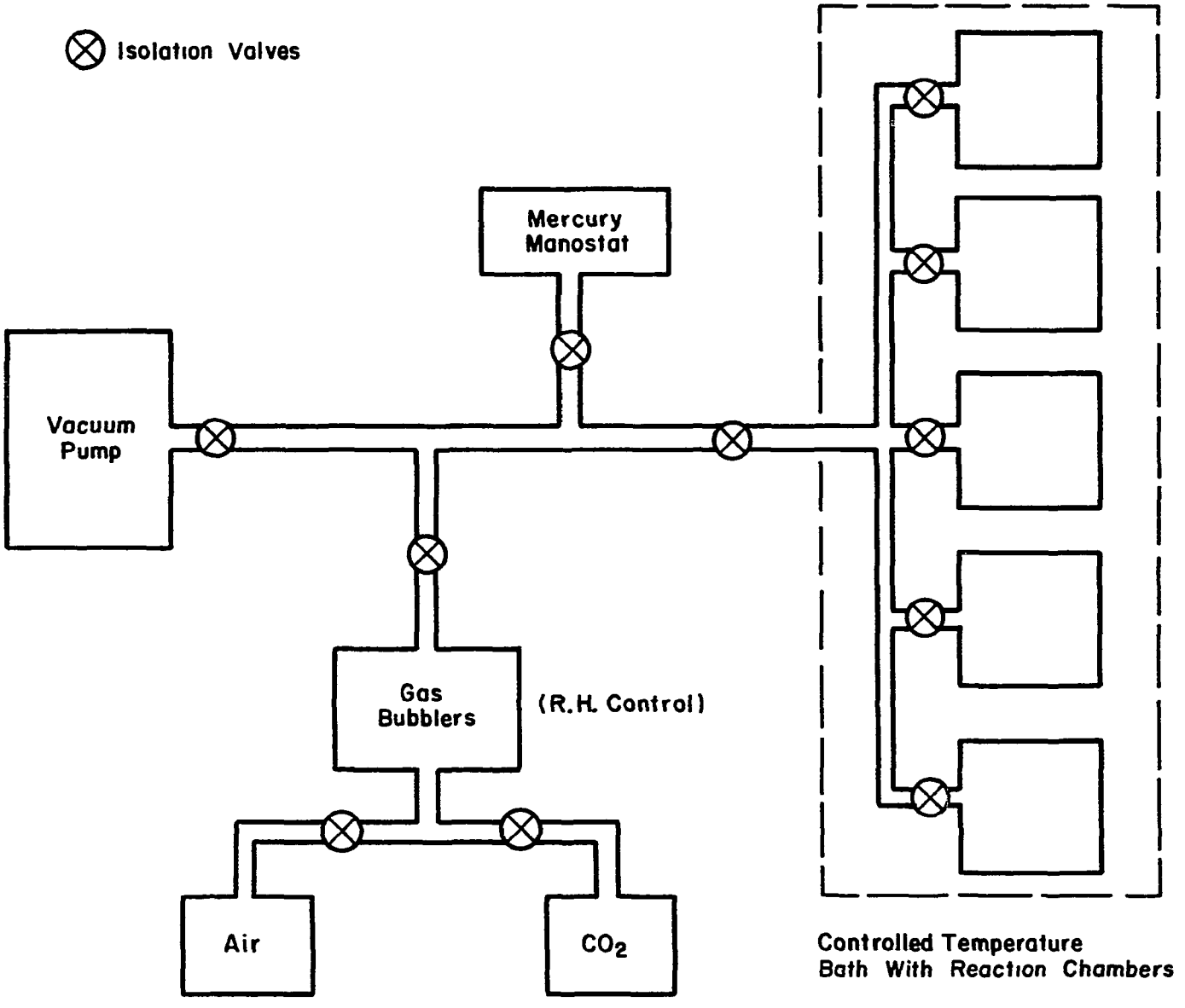

Figure 1a. Carbonation Apparatus

using an 8 ton Denison hydraulic press. It was necessary to double press the dry samples to form long specimens and to prevent pressure delaminations. The first pressing operation was carried out at 3.4 MPa (0.5 Ksi). The pellets were granulated to -40 mesh and repressed at 21 MPa (3 Ksi) and stored in a desiccator until reacted or tested for strength. The pellets were formed in two sizes (7.9 mm and 12.7 mm in diameter). The height of the specimens depended on the testing which was to be performed.

4. Wet Pellets

The β-C_2S and C_3S powders were mixed by hand with 6 wt.% excess water relative to the desired w/s ratio. The wetted powder was pressed using an 8 ton Denison hydraulic press. Only a single pressing operation at 21 MPa (3 Ksi) was necessary with the wet powders. The water content of the pressed pellets was determined by weighing the pellet as formed, burning-out the sample at 1000°C for 1 hour and reweighing the sample. The water loss on ignition was calculated using the following formula:

$$\text{LOI} = (\text{wt. room temp.} - \text{wt. } 1000°\text{C})/(\text{wt. } 1000°\text{C}) \qquad (36)$$

The same method was used to determine the amount of atmospheric contamination of the dry calcium silicate powders. Some of the pellets were carbonated immediately and were designated hydrating carbonated samples. Other samples were hydrated to 25-50% of theoretical in a saturated solution of CH and distilled water. The equations used to determine the degree of hydration are:

$$\%\ \text{Hyd.}_{C_2S} = \frac{\text{wt. } 105°\text{C} - \text{wt. } 1000°\text{C}}{\text{wt. } 1000°\text{C } (0.2091)} \qquad (37)$$

$$\% \text{ Hyd.}_{C_3S} = \frac{\text{wt. } 105°C - \text{wt. } 1000°C}{\text{wt. } 1000°C \ (0.2366)} \qquad (38)$$

If the hydrated samples were later carbonated, the sample type was designated as hydrated-carbonated calcium silicates.

The porosity of the wet pellets was determined by vacuum saturating the pellet, weighing the sample wet, then drying the sample at 105°C for 4 hours and reweighing the sample. The formula for determining the porosity is:

$$\% \text{ Porosity} = \frac{(\text{Wt. saturated} - \text{wt. dried})(1 g/cm^3)}{\pi x \text{Dia.}^2/4 x \text{Ht. (dry dimensions) } cm^3} \qquad (39)$$

5. Carbonation Method

Figure 2 shows the carbonation equipment. The procedure involves evacuating the desiccators and reintroducing $\overline{C}$ and air which have been conditioned to the proper relative humidity. The fractions of $\overline{C}$ and air were monitored using a mercury manostat since the pressure of each gas was proportional to its volume fraction. If the carbonation reaction was to continue for extended testing, the desiccators were connected in series to form a larger volume of conditioned gas in order to avoid appreciable change in $P_{\overline{C}}$. The specimens were placed into the desiccators of the glove bag through a double-sealed portal which isolated the reaction gas from the laboratory atmosphere. The partial pressure of $\overline{C}$ ($P_{\overline{C}}$) was varied from 0.0003-1.0 atm.

6. Relative Humidity (RH)

The $\overline{C}$ and air were conditioned to the proper relative humidity using saturated salt solutions to equilibrate the water vapor. When long term testing was necessary, the bottom of the desiccator was filled with the

appropriate solution (Table 3). When the glove bag, or a desiccator, was filled for short term testing, two 1000 ml bubbler flasks were connected in series and the dry $\overline{C}$ was introduced at a rate of 2 ℓ/min. Dry $\overline{C}$ (Union Carbide-High Purity) from a tank was not used since it had a tested dew point of -42°C which severely desiccated the reacting calcium silicates. All of the relative humidity conditions were checked with an Alnow Dew Pointer (Illinois Testing Laboratories, Chicago, IL).

Table 3
Constant Humidity Saturated Salt Solutions

Salt	%RH
$H_2PO_4 \cdot \frac{1}{2}H_2O$	9.0
$MgCl_2 \cdot 6H_2O$	33.0
$Na_2Cr_2O_7 \cdot 2H_2O$	55.0
NH_3Cl	79.5
H_2O	100.0

C. Experimental Methods

1. Specific Gravity Determination

Unreacted β-C_2S and C_3S were analyzed with a constant volume pycnometer using water or benzene as the liquid medium. The vials were washed with methyl alcohol, then dried at 105°C and stored in a desiccator until needed. The vials were packed 75% full with material passing 100 mesh (147 μm) and weighed again. Liquid was added to within 5 mm of the top of the vials and

the filled pycnometer vials outgased in a vacuum desiccator at 30 torr for 2 hours. The vials were filled to the prescribed mark and weighed again. The specific gravity was calculated using the formula listed below and all determinations were run in triplicate.

$$\text{Sp. Gr.} = \frac{\text{Dry wt. powder}}{\left(\begin{array}{c}\text{Wt. liquid displaced} \\ \text{by the powder}\end{array}\right)\left(\begin{array}{c}\text{liquid density} \\ \text{at T°C}\end{array}\right)} \text{ g/cm}^3 \qquad (40)$$

2. Surface Area Determination

The surface area of the milled powders was determined using the Blaine air permeability method.[91] Three grams of freshly milled calcium silicate were placed in the apparatus and a vacuum developed across the sample. The time for the pressure differential across the specimen to approach equilibrium was recorded and compared to standard calcium silicates with known surface areas. The equation used to determine Blaine surface area was

$$\text{Surface area} = \frac{1294. \times \sqrt{\text{time (sec)}}}{\text{density of the powder}} \text{ cm}^2/\text{g} \qquad (41)$$

The second method for determination of surface area of carbonated samples (dried at 105°C) was the B.E.T. molecular adsorption technique. A static measurement of the surface area using water as the adsorbed material was conducted using a gravimetric technique in which the sample was weighed as the relative humidity over the sample was varied by changing the concentration of the sulphuric acid-water solution. A dynamic B.E.T. study was conducted using nitrogen N_2 as the adsorbate. The testing was carried out on a Quantasorb apparatus (Quantachrome Corp., Greenval, New York) by mixing the N_2 with He to obtain controlled concentrations of N_2 in the gas stream. The water B.E.T. method always gives

higher indicated surface areas than the N_2 method. It has been suggested that nitrogen will not diffuse into all of the pores and capillary space that is accessible to water.

3. Thermogravimetric Analysis (TGA)

TGA was used to evaluate the relative rate and amount of volatiles lost during heating of reacted calcium silicates. A DuPont Model 900 Thermal Analyzer and a Model 950 Thermogravimetric Analyzer (E.I. Du Pont de Nemours & Co., Inc., Instrument Products Division, Wilmington, Delaware) were used for this study. A 100 mg sample of reacted calcium silicate which had been dried at 105°C for 6 hours was used as the standard sample size. Oxygen was bubbled through the apparatus at a flow rate of 0.05 ft^3/min during the runs and a constant heating rate of 10°C/min was used. The sensitivity of the instrumentation was as high as 4 mg/inch on the weight vs. temperature plots. The TGA data were used to develop the constant temperature pyrolysis technique.

4. Mass Spectrometer (MS)

A constant field MS (AEI, Model MS10) was used to determine the atomic weight of the gases evolved during the decomposition of the carbonated calcium silicates. The sample and test conditions were identical to those used for the TGA data and direct comparisons could be made. The MS was set for a mass/charge (m/e) of 18 for water and 44 for carbon dioxide. The rate of evolution of H or $\overline{C}$ was plotted as a function of temperature from room temperature to 1000°C. The m/e calibration was set before the first run and held constant throughout the series of MS runs. MS data were also used to develop the constant temperature pyrolysis method.

5. Constant Temperature Pyrolysis

All of the reacted calcium silicates which required stoichiometry determinations were dried at 105°C for 6 hours and weighed. The samples were then placed in dense 92% alumina crucibles and heated for 4 hours at 350°C, cooled and weighed again. The weight change between 105°C and 350°C represented the combined water. The samples were heated again to 1000°C and weighed. The weight difference from 350-1000°C was due to combined $\overline{C}$. These data (combined H and $\overline{C}$) were used to calculate the gel stoichiometry. Up to 40 samples were run at a time; the furnace had a temperature gradient of ±4°C over the array of crucibles. Typical sample weight was 1.0 g and all of the constant temperature pyrolysis specimens were run in duplicate. All weighings were carried out on an electronic Right-A-Weigh balance (William Ainsworth & Sons, Denver, CO) with a precision of ±0.0002 g.

6. Strength Testing

Two testing machines were used in this study. The first was an Instron testing machine (Instron Corp., Canton, MS) which had a load capacity of 200 kg. The Instron was used for unreacted and short term carbonated samples. The second device was made by Tinius Olsen Testing Machine Co. (Willow Grove, PA) and had a maximum load capability of 13,600 kg. The normal loading rate used on both machines was 200 kg/min. All of the compression specimens were polished plane parallel where necessary, before they were reacted or tested. The normal compression specimen had aspect ratios of 2.0 while the diametral compression specimens had aspect ratios of 1.0. Each of the strength tests was run with five specimens and the average of the three highest strength values was recorded.

7. X-ray Diffraction Analysis

a. Sample Preparation

Powdered, reacted materials were ground to 5 μm in a Spex mixer. Pelletized silicates were either ground to the same fineness or polished parallel to the cleavage plane for the diametral compression specimens with 400 grit SiC abrasive. Initial phase identification of the powders was conducted using the 5 μm material. When quantitative amounts of the phases were required, 0.25 g of TiO_2 (anatase) was added to 1 g of reacted, powdered calcium silicate and the relative amount of calcium silicate or carbonate determined by an internal standard x-ray technique. All of the powdered samples were dried at 105°C for 4 hours prior to being x-rayed and were stored in glass vials before and after testing. Pelletized samples were also dried and stored in plastic vials in a desiccator until needed.

b. Specimen Mounting

One x-ray specimen holder consisted of an aluminum plate 30 mm x 30 mm x 0.3 mm with a 21 mm x 9.5 mm x 1 mm groove milled into the top surface and was used to hold powder for qualitative phase analysis. A glass slide was placed over the groove, taped in place, then powder was packed into the slot between the glass slide and the bottom of the groove. This method minimized preferred orientation of the powders. The slide was removed and the sample run on a diffractometer.

A second x-ray sample holder consisted of an aluminum plate 30 mm x 30 mm x 1.5 mm which had a rectangular window machined into the plate (Figure 1b). Fractured and polished diametral compression specimens were mounted in the window and held in place with modeling clay applied to the

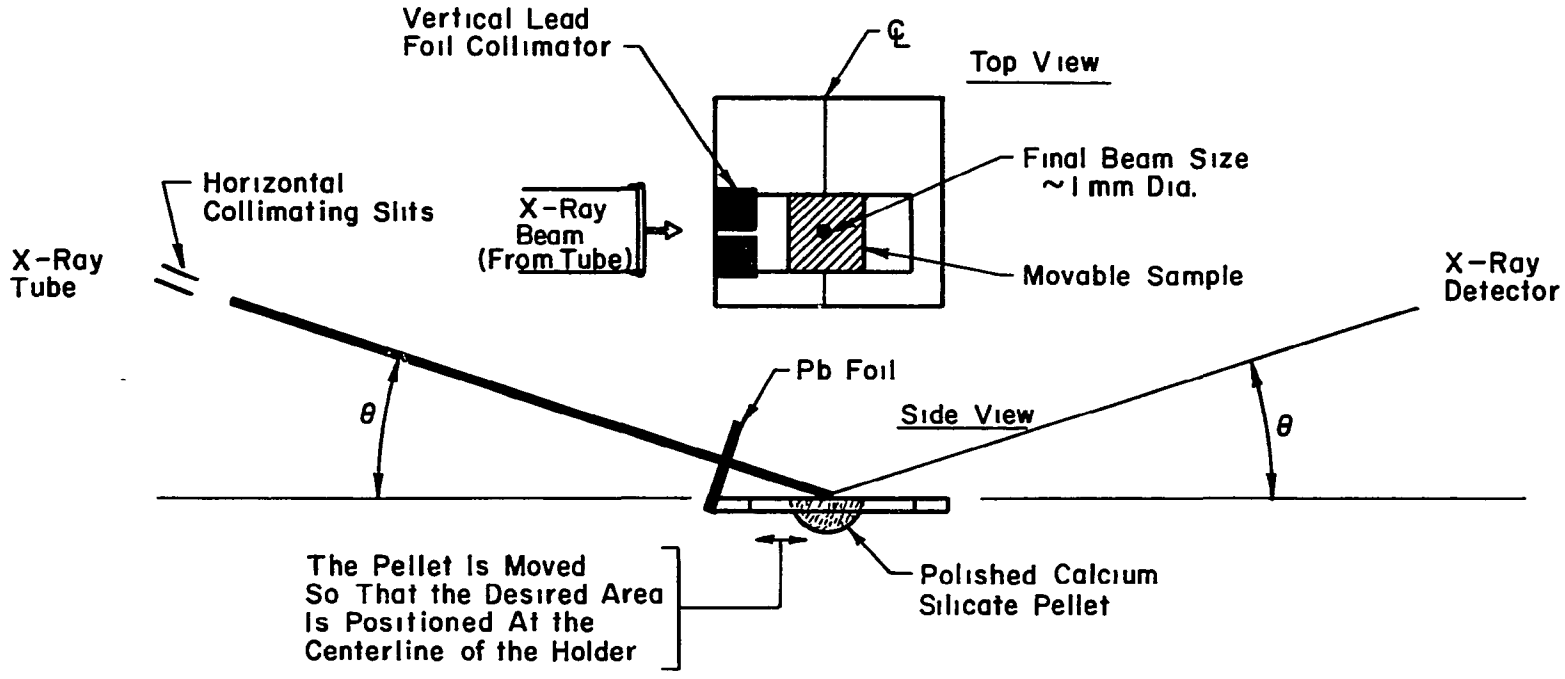

Figure 1b. Modified X-ray Sample Holder

bottom of the sample. A piece of lead foil 0.5 mm thick with a 1 mm vertical slit was fastened to the edge of the holder to collimate the x-ray beam and form a 1 mm beam at the centerline of the holder. The composition and the relative amounts of selected phases were determined as a function of position by moving the specimen relative to the scribed centerline mark on the holder. The polished sample was aligned with the top surface of the holder by forcing the pellet against a glass slide which was taped over the top surface of the holder.

c. Qualitative Phase Identification

Two North American Philips Norelco X-ray Diffractometers (Philips Electronics and Pharmaceutical Industries Corp., Mount Vernon, NY) were used to determine the phases of the unreacted calcium silicates and the reaction products of carbonation, using Cu K_{α} radiation. One diffractometer was equipped with a graphite crystal monochromator which allowed the use of the Cu x-ray spectrum without a Ni filter thus allowing a higher intensity beam to reach the specimen and greater accuracy. The phase identification was conducted at a scanning speed of 1°2θ/min with a tube voltage and current of 25 Kv and 10 ma, respectively. The angular range of scanning for phase identification was 10-70°, 2θ. The rate meter was set at 500 counts per second (CPS) full scale. The reacted and unreacted phases were identified through use of the ASTM Powder Diffraction File.[85]

d. Quantitative X-ray Diffraction Analysis (QXDA)

The extent of the reaction in the carbonated samples and the amount of carbonates was determined using QXDA. The diffraction peaks for the carbonates and the calcium silicates are given in Table 4. These peaks were

Table 4

List of Diffracting Planes Analyzed by QXDA Methods

(Ref. 85)

Phase	2θ Value	d (Å)	Diffracting Plane (hkl)	I/I_o
β-C_2S	31.04	2.878	$12\bar{1}$	8
	32.00, 32.11	2.794, 2.785*	D($10\bar{4}$, $12\bar{2}$)	(100)
	32.56	2.748*	D($20\bar{2}$)	(100)
	34.35	2.608	$21\bar{2}$	20
	41.20	2.189	031	21
C_3S	29.53, 30.20	3.022, 2.957	021, 202	(44, 13)
	32.22	2.776*	D(009)	(100)
	32.77	2.730*	D(024)	(100)
	34.44	2.602	205	52
	41.28	2.185	208	33
$CaCO_3$ (calcite)	29.40	3.035	104	100
	35.96	2.495	110	14
	39.40	2.285	113	18
	43.14	2.095	202	18
$CaCO_3$ (aragonite)	26.24	3.396	111	100
	27.25	3.273	021	52
	36.20	2.481	200	33
	37.93	2.372	112	38
$CaCO_3$ (vaterite)	24.85	3.580	110	100
	27.00	3.300	111	100
	43.94	2.059	300	100
TiO_2 (anatase)	25.35	3.510	101	100
	37.78	2.379	004	22
	48.07	1.891	200	33

*The total area of the doublet was used for the reference peak.

scanned at $\frac{1}{4}$ or $\frac{1}{2}°2\theta$/min and each sample was run in triplicate. The QXDA analysis was conducted on a second diffractometer which was equipped with a fine-focus Cu x-ray tube which was run with a Ni filter at 36 Kv and 14 ma. The rate meter was run at 1000 CPS.

(1) Internal Standard Method

The amount of unreacted calcium silicates was determined by mixing 0.25 g of TiO_2 (anatase) with 1.0 g of reacted dried calcium silicate. A calibration curve was determined for weighed mixtures of β-C_2S and C_3S with calcium carbonate using TiO_2 as the internal standard. The relative intensity under selected diffraction peaks was evaluated for the β-C_2S, C_3S, calcite and aragonite and compared to TiO_2. Separate calibration curves were made for the weight fractions of calcium silicates and the weight fractions of carbonate. Most reacted samples were evaluated by internal standard QXDA and compared directly with the calibration curve to determine the amount of unreacted silicate or the amount of carbonate formed. The relative areas for the diffraction peaks were determined with a K&E compensation polar planimeter (Keuffel & Esser Co., Chicago, IL). The background intensity of the diffraction peaks was determined visually. Various carbonate peaks interfere with the calcium silicate peaks and visual extrapolation or mathematical deconvolution of the mixed silicate-carbonate peaks was necessary. Visual extrapolation consisted of finding one portion of the silicate peak of interest which was not affected by the carbonates or hydrates and drawing a symmetrical peak for the silicate using the unencumbered side of the silicate peak as a template. Many silicate peaks were overwhelmed by the carbonate formation and the spectra of the calcium silicate

was analyzed for the relative I/I_o values for five selected peaks. The carbonates do not interfere with all of the silicate peaks, so that when carbonation occurs, the unencumbered silicate peaks can be used to give a specific area under the diffraction peak. The mixed silicate-carbonate peaks can thus be analyzed by mathematically evaluating the area attributed to the silicate predicted from the ratios of intensities of the other silicate peaks. The silicate peaks can then be subtracted from the mixed total and the remaining $\overline{CC}$ compared to the calibration curve for the carbonation weight fraction. Both the amount of unreacted calcium silicate remaining and the amount of carbonate formed can be crosschecked using this method. Each sample of reacted cement was run twice and each trace was evaluated with the polar planimeter three times.

(2) External Standard Method

Calcium silicate samples which were carbonated directly in the x-ray holder, or pellets which had been carbonated, fractured and polished, could not be mixed with an internal standard (such as TiO_2) to determine the relative amounts of unreacted silicate or formed carbonate. Unreacted calcium silicate powder was run immediately prior to the diffraction run on the reacted sample to eliminate variation in the x-ray flux. If powders were being analyzed, then powdered silicate standards were used and if pellets were being x-rayed, standard pellets were run. The external standard method was not as accurate as the internal standard method because the ratio of calcium silicate to carbonate depended on the degree of reaction. As the area under the carbonate peak approached zero, the ratio of silicate to carbonate approached infinity. The early reaction times, where the silicate is only

slightly reacted, were evaluated by directly comparing the silicate peak to unreacted calcium silicate. Direct comparison was used for very long reaction times and crosschecked with TGA and external standard data obtained by the ratio of silicate and carbonate. This external standard method allowed carbonated powders or pellets to be analyzed for relative composition as a function of position.

8. Scanning Electron Microscopy (SEM)

The specimens examined with the SEM included reacted and unreacted powders and pellets of β-C_2S and C_3S. The fractured and polished surfaces of the reacted calcium silicates were studied.

Photomicrographs of selected specimens were obtained using a JEOL JSM-U3 microscope (Japan Electron Optics Laboratory Co., LTD, Medford, MS). The samples were glued to 12.5 mm diameter aluminum stubs with a mixture of Duco Plastic Cement (E.I. Du Pont) and Dag #154 colloidal graphite suspension (Acheson Colloids Co., Port Huron, MI). The specimens were dried for 4 hours at 70°C after the glue was applied and stored in a desiccator until required. The calcium silicate samples were sputter coated with gold approximately 250 Å thick. Additional information on the reaction products was obtained by using an Ortec nondispersive x-ray analyzer on the U3 microscope (Nuclear Diodes, Inc., Prairie View, IL). The relative amounts of Ca and Si could be determined directly at selected areas of the reacted β-C_2S or C_3S. Reaction products could be evaluated to determine if the particle was gel or carbonate since the carbonates contained no silicon.

III. RESULTS

A. Reaction Rate Kinetics

1. QXDA Internal Standard Method

The amount of unreacted calcium silicate and the amount of calcium carbonate formed during the carbonation reaction was monitored by QXDA. Figure 2 shows the calibration curves for the calcium silicates and Figure 3 shows the calibration curves for the predominant carbonate phases (calcite and aragonite). Each data point on the calibration curves was an average of ten separate diffraction runs. The calibration curves for the calcium silicates and the carbonates were linear and the error of the QXDA method was approximately ±3%.

2. QXDA External Standard Method

The amount of unreacted calcium silicate and the amount of calcium carbonate formed during the reaction were evaluated by comparison to an external standard. Four calibration curves were derived from the internal standard curves (Figures 4 and 5), since both the calcium silicates and the carbonates were evaluated with respect to a constant amount of TiO_2. Unreacted powdered or pelletized calcium silicates were run immediately preceding each external standard run so that the x-ray spectra could be directly compared and the short term degree of reaction determined. Since both calcium silicates and carbonates were present in the initial internal standard mixtures, any amount of diluting materials could be added without affecting the ratio of the peak areas of the silicate and the carbonate; thus, the formation of either C-S-H or S-H gels was not an experimental difficulty. The external standard method was not as accurate as the internal QXDA method especially

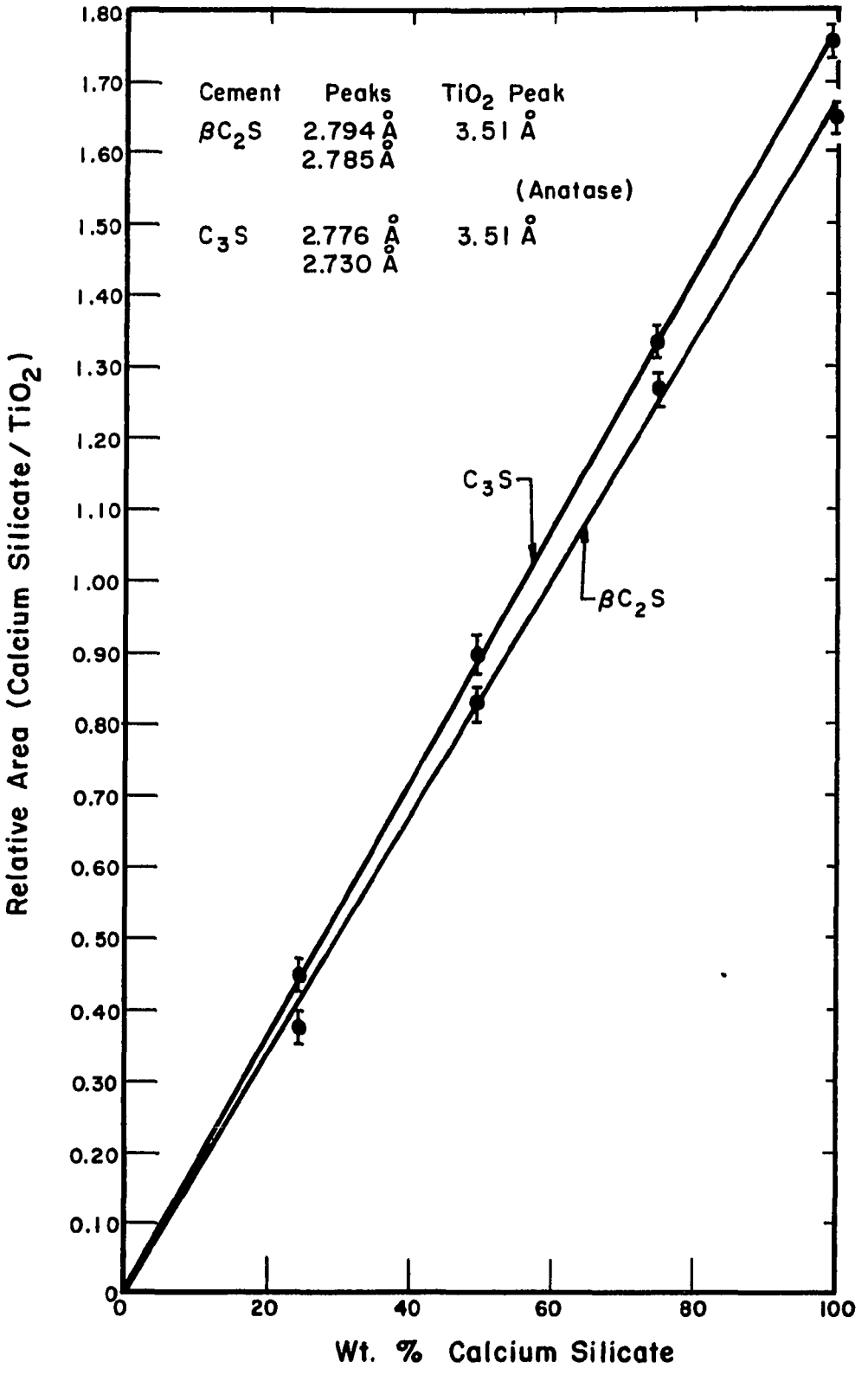

Figure 2. Internal Standard Calibration Curve for β-C_2S and C_3S

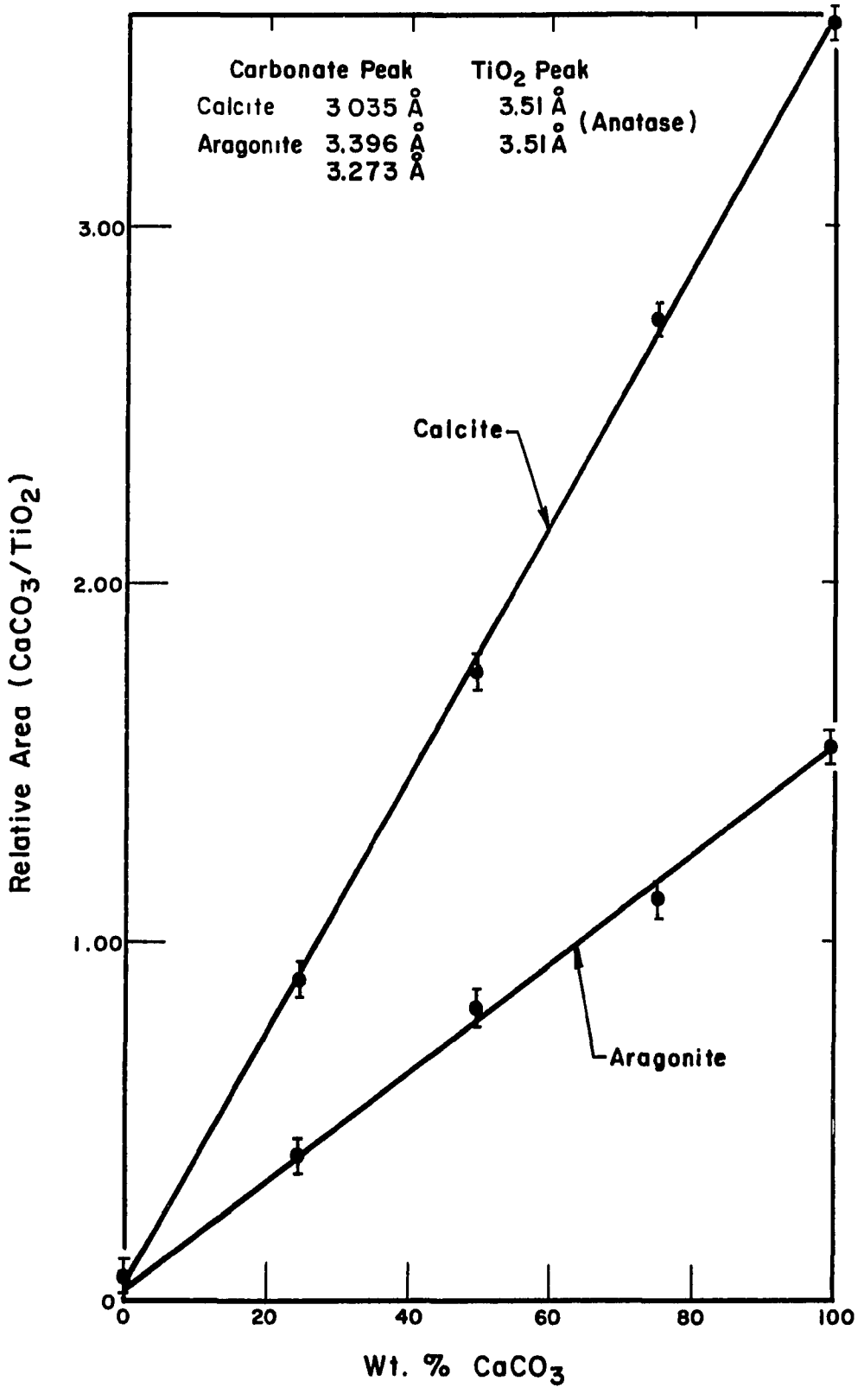

Figure 3. Internal Standard Calibration Curve for Calcite and Aragonite

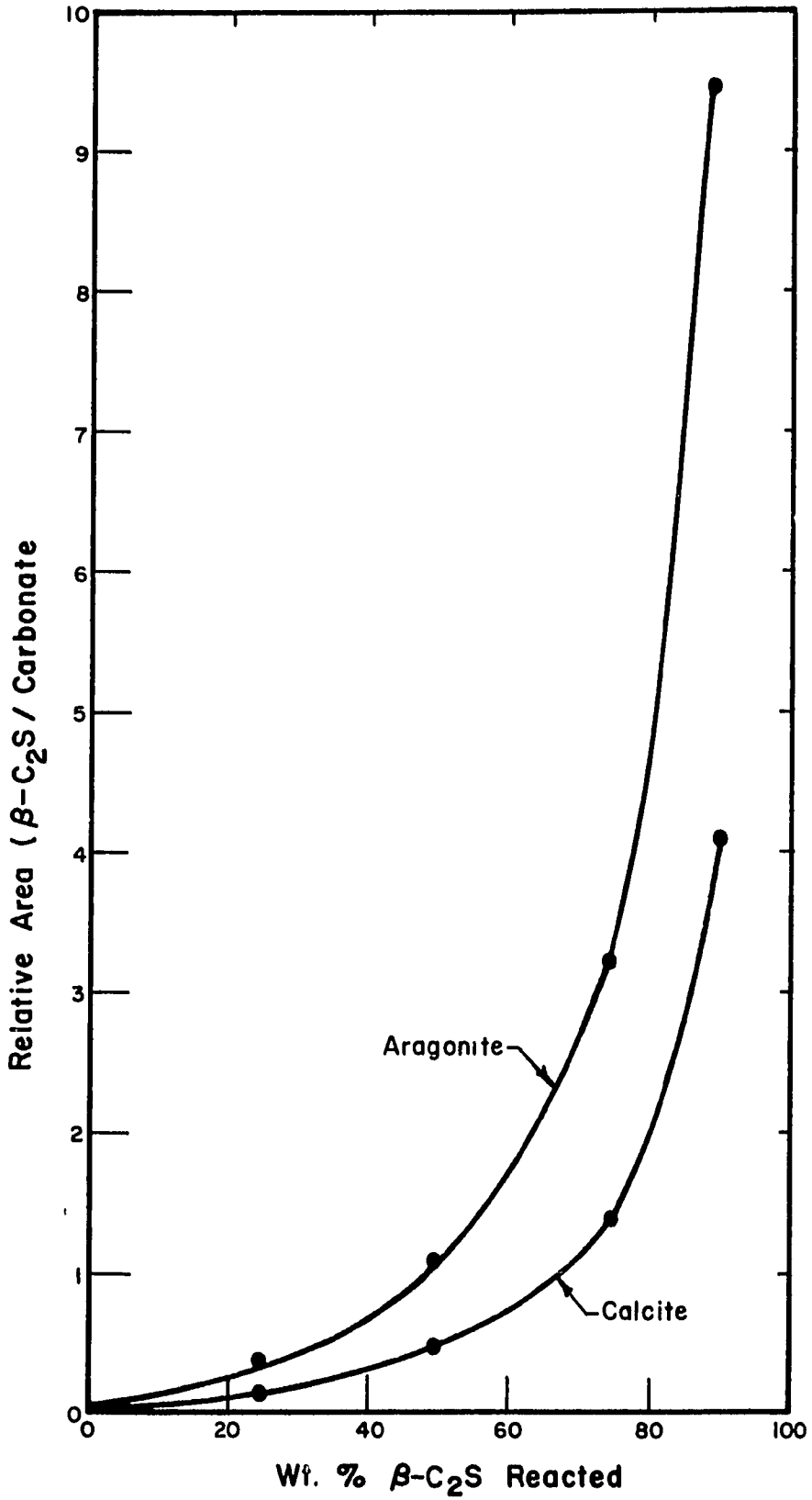

Figure 4. External Standard Calibration Curve for β-C_2S

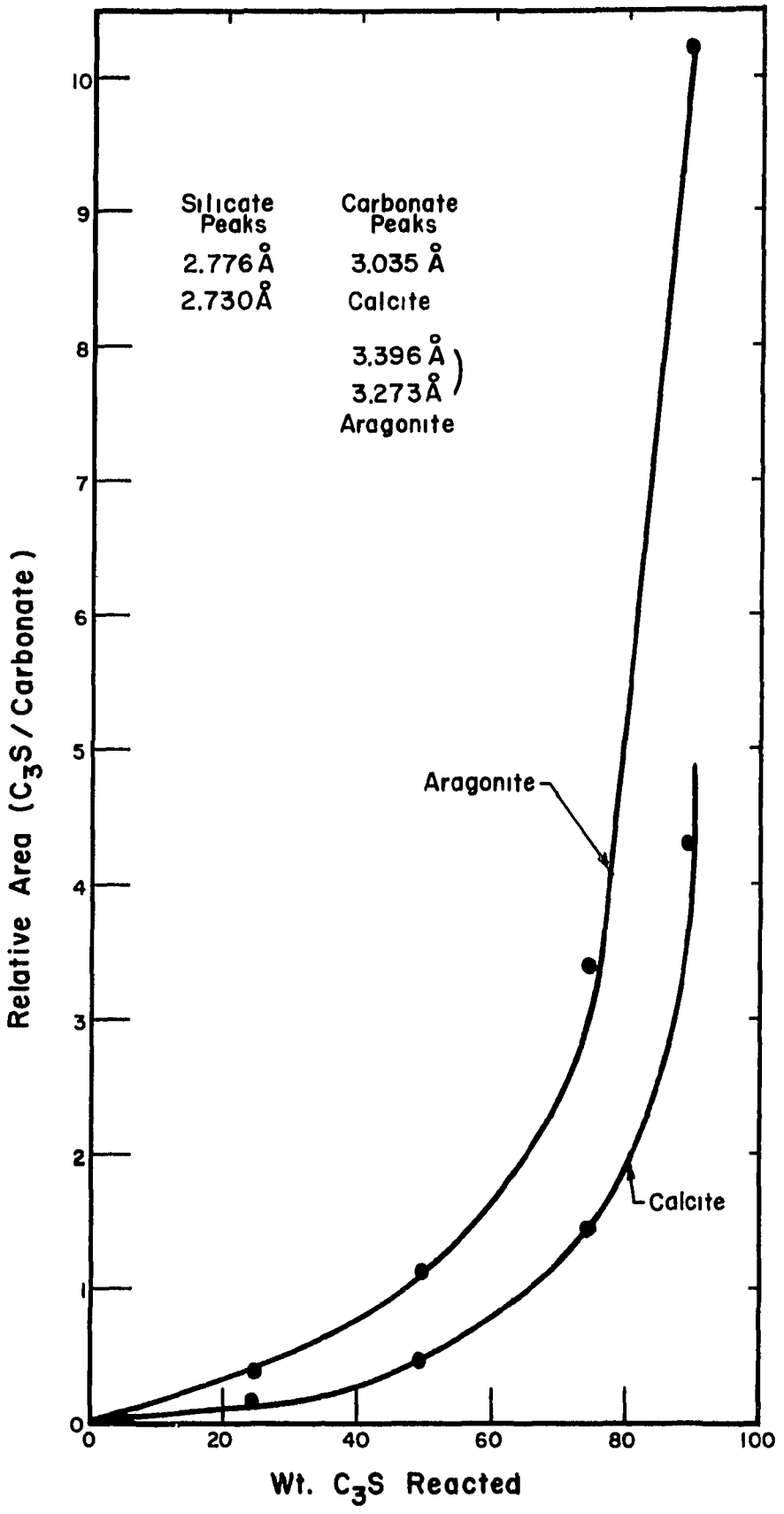

Figure 5. External Standard Calibration Curve for C_3S

at low degrees of reaction where the calcium silicate/carbonate ratio approached infinity. The weight percent carbonate was always cross checked against the TGA weight loss associated with carbonate decomposition. The nominal accuracy for the external standard method was ±5 wt.%.

A completely external standard technique which measured the peak area of the calcium silicate or the carbonate directly was attempted but the influence of the secondary reaction products such as gel and various forms of carbonate limited accuracy to ±10 wt.%.

3. Dry Calcium Silicate Powders

Dry powders were the easiest materials to work with and showed the greatest reproducibility with respect to reaction rate because the silicates received all of the reactants ($\overline{C}$ & H) from the vapor phase, which was carefully controlled. Figures 6 and 7 show the degree of reaction of β-C_2S powders with different Blaine finenesses. All β-C_2S powders showed increased reactivity with increased temperature and increased surface area.

The same behavior was noted for C_3S powders (Figures 8 and 9). Generally, the C_3S reacted faster than the β-C_2S dry powders with similar surface area.

4. Wet Calcium Silicate Powders

Figures 10-12 show the reaction behavior of β-C_2S with initial w/s ratios of 0.05, 0.1, and 0.2 wt.% of the dry β-C_2S and varying $P_{\overline{C}}$ and RH. The 0.1 w/s ratio gave the greatest degree of reaction for β-C_2S. An induction period for carbonation of 1-2 minutes was visually observed. The reaction was quite rapid from 2-15 minutes, but then slowed down appreciably. The initial rate of carbonation and the final degree of reaction were

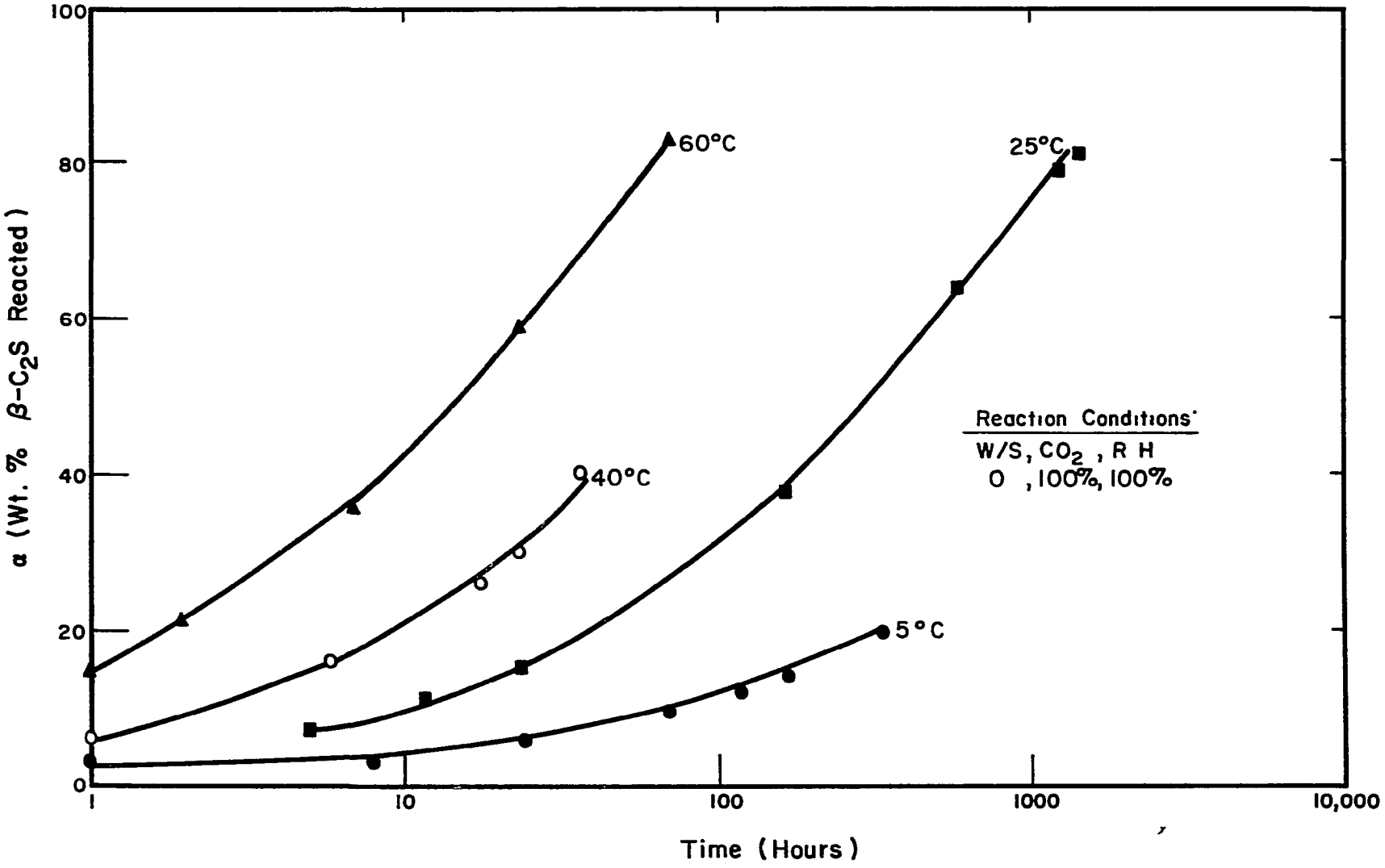

Figure 6. Degree of Carbonation for Anhydrous β-C_2S Powder (3850 cm^2/g)

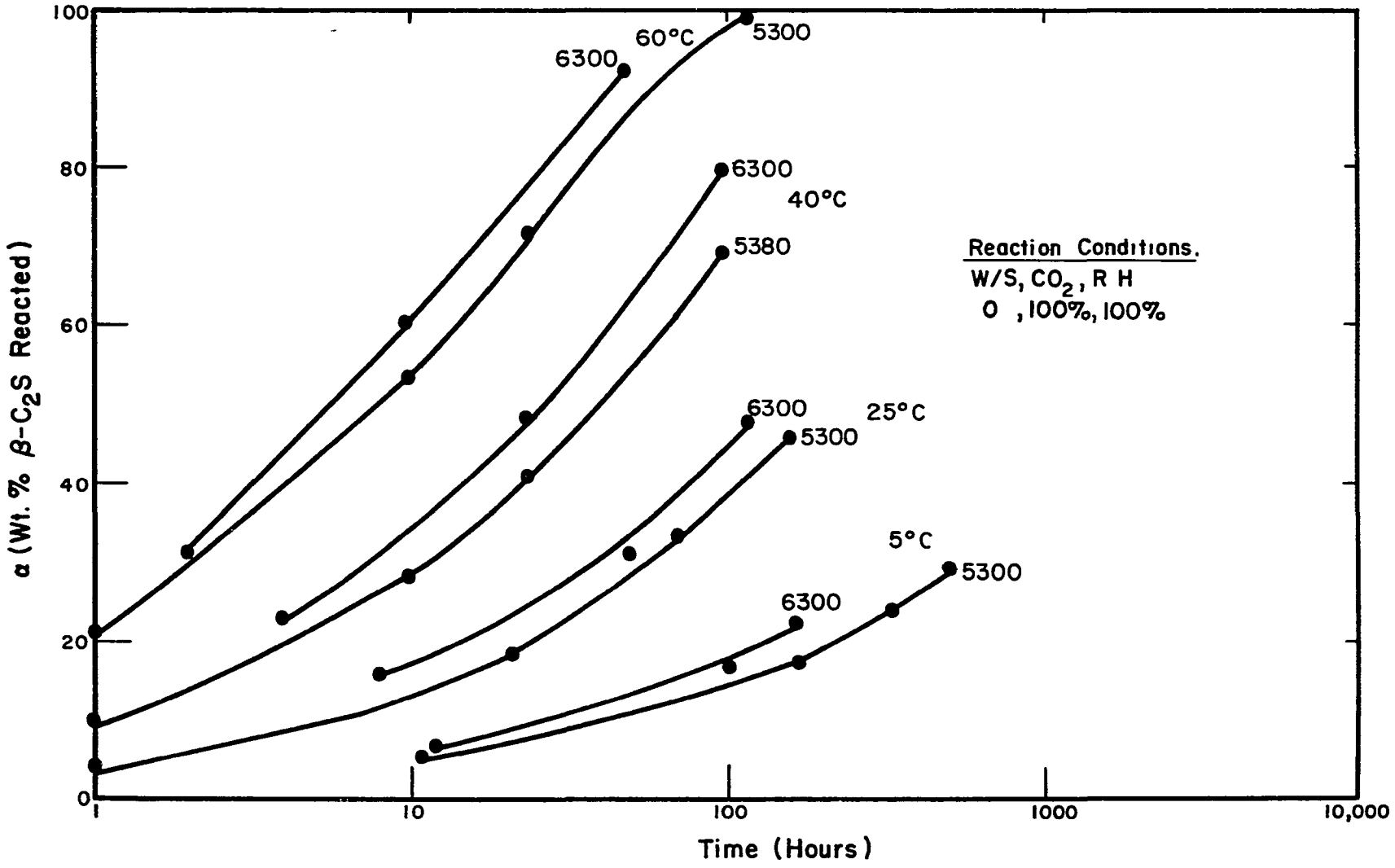

Figure 7. Degree of Carbonation for Anhydrous β-C_2S Powder (5300 and 6300 cm^2/g)

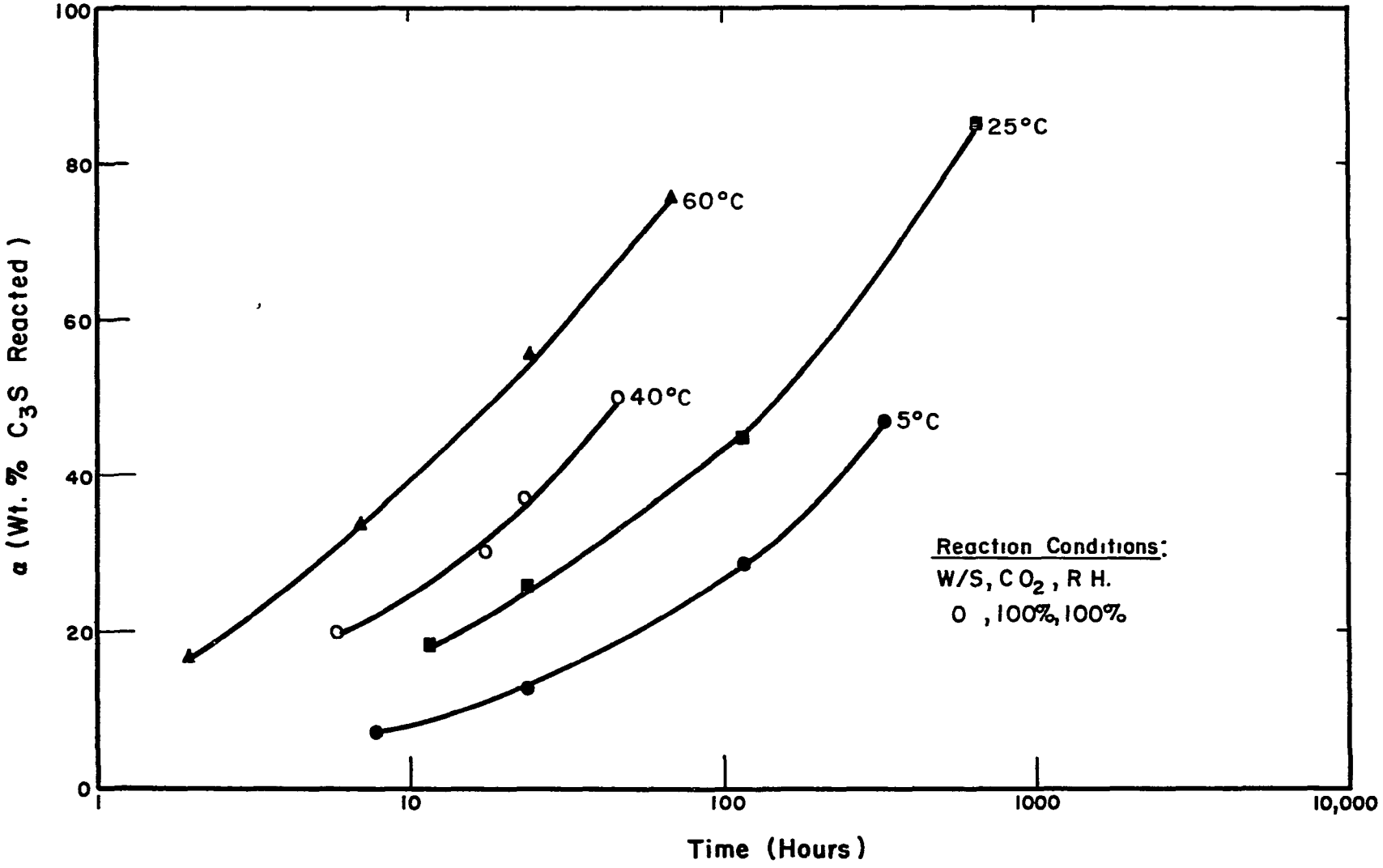

Figure 8. Degree of Carbonation for Anhydrous C_3S Powder (3900 cm^2/g)

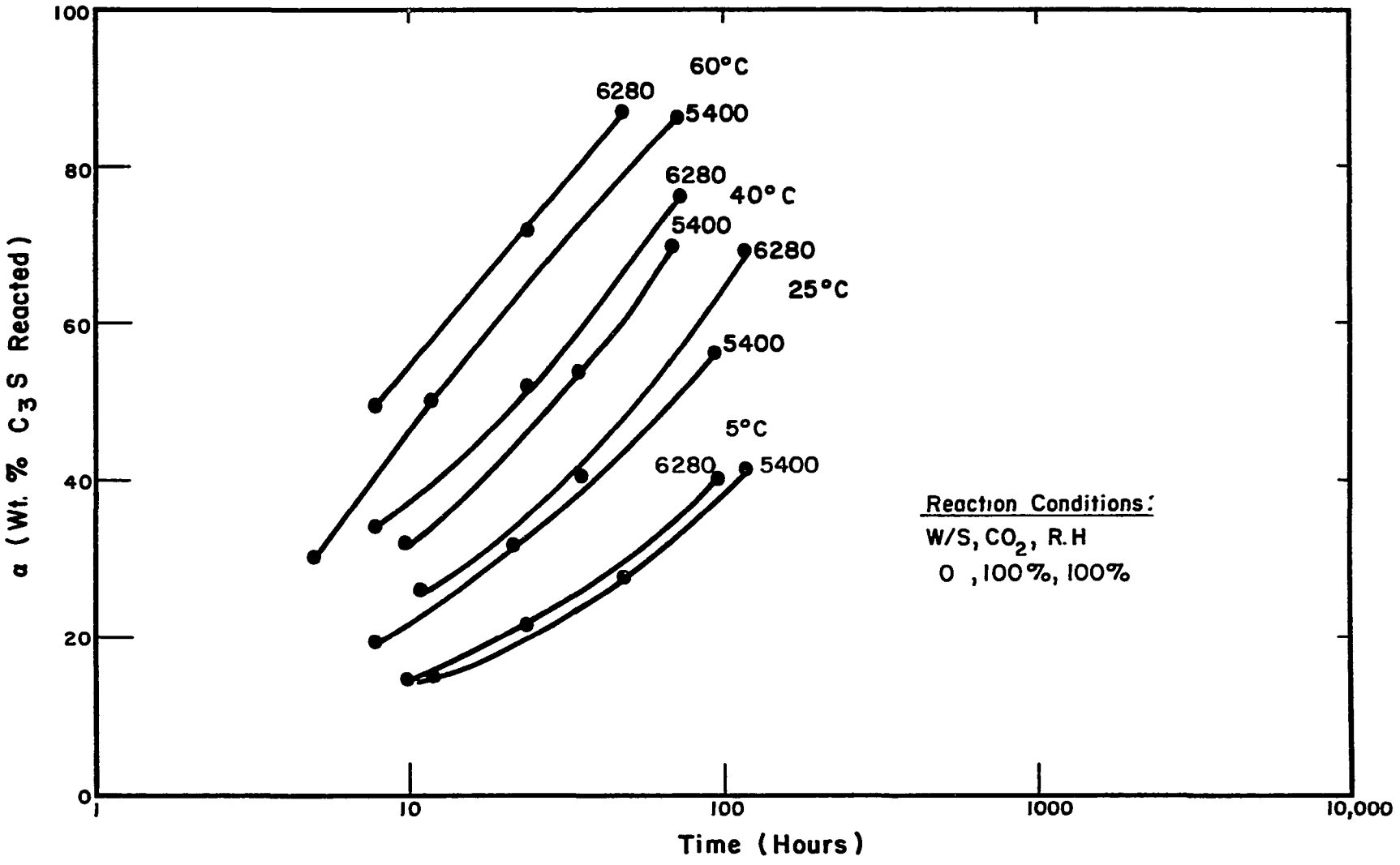

Figure 9. Degree of Carbonation for Anhydrous C_3S Powder (5400 and 6280 cm^2/g)

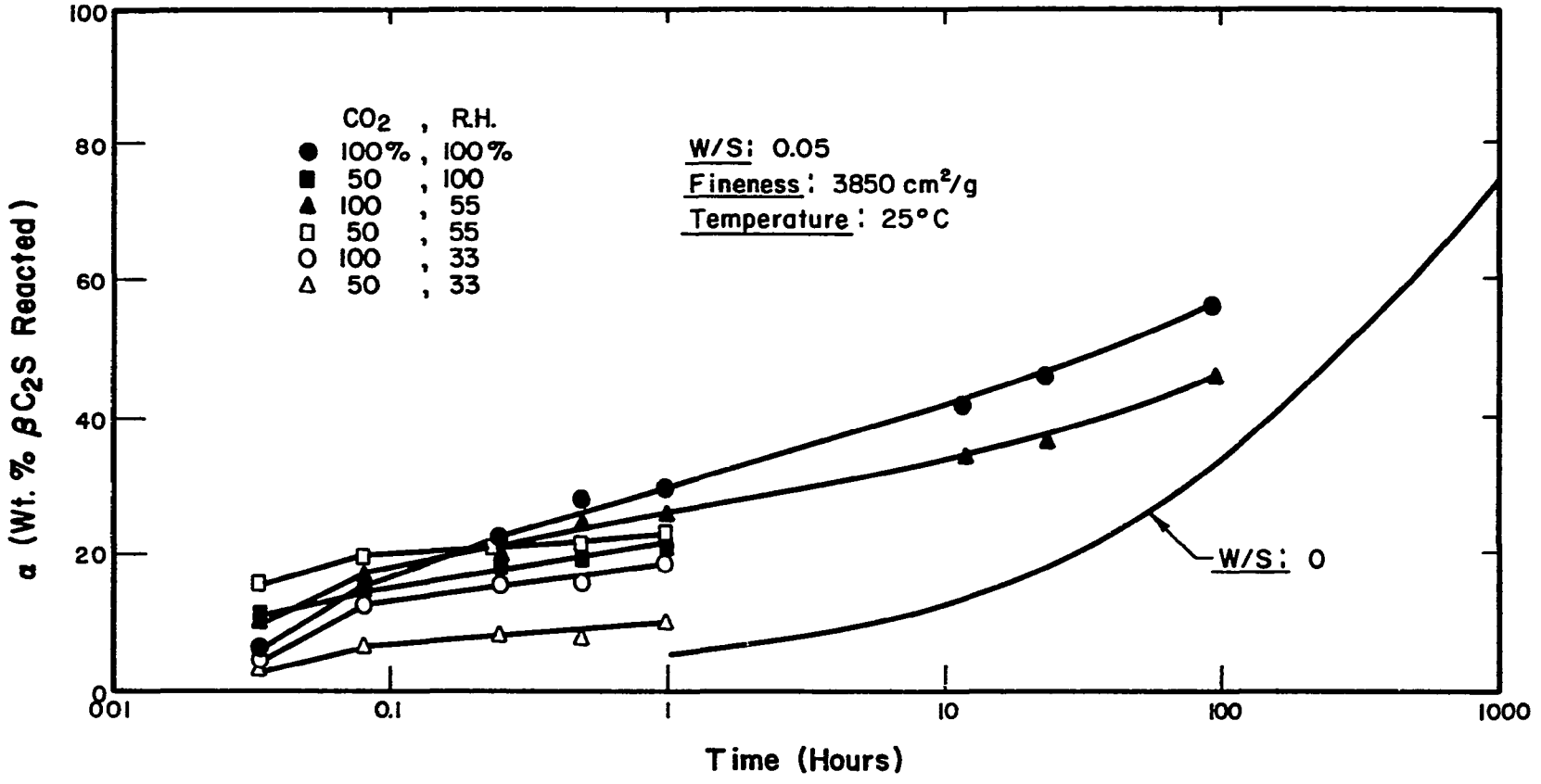

Figure 10. Degree of Carbonation for 0.05 w/s β-C_2S Powder

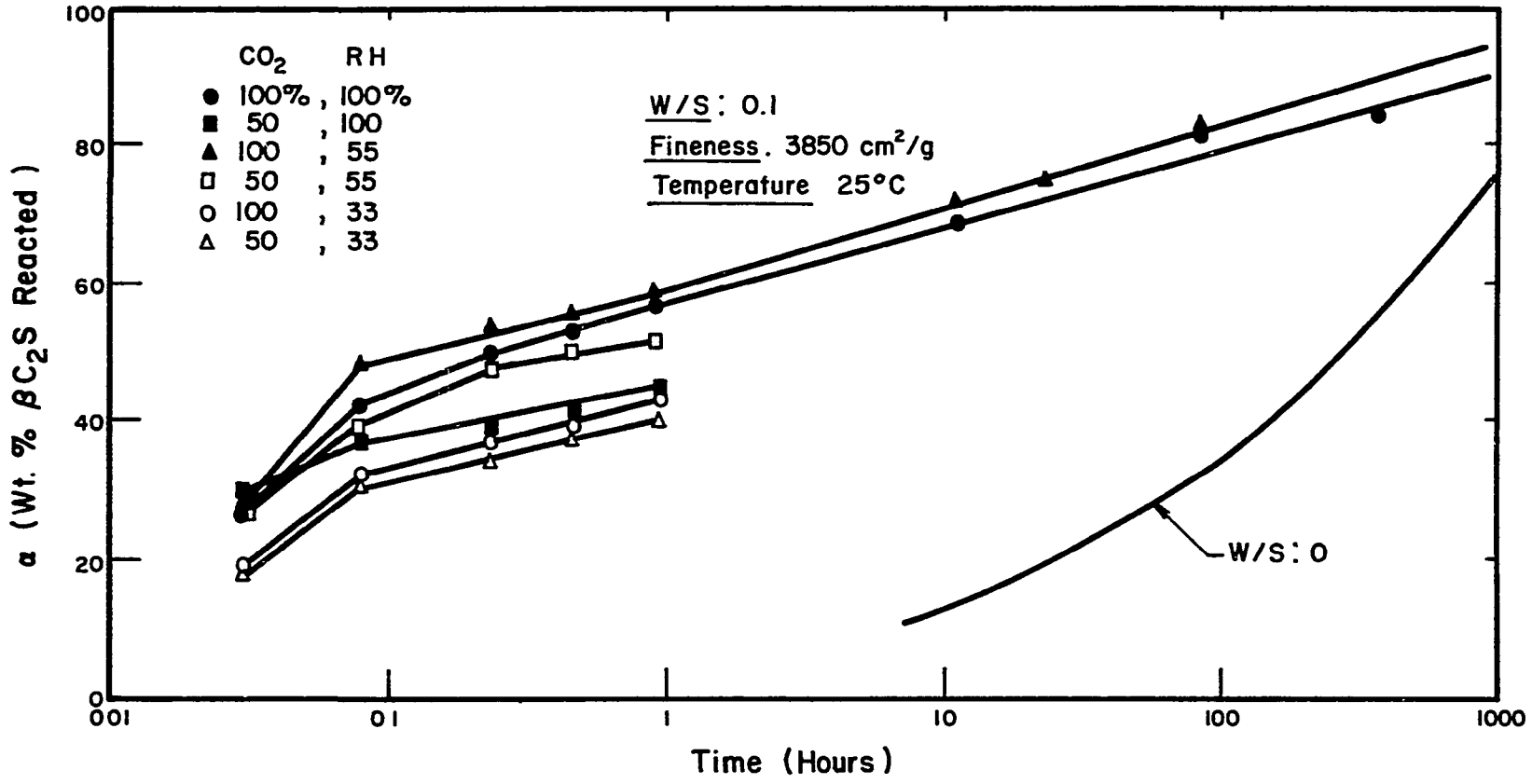

Figure 11. Degree of Carbonation for 0.10 w/s β-C_2S Powder

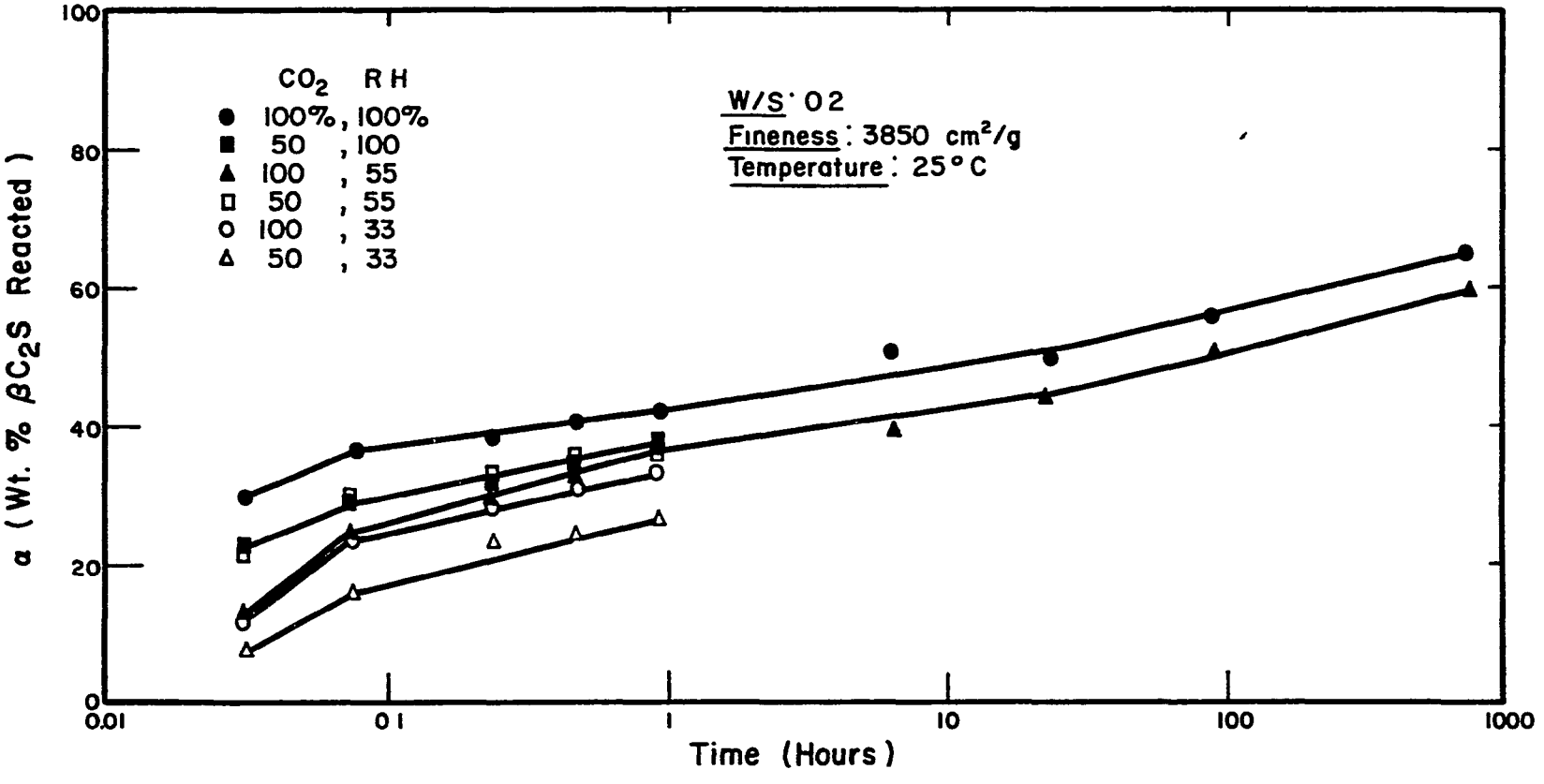

Figure 12. Degree of Carbonation for 0.20 w/s β-C_2S Powder

substantially higher for the wet calcium silicates than for the anhydrous samples. The shape of the reaction curves vs. time for the wet and dry carbonation runs were similar but not identical. Figure 13 shows the results for carbonated C_3S powder with w/s ratios of 0.1, 0.15, and 0.2. The 0.15 w/s ratio gave the greatest degree of reaction for C_3S and, again, C_3S reacted faster than β-C_2S under identical conditions.

5. Dry Pellets

The dry calcium silicate pellets reacted in a manner similar to the dry powders but the degree of reaction depends on the composition, shape and porosity of the pellet. For example, pellets with an aspect ratio of 2 carbonated faster than those with an aspect ratio of 1. Figure 14 shows the degree of reaction of the silicate in the pellet as a function of position across the diameter (aspect ratio of 1). β-C_2S, C_3S and an equimolar mixture of β-C_2S and C_3S were evaluated. All of the samples had a thin layer of 40-100% pure carbonate on the surface which was predominantly aragonite. The sample was moved as explained in Sect. II-7 and the reaction gradient was determined. The reaction gradients for the anhydrous silicates were relatively flat throughout the central portion of the samples. Long reaction times formed flat reaction gradients and produced 30-50% complete reaction of the pellets.

6. Wet Pellets

Wet pelletized silicates showed greater variation in the central part of the samples than the dry samples (Figure 14). At early times the minimum reaction occurred in the center of the specimen (6.25 mm), but the reaction gradient leveled out across the wet specimens with time. The wet β-C_2S,

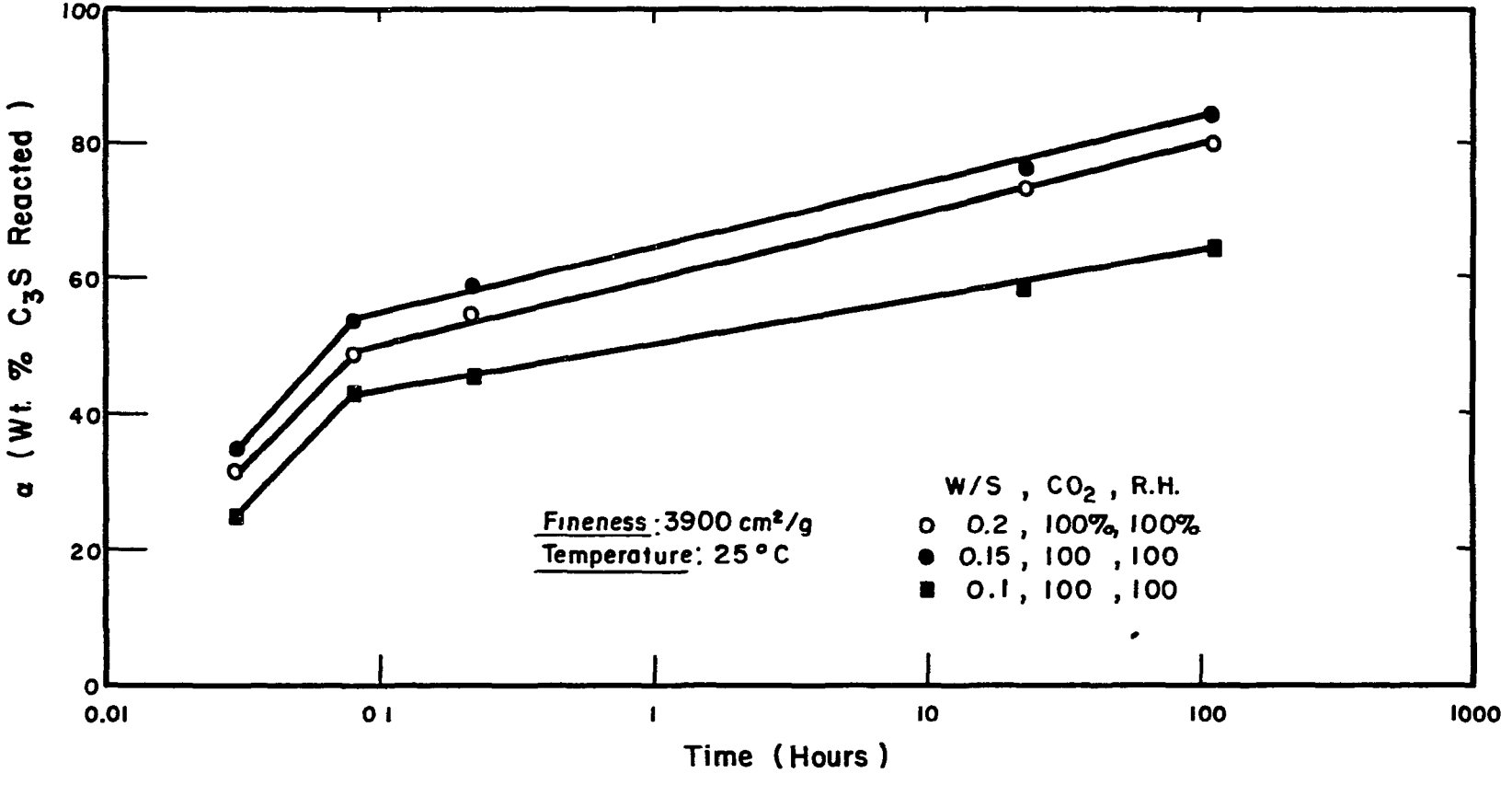

Figure 13. Degree of Carbonation for Wetted C_3S Powder

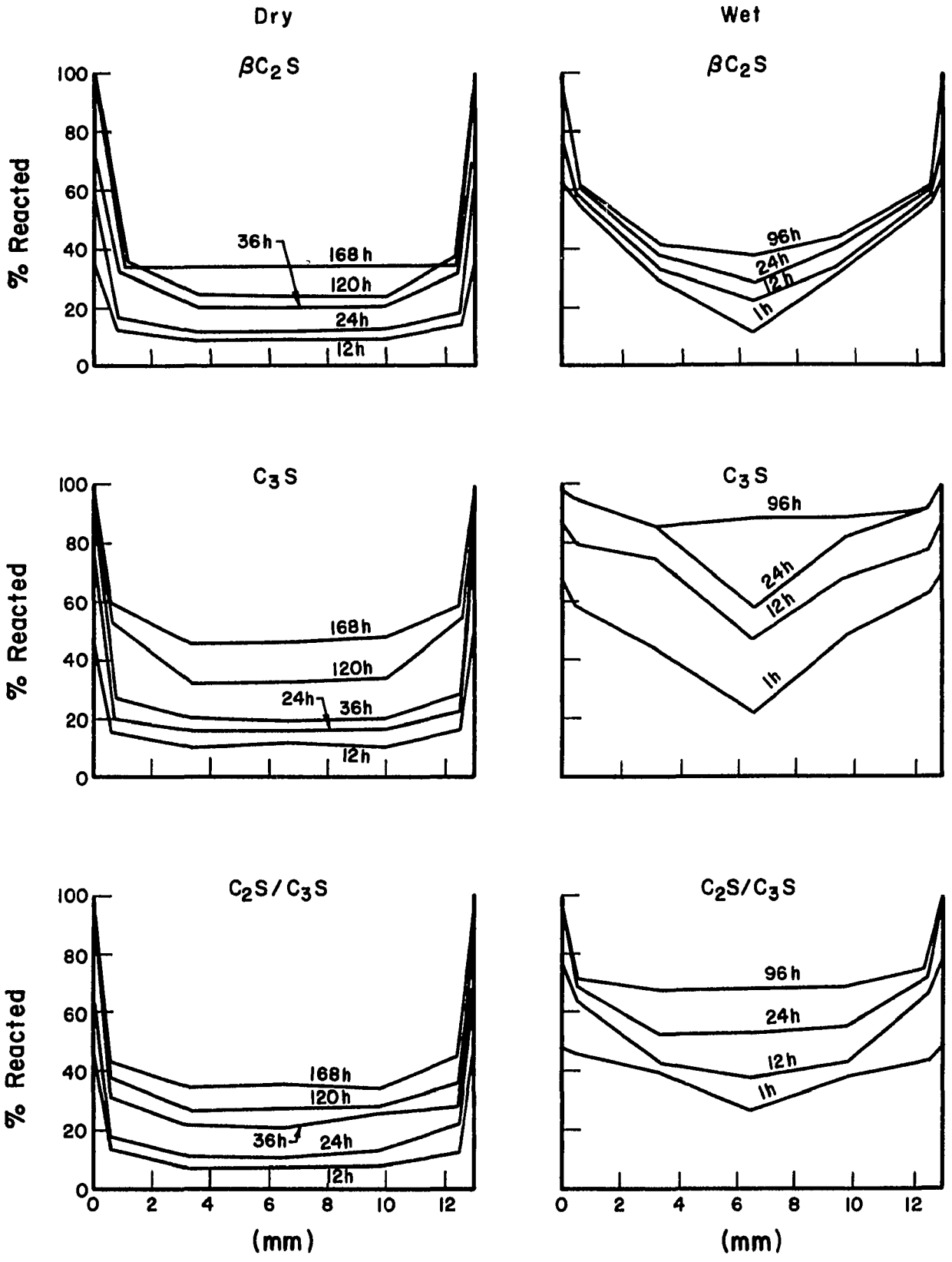

Figure 14. Degree of Carbonation Across the Diameter of Calcium Silicate Pellets

C_3S, and β-C_2S/C_3S pellets all reacted to a greater extent than their dry counterparts. The maximum percent reacted for the wet pellets was experienced in the C_3S pellet which was 90% reacted at 96 hours. Generally the C_3S reacted the fastest, then the β-C_2S/C_3S mixture, and finally the β-C_2S.

7. Rate of Hydration

The hydration rate for pressed pellets of β-C_2S, C_3S and β-C_2S/C_3S is shown in Figure 15. The rate of hydration of β-C_2S and C_3S compared favorably with other hydration studies.[2,3] The hydration rate of the equimolar mixture fell between the hydration rates of β-C_2S and C_3S.

8. Carbonate Formation

The degree of carbonate formation is shown in Figures 16-18. The dry powders form calcium carbonate as soon as the calcium silicates are wetted by atmospheric humidity or by condensed liquid water and as soon as the $\overline{C}$ content reaches a threshold value. After a short induction period (0-2 minutes), the carbonate begins to form and the rate at which $C\overline{C}$ appears coincides with the disappearance of the calcium silicate. Theoretically, 1 mole of β-C_2S can form 2 moles of $C\overline{C}$ while 1 mole of C_3S forms 3 moles of $C\overline{C}$, according to Eq. 42.

$$C_nS + n\overline{C} + H \rightarrow nC\overline{C} + S\text{-}H \qquad (42)$$

The theoretical formation of calcium carbonate is shown in Figures 16-18, where the limits are given as the g theoretical carbonate/g calcium silicate. The values are 1.162 and 1.315 g $C\overline{C}$/g calcium silicate for β-C_2S and C_3S, respectively. Thus it can be seen that the deviation from the theoretical lines in Figures 16-18 is an indication of the amount of gel

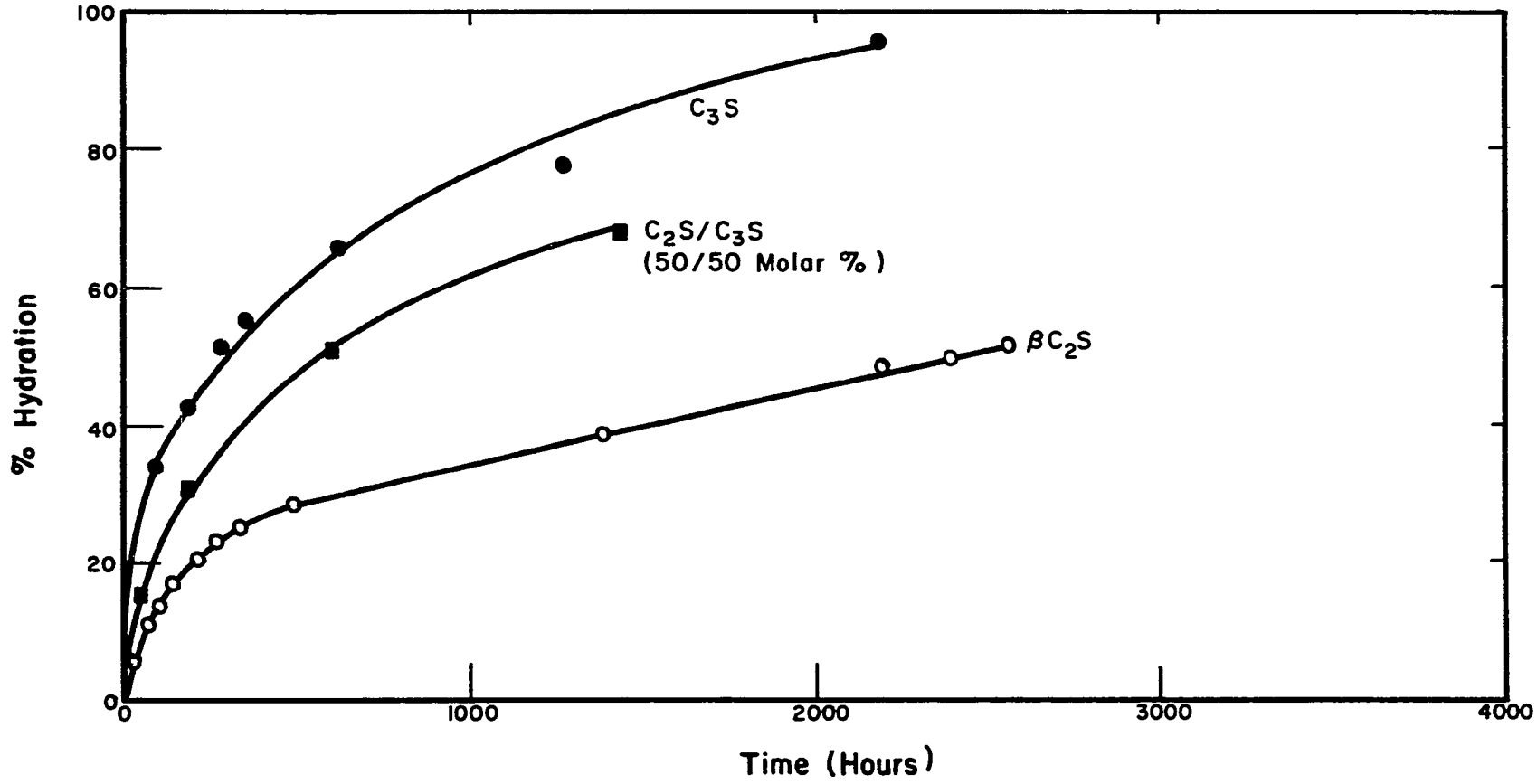

Figure 15. Degree of Hydration for Calcium Silicate Pellets Formed From 3900 cm^2/g Powder

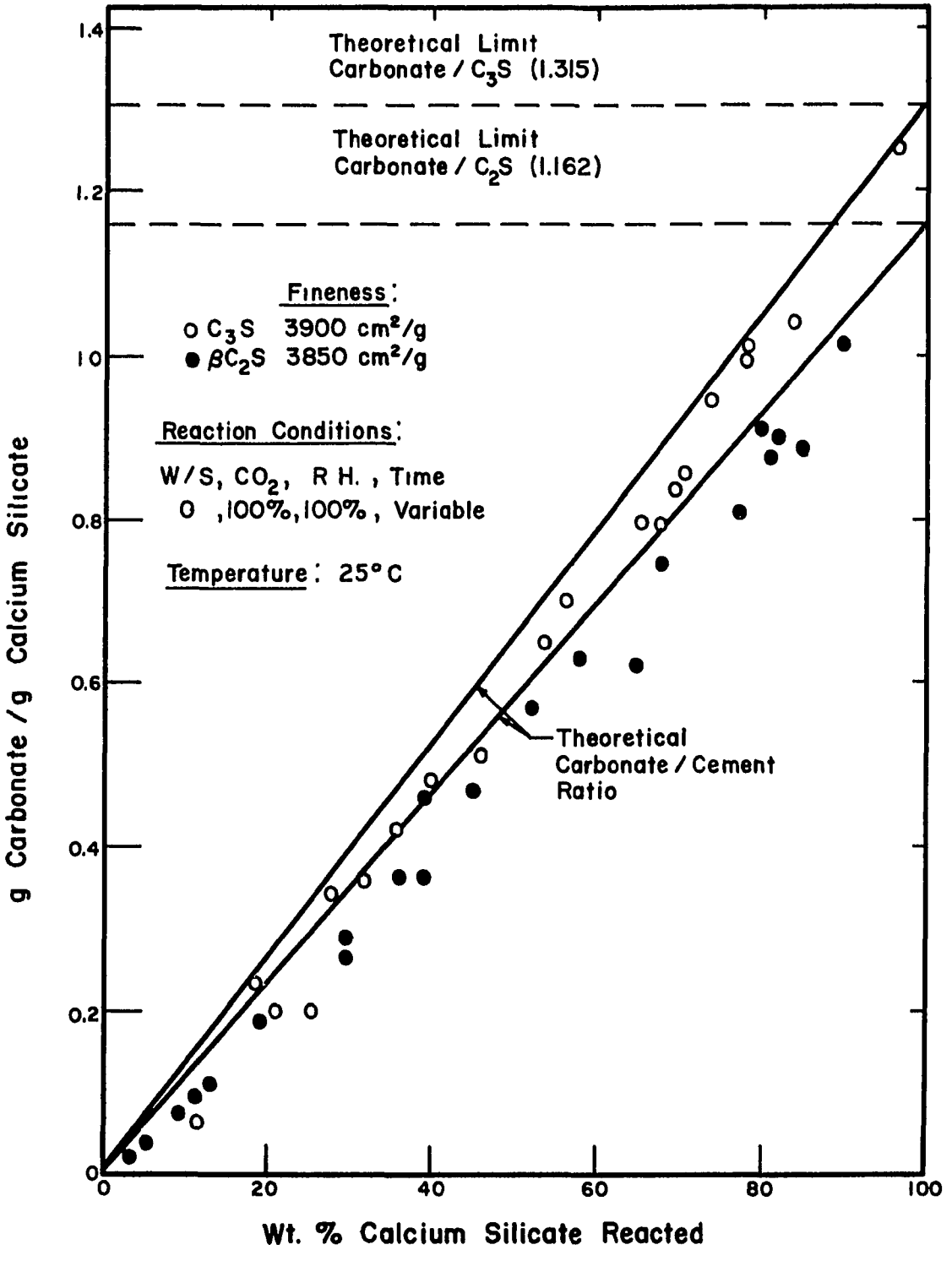

Figure 16. Amount of Carbonate Formation Versus Degree of Carbonation of Dry Calcium Silicate Powders

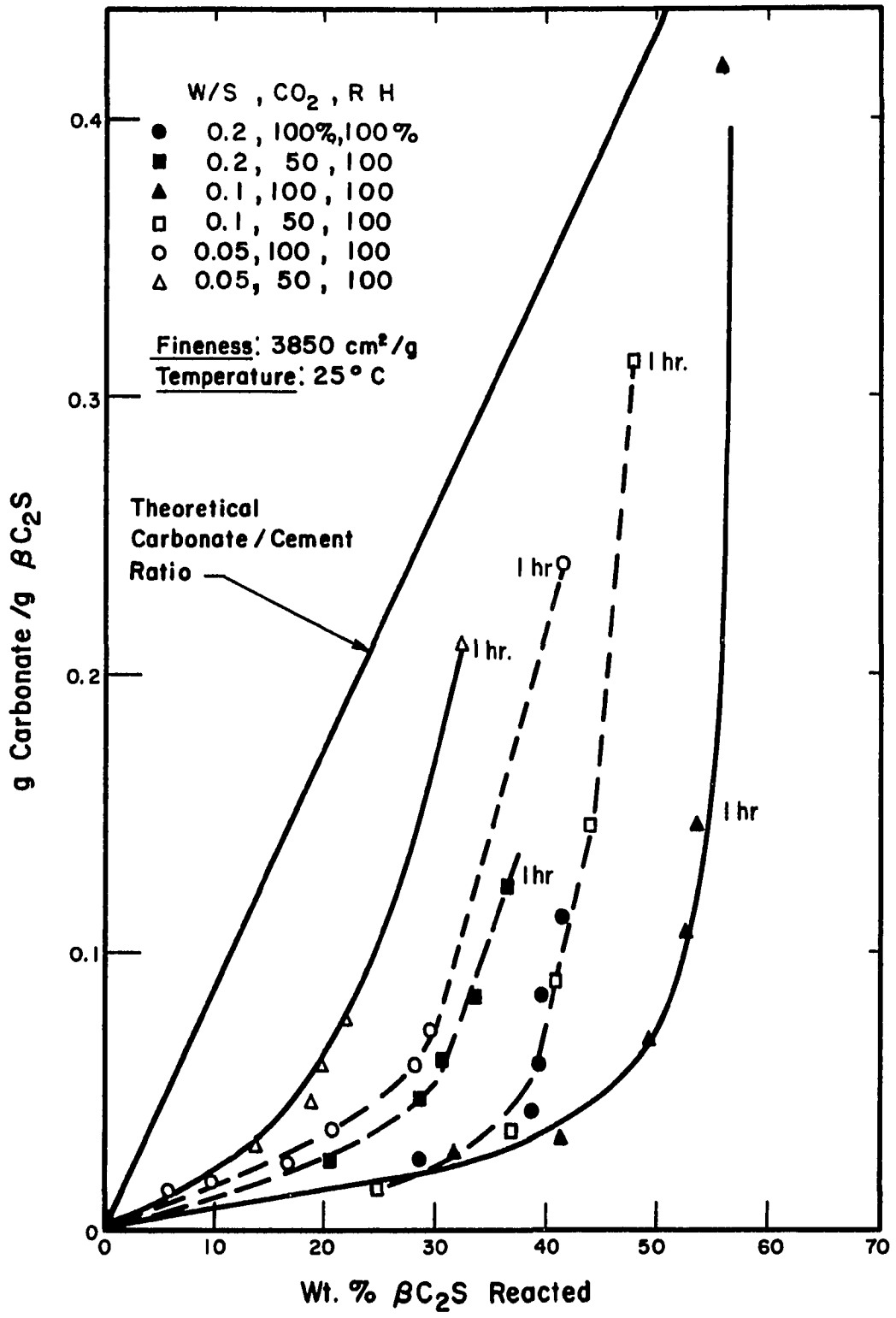

Figure 17. Amount of Carbonate Formation Versus Degree of Carbonation of β-C_2S Powders of Different w/s Ratios

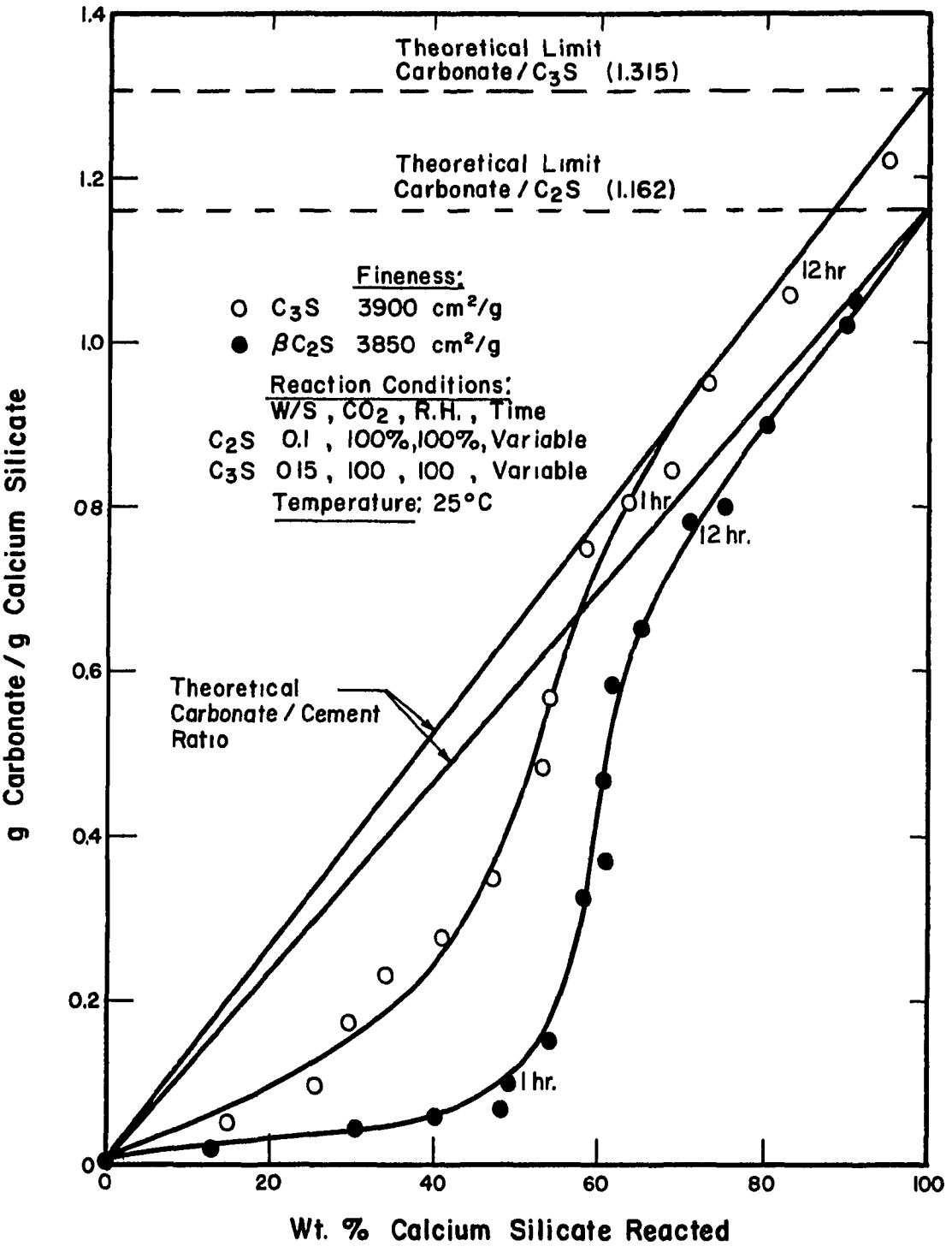

Figure 18. Amount of Carbonate Formation Versus Degree of Carbonation of Wetted Calcium Silicate Powders

formed. The dry powders form little gel and form carbonate immediately upon the reaction of the silicate (Figure 16).

However, when the wet powders were carbonated (Figures 17 and 18), the deviation from the theoretical carbonate line was quite pronounced, especially at early times. A large amount of gel formed initially in the wetted powders which were carbonated but after 2 hours the amount of carbonate approached the theoretical limit indicating that the gel itself was carbonated. Higher w/s ratios (0.1 and 0.2 for β-C_2S, and 0.15 for C_3S) deviated significantly from the carbonate limit while the lower w/s ratios approached the dry (0 w/s) condition and the theoretical line. Figure 17 shows a reaction envelope for various w/s ratios.

9. Water/Solids (w/s) Ratio

The effect of w/s ratio on the wet β-C_2S and C_3S is shown in Figure 19. The degree of reaction is maximized at 0.125 and 0.16 for β-C_2S and C_3S, respectively, and w/s values higher or lower than the optimum value cause a decrease in the reaction rate for both calcium silicates. Although the curves in Figure 19 have maxima, they are not symmetrical and reaction rate drops faster at low w/s ratios than at high w/s ratios.

10. Relative Humidity (RH)

The effect of RH on the degree of reaction is shown in Figure 20. The wet samples of β-C_2S and C_3S react more rapidly than the dry samples. The wet samples showed approximately linear dependency on the relative humidity from 0-55% but virtually no effect from 55-100% RH. The dry β-C_2S and C_3S reacted less than the wet samples but showed a continuous increase in reactivity with increased RH from 0-80%.

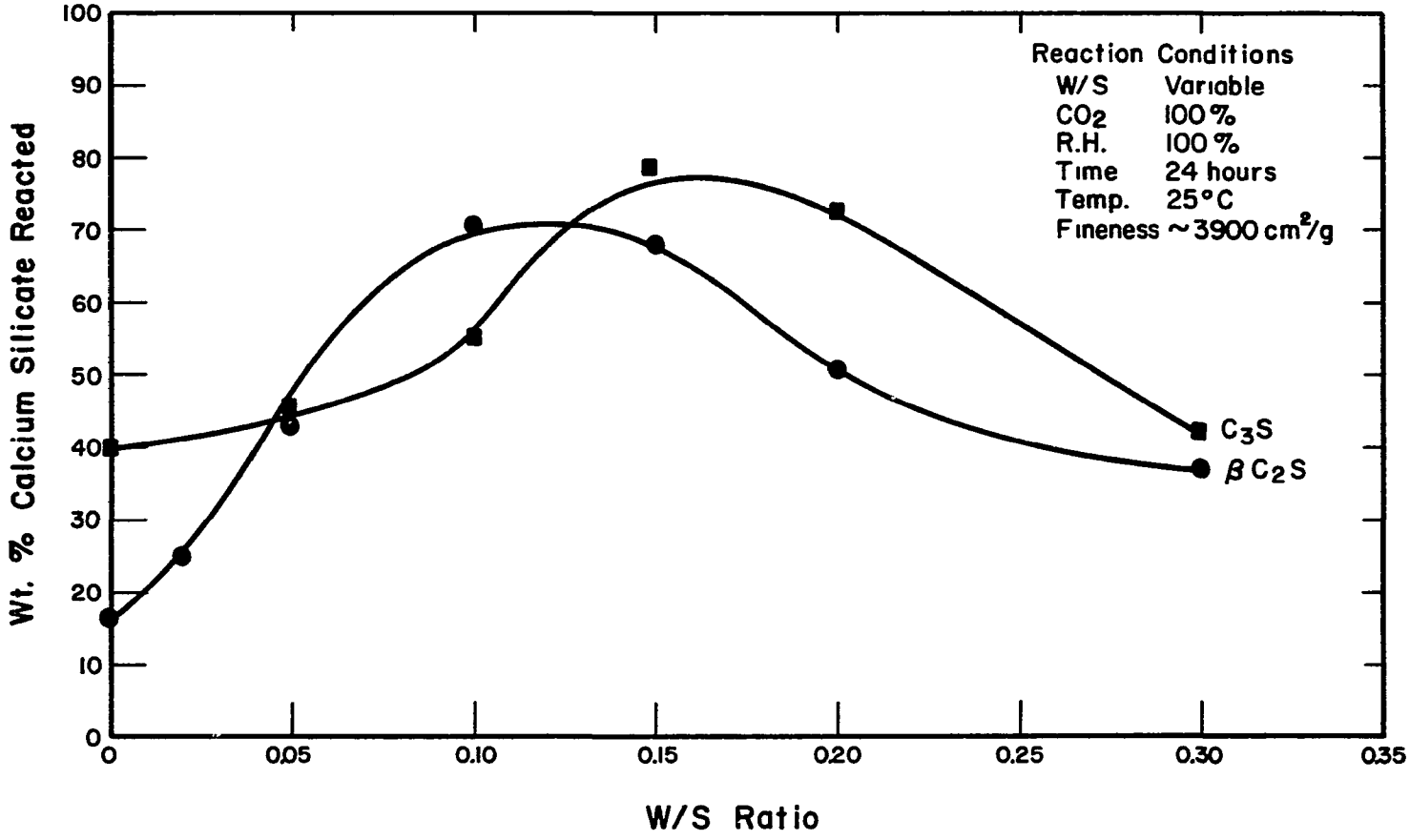

Figure 19. Effect of w/s Ratio on the Degree of Carbonation for β-C_2S and C_3S Powders

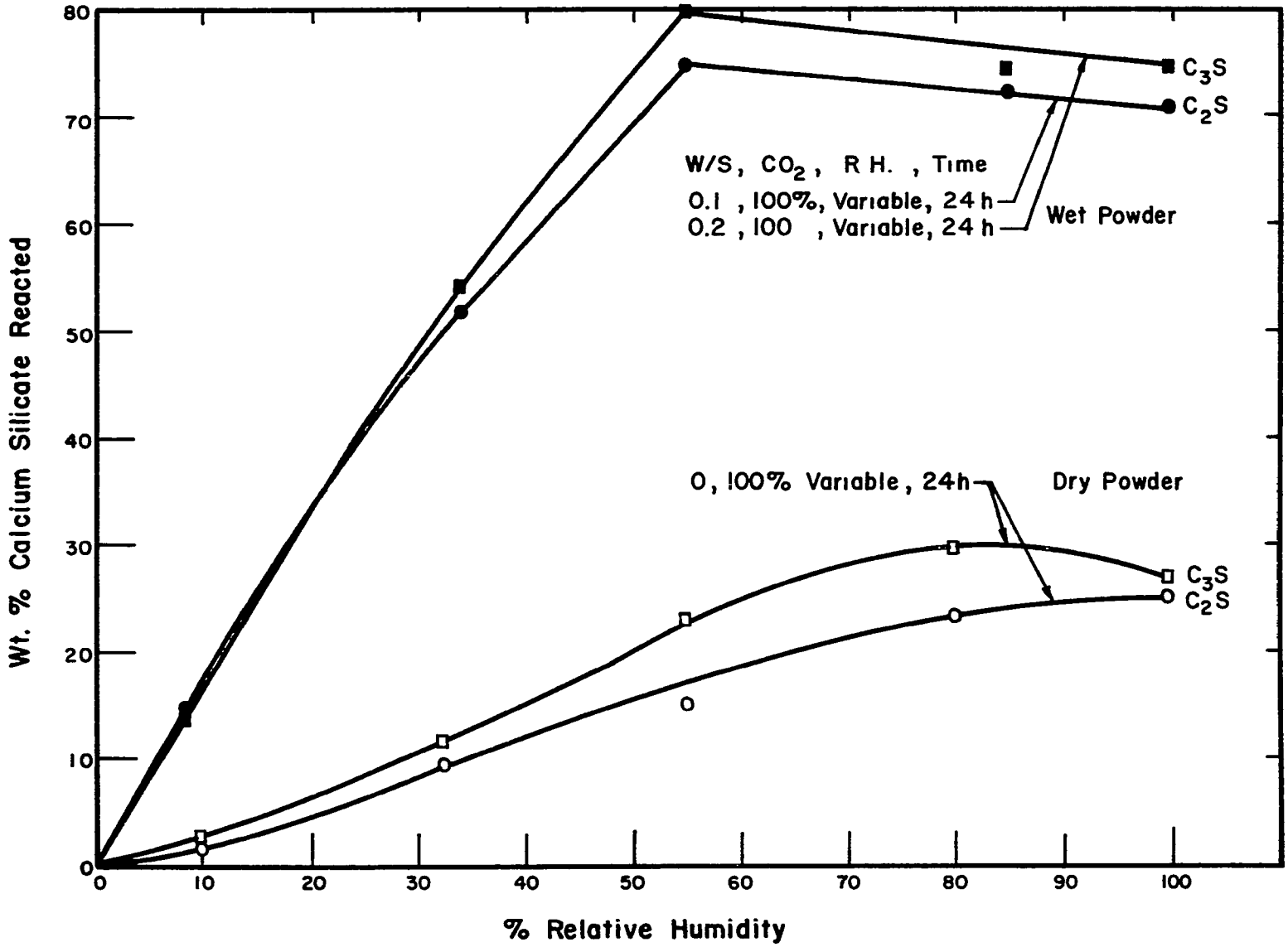

Figure 20. Effect of Relative Humidity on the Degree of Carbonation of β-C_2S and C_3S Powders

11. Partial Pressure of $\overline{C}$ ($P_{\overline{C}}$)

Figure 21 shows the effect of $P_{\overline{C}}$ from 0.025-1.0 atm on the degree of reaction of calcium silicates. The dry samples showed a breakpoint value of 0.125 atm for rapid reaction and a slow rate of increase in the rate of carbonation. The wet β-C_2S and C_3S also showed a two-step dependence on $P_{\overline{C}}$. A threshold value of 0.025-0.05 atm was observed in all samples, below which no appreciable reaction occurred. Subsequently, the degree of reaction increased rapidly from 0.025 or 0.05 to 0.15 atm $\overline{C}$ followed by a slower reaction at $P_{\overline{C}}$ values from 0.15 to 1.0 atm. The second portion of the carbonation curve was shallower for the higher $P_{\overline{C}}$.

B. Determination of Stoichiometry

1. Mass Spectrometer-Thermogravimetric Analysis (MS-TGA)

Two separate tests were conducted on selected calcium silicate pastes and reacted dry powders to determine when H and $\overline{C}$ were lost from the samples during heating. All MS and TGA specimens were dried at 105°C for 6 hours and showed no weight loss or evolved water at temperatures below 105°C (Figure 22a&b). Water was driven from the samples from 105° to 350°C. The samples with shorter reaction times had more water as shown in the MS data and the water peak shifts to slightly higher temperatures and broadens with longer reaction times. The $\overline{C}$ was driven from the samples at 350°-1000°C and the longer reaction times shifted the $\overline{C}$ to higher temperatures. Shifting of the water and $\overline{C}$ peaks to higher temperatures is an indication of increased crystallinity. The areas under the water and $\overline{C}$ peaks are an indication of the amount of material which was lost at a given temperature. Generally, the water decreased and the $\overline{C}$ increased as the samples were carbonated for longer times.

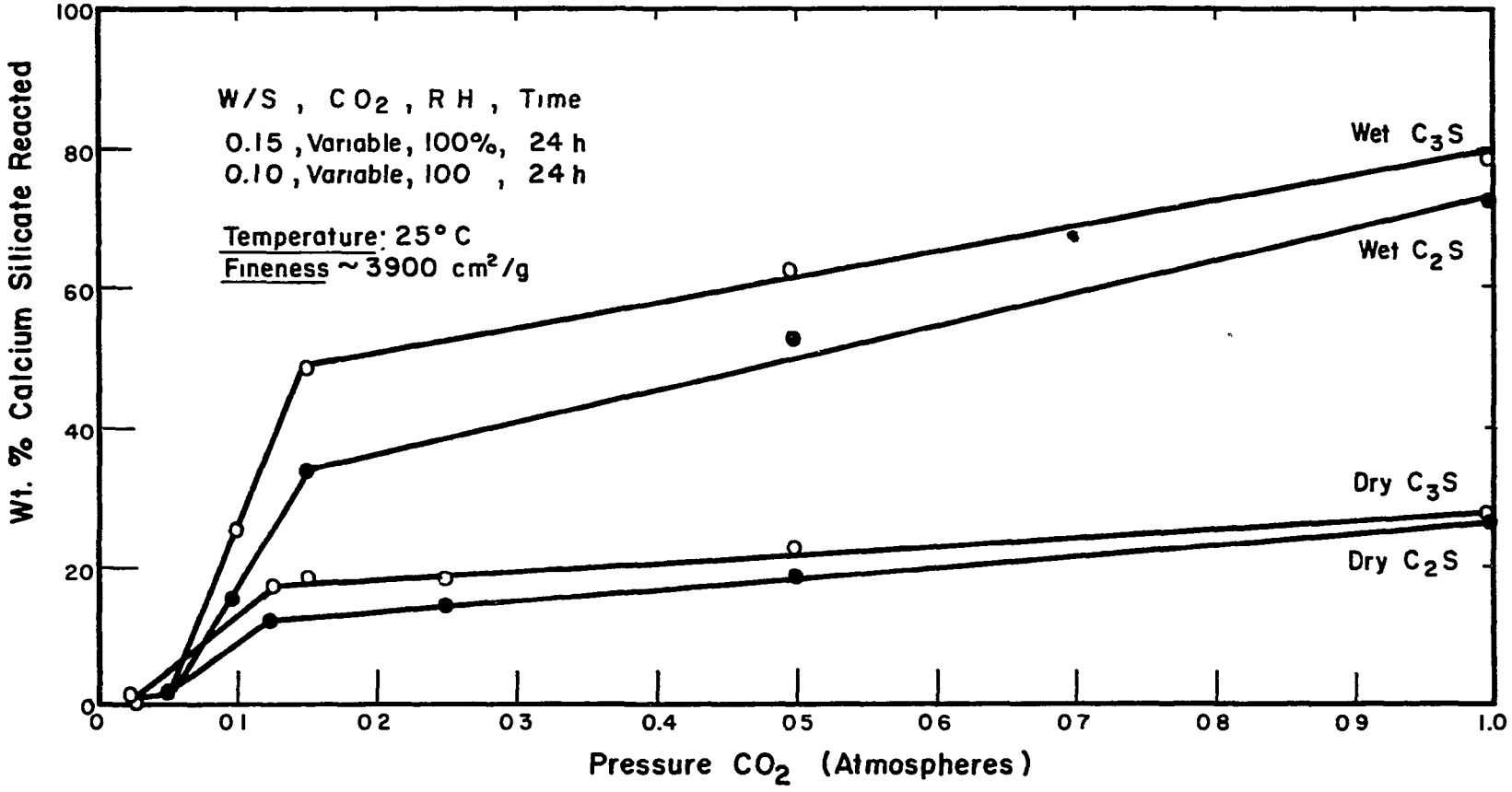

Figure 21. Effect of CO_2 Partial Pressure on the Degree of Carbonation of β-C_2S and C_3S Powders

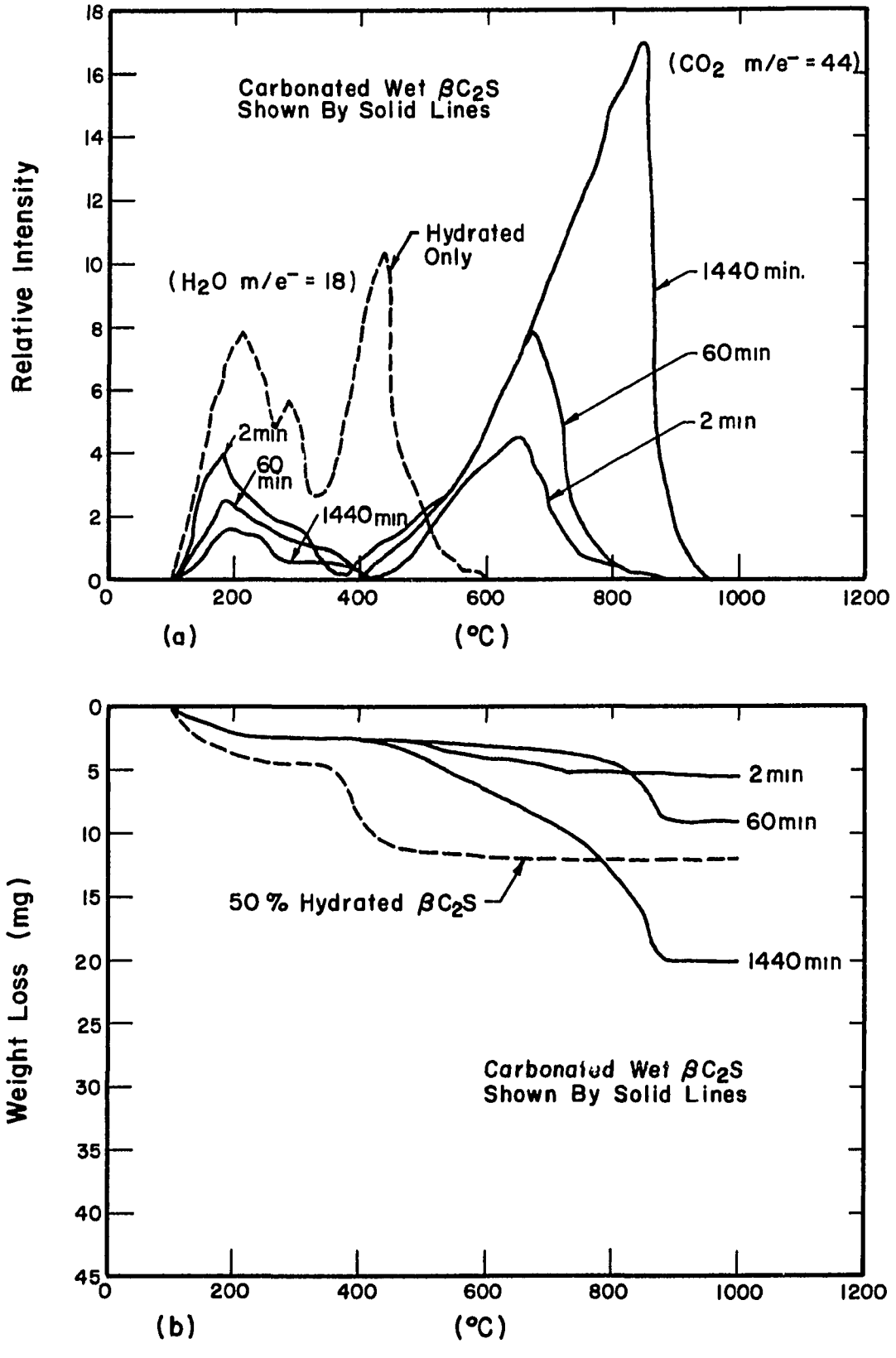

Figure 22(a). Mass Spectrometer Analysis of Carbonated β-C_2S and C_3S Powders

(b). TGA Data for Carbonated β-C_2S and C_3S Powders

Samples which were hydrated then carbonated as shown in Figure 22a&b by the dashed line were included to show the interference of the hydration products (CH and C-S-H gel) compared to the sharp water and $\overline{C}$ delineation which is possible with the dry carbonated samples. Since the water and $\overline{C}$ could only be separated for the dry powders, only these samples were used in the constant temperature pyrolysis procedure. No wetted calcium silicate powders were evaluated for stoichiometry using MS-TGA methods.

2. Stoichiometry

The C/S and H/S ratios for reacted dry β-C_2S and C_3S powders are shown in Figures 23 and 24. The initial C/S ratios approximate to the C/S ratios of the anhydrous calcium silicates; i.e., 2.0 and 3.0 for β-C_2S and C_3S, respectively. However, the C/S ratios dropped rapidly as carbonation proceeded, to about 0.4 at 40% reaction, then more slowly toward zero as the reaction approached 100%. The H/S ratios similarly dropped from 3-4 initially, toward zero as the reaction approached 100%. Analogous behavior was noted for the C/S and H/S values for wet powdered β-C_2S and C_3S, but only a limited amount of testing was conducted due to uncertainty in the exact temperature where the H and $\overline{C}$ decomposed from the reacted silicates. The wet powders had scatter in C/S and H/S ratios, especially H/S ratios. Figure 25 shows the C/S data for a set of w/s ratios on carbonated β-C_2S. The decrease in the C/S as the carbonation reaction continued is similar to the dry β-C_2S which was carbonated. Only the wet powders formed an appreciable amount of gel which subsequently was carbonated.

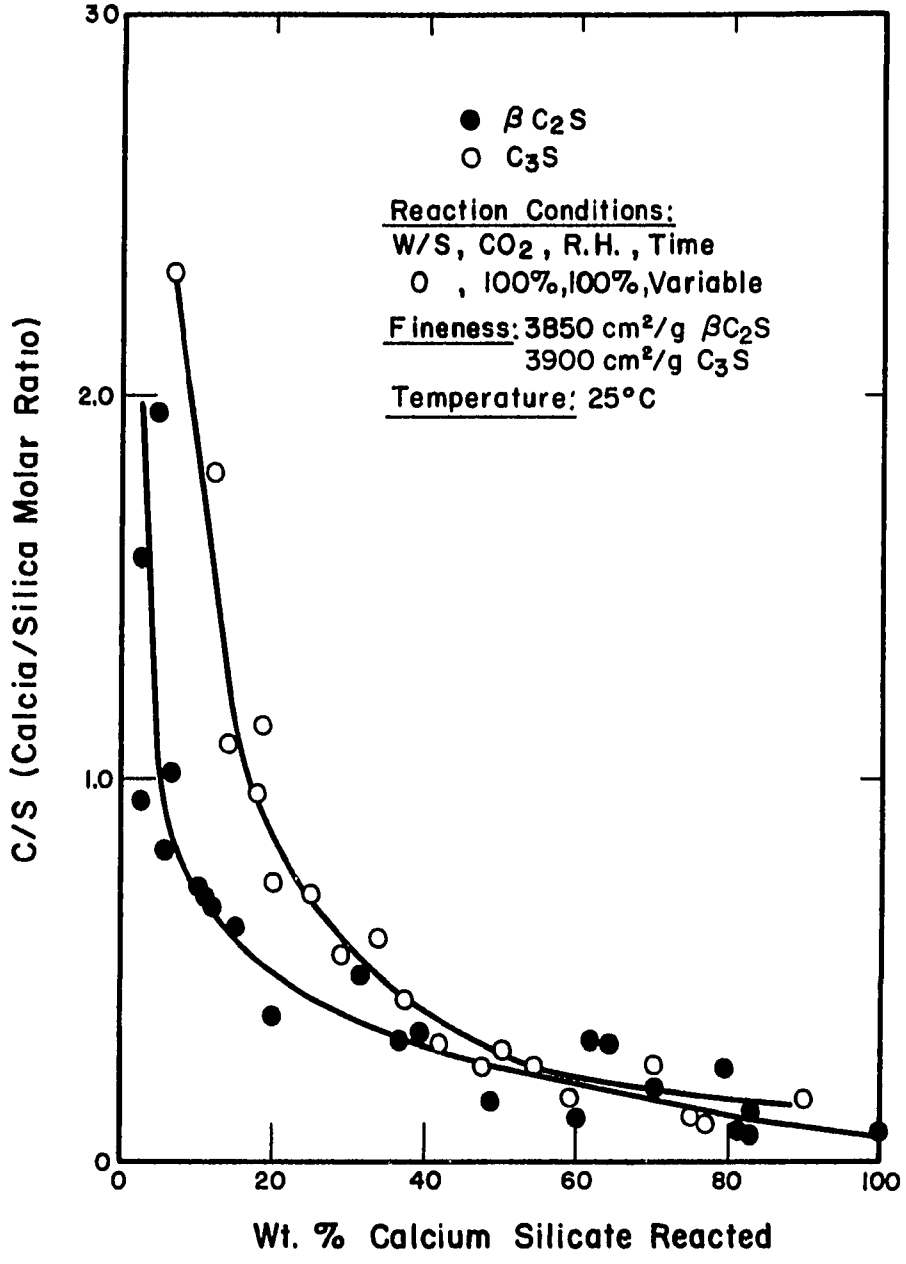

Figure 23. C/S Ratio of C-S-H Gel Formed From Anhydrous β-C_2S and C_3S Powders, as a Function of Calcium Silicate Reacted

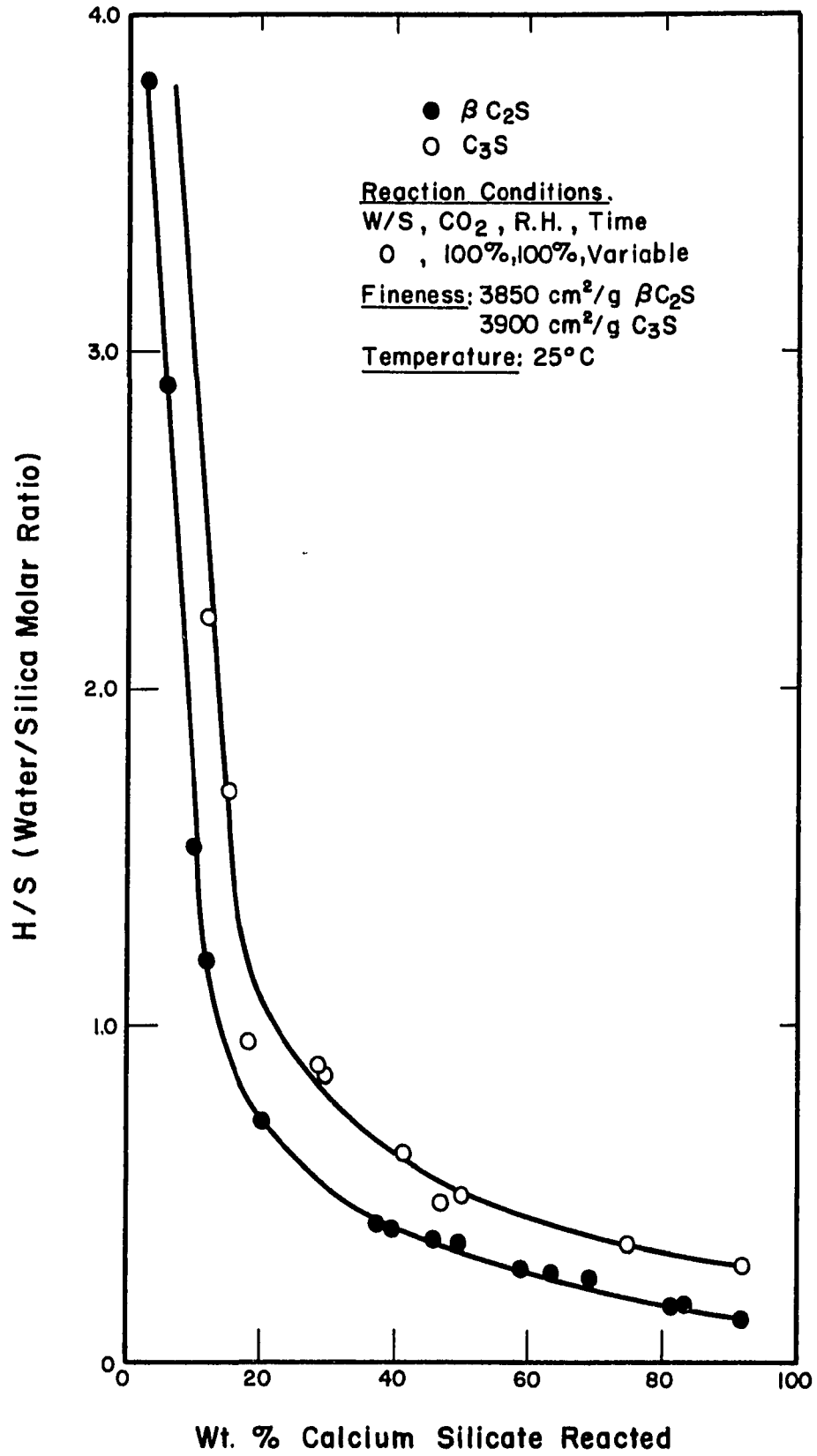

Figure 24. Variation of H/S Ratio of C-S-H Gel Formed From Anhydrous Carbonated β-C_2S and C_3S Powder, as a Function of Calcium Silicate Reacted

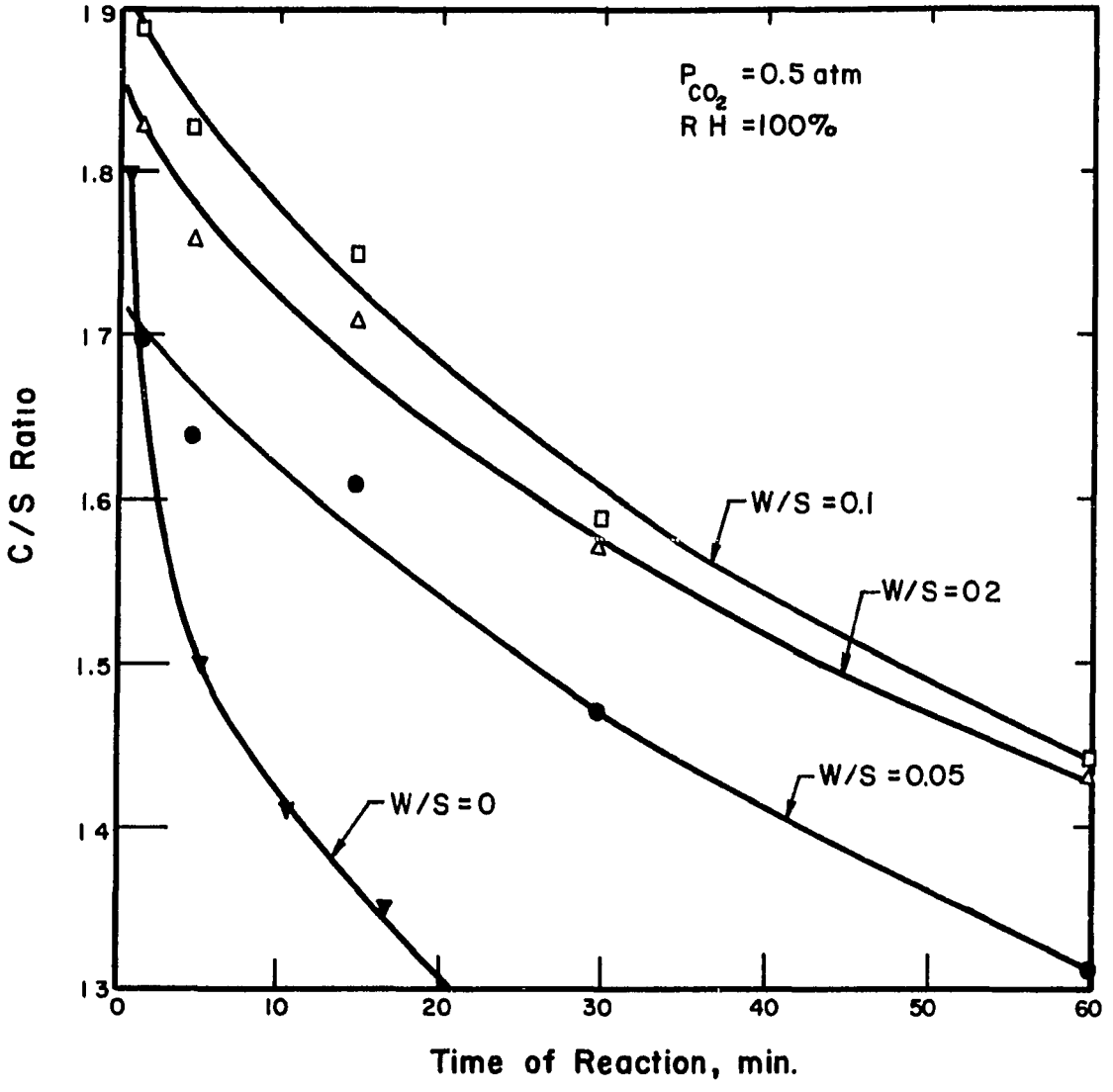

Figure 25. Variation of C/S Ratio of C-S-H Gel Formed During Carbonation of β-C_2S Powder

C. Properties of Reaction Products

1. Surface Area Determination

The surface area of the anhydrous calcium silicates used in this study ranged from 0.385-0.630 m^2/g. The reaction products (C-S-H gel and calcium carbonate) had surface areas which were much higher than the starting materials. Typical surface areas for carbonated calcium silicates ranged from 120-400 m^2/g (H_2O adsorption values), depending on the length of reaction. The surface area peaked at approximately 1 hour and was lower at shorter and longer reaction periods. Surface area was evaluated on the carbonated silicates using water and N_2 as adsorbents for the BET technique of surface area measurement. The N_2 adsorption values were in the range of 70-260 m^2/g for the same carbonated samples quoted for the water adsorption method. The surface area of the dry powders was more reproducible than the wetted powders. The surface areas of the carbonates (calcite and aragonite) were estimated from photomicrographs to be 4-20 m^2/g for the crystallites which could be resolved using a SEM. Some of the carbonate was intermediate in size compared to the gel and crystallite calcite or aragonite.

2. Morphology of Carbonated Calcium Silicates

Figure 26A&B shows the unreacted morphology of the β-C_2S and C_3S powders while Figure 26C&D shows the center and the edge of anhydrous pressed pellets which had been reacted only 1 hour. The unreacted β-C_2S (Figure 26A) had numerous small crystallites on the surface of the larger grains which were analyzed by x-ray diffraction (XRD) and x-ray fluorescence (XRF) and found to be β-C_2S. The C_3S (Figure 26B) powder had clean equiaxed grains. The center and the unreacted portion of the edge of the pellets showed no

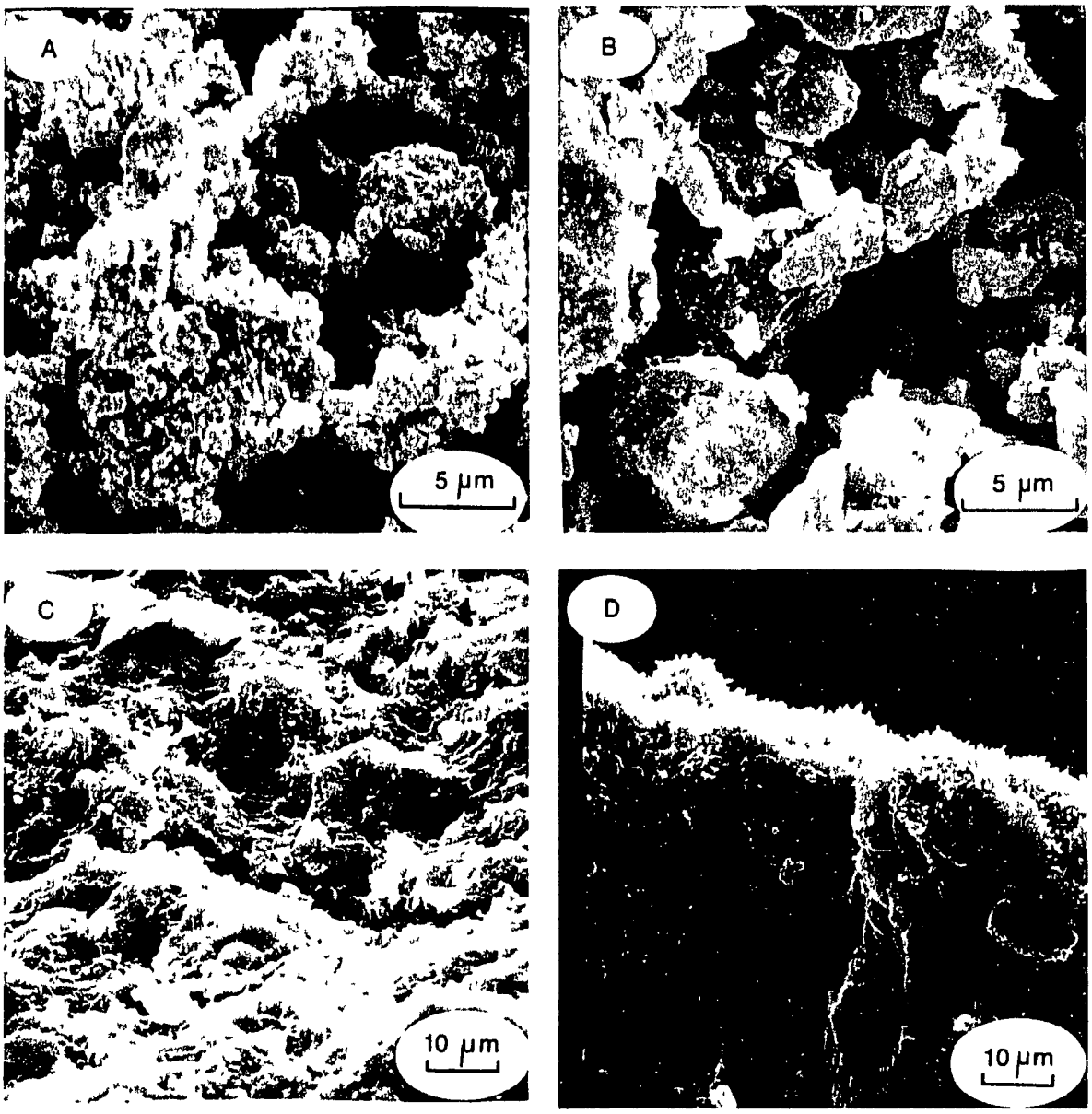

Figure 26. Characteristic Features of Unreacted β-C_2S and C_3S

A) Unreacted β-C_2S Powder
B) Unreacted C_3S Powder
C) Central Portion of Dry Pressed β-C_2S Pellet (Carbonated 15 minutes)
D) Edge of a Dry Pressed C_3S Pellet (Carbonated 15 minutes)

secondary phases. The reacted surface of the pellet was coated with fine aragonite crystals.

Figure 27 shows the typical microstructure of the dry calcium silicates after carbonation from the vapor phase. Normal reaction conditions were 100% $\overline{C}$ and 100% RH. Figure 27A&B shows the surface of a pellet which was covered with blocky aragonite crystals. This morphology was observed only in densely pressed C_3S pellets or wet or dry powder at very short reaction times. Figure 27C&D shows the more typical aragonite crystals which grow on loosely packed powders. The aragonite morphology is acicular and tends to form only as long as pore space exists. Both the blocky and lath-like morphologies were expected since aragonite is an orthorhomic crystal.

Figure 28 also shows morphologies for anhydrous calcium silicates which were carbonated. Figure 28A shows the reaction zone approximately 0.1 mm below the surface of the pellet. Note the cleaved silicate grain and the aragonite growing around the grain and the aragonite growing into pore space across the sample. Figure 28B shows the acicular habit of aragonite crystals growing over a large surface silicate grain. Figure 28C shows the unreacted surface and hair-like carbonate growing on a C_3S specimen reacted at 60°C for 3 days. Figure 28D shows the two forms of carbonate morphologies growing together. Both morphologies were determined by SRF, SRD and acid etching to be carbonates.

The morphologies observed when the calcium silicates which were reacted wet are collected in Figure 29. The predominant carbonate phase was calcite which commonly occurred as large rhombohedral crystals or very small, sharply defined crystallites on the surfaces of the silicate grains. Figure 29A&B shows the large calcite crystals on the surface of a C_3S pellet with

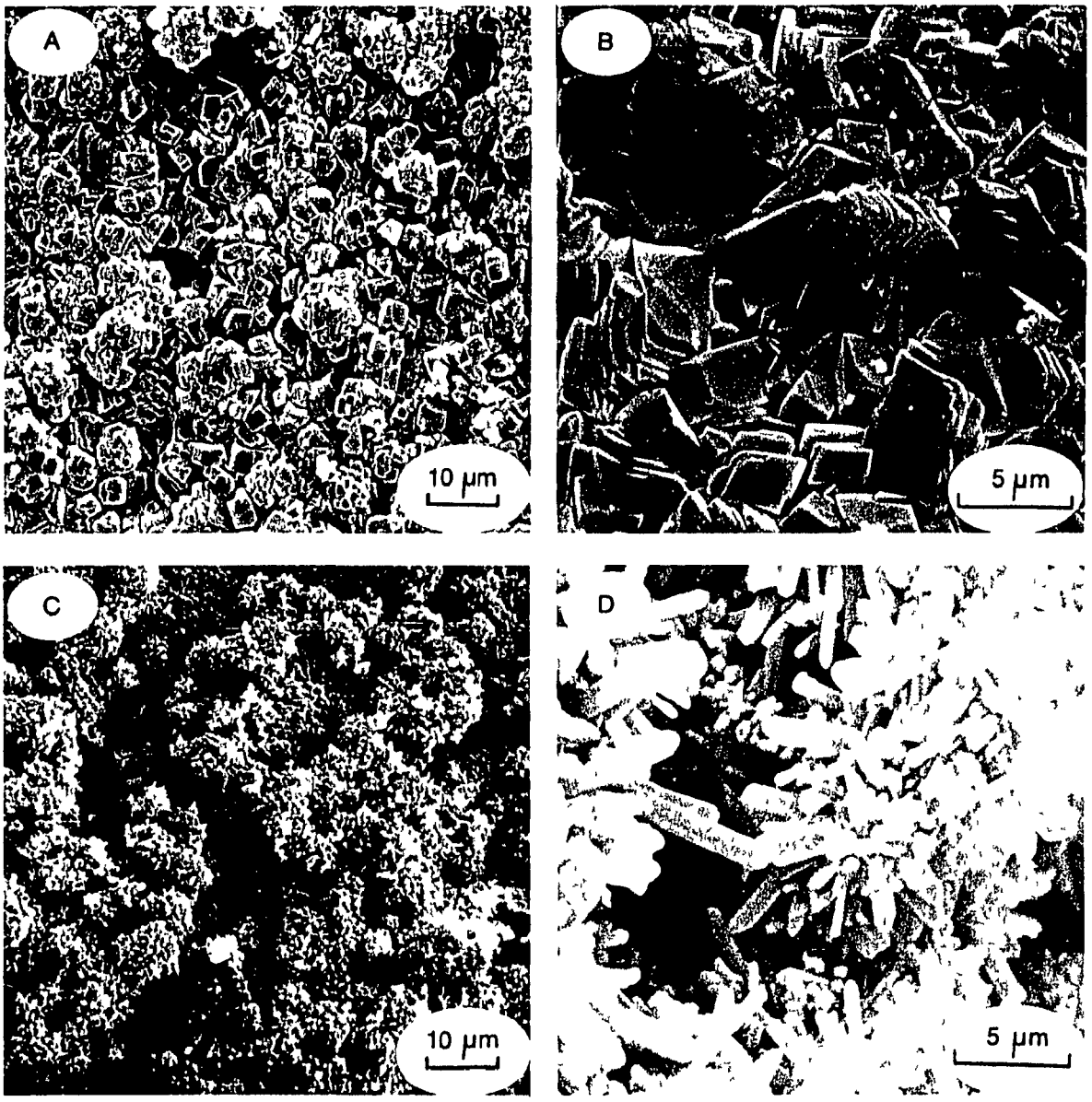

Figure 27. Characteristic Features of Carbonated Anhydrous β-C_2S and C_3S Powders

A) Pellet of β-C_2S Carbonated Dry 22 Days
B) Pellet of β-C_2S Carbonated Dry 22 Days
C) Powdered Sample of C_3S Carbonated Dry 3 Days at 60°C
D) Powdered Sample of C_3S Carbonated Dry 3 Days at 60°C

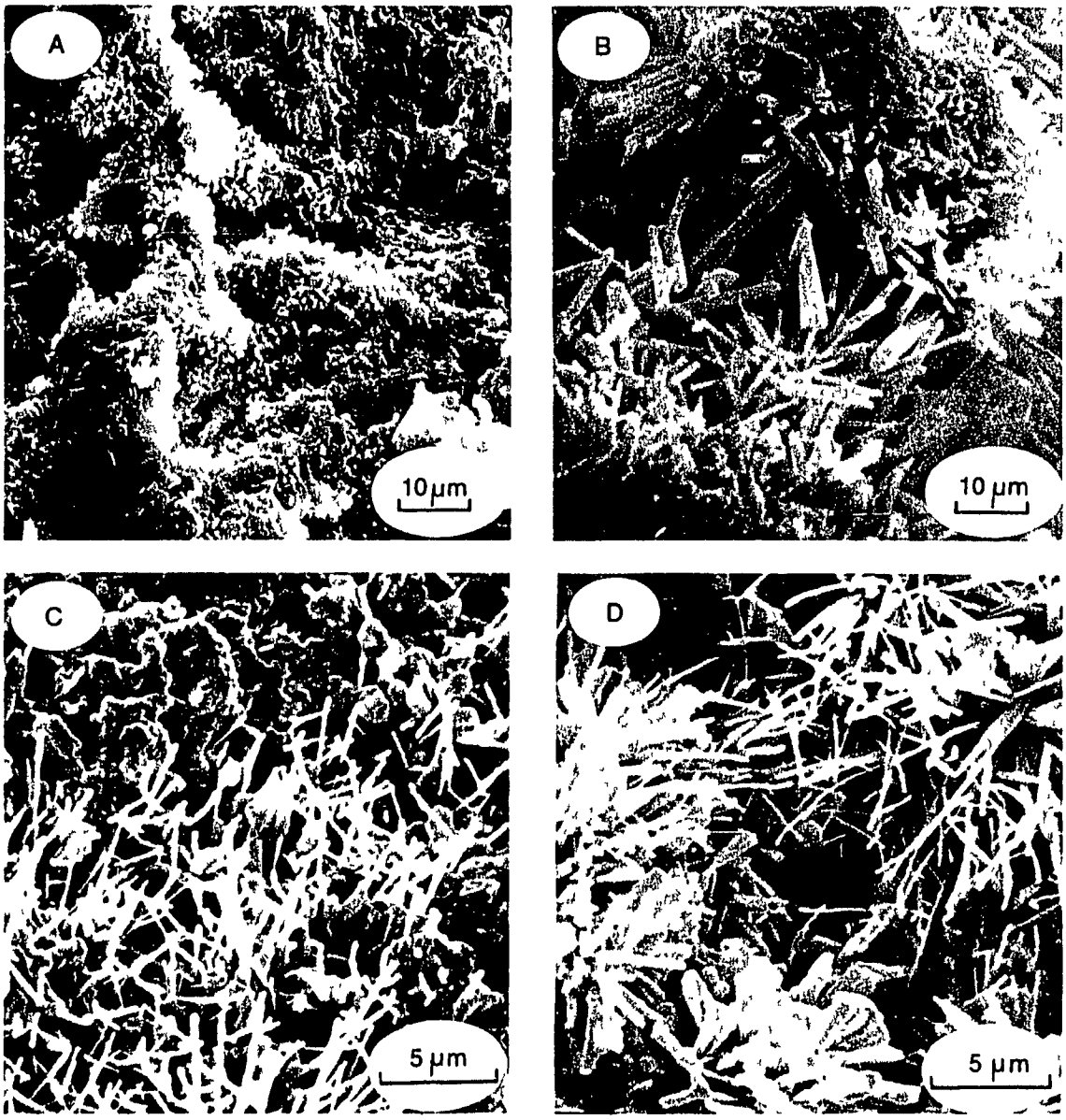

Figure 28. Characteristic Features of Carbonated Anhydrous β-C_2S and C_3S Powders

A) β-C_2S Pellet Carbonated 3 Days (Surface of Pellet at Extreme Right)
B) β-C_2S Pellet Carbonated 7 Days
C) C_3S Powder Carbonated 3 Days at 60°C
D) C_3S Powder Carbonated 3 Days at 60°C

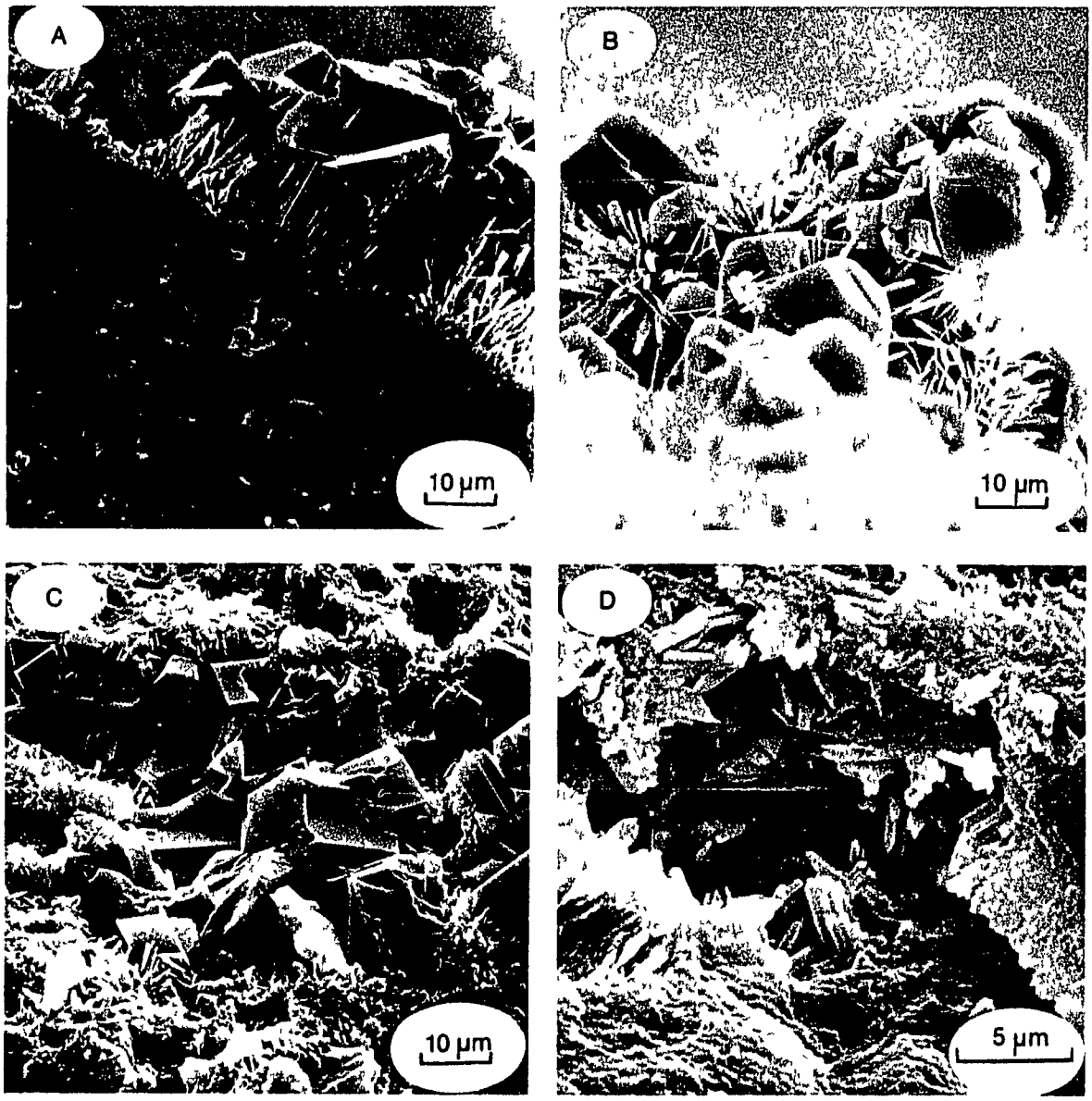

Figure 29. Characteristic Features of Carbonated Wetted β-C_2S and C_3S Pellets

A) C_3S Pellet 0.15 w/s, Carbonated 14 Days
B) C_3S Pellet 0.15 w/s, Carbonated 14 Days
C) C_3S Pellet 0.20 w/s, Carbonated 3 Days
D) β-C_2S Pellet 0.15 w/s, Carbonated 3 Days

{Surface Area} (Interior)

aragonite needles growing from the surface of the pellet and apparently from the immediate area of the calcite crystals. Figure 29C shows large calcite crystals and small aragonite crystals on another C_3S pellet while Figure 29D shows the area just below the surface of the same pellet and small aragonite crystals growing into the pore space. No apparent gel structure was evident for any of the powders or pellets of calcium silicate which were reacted dry or wet.

Other calcite morphologies that were observed on both β-C_2S and C_3S are shown in Figure 30. Crystallites of calcite at three magnifications were examined on a sample which had 100% calcite and no aragonite (Figure 30A-C); these powders were not allowed to dry during carbonation. Figure 30D shows massive calcite crystals formed by carbonating the β-C_2S in carbonated water; only the surface of the sample showed any signs of carbonation.

Figure 31 shows the difficulty in trying to identify the carbonate phases solely by microscopic examination. Figure 31A&B shows carbonated wet silicate powders which were analyzed to contain 100% calcite and were 80% reacted. Figure 31C&D shows similar micrographs, but in this case the carbonate was 50% calcite and 50% aragonite and the powder was 85% reacted. This sample had been allowed to dry partially during carbonation and the 50% aragonite formed during that period. Whichever form of carbonate nucleated initially predominated during the later stages of carbonation.

Figure 32 shows the interaction of the gel and the carbonates as binding phases for pelletized silicates used in this study. Figure 32A shows a typical powdered unetched carbonated sample with aragonite crystals on the surfaces of the silicate grains. After 3 minutes etching in 0.5 molar HCl, the carbonate dissolved leaving the highly polymerized, amorphous silica

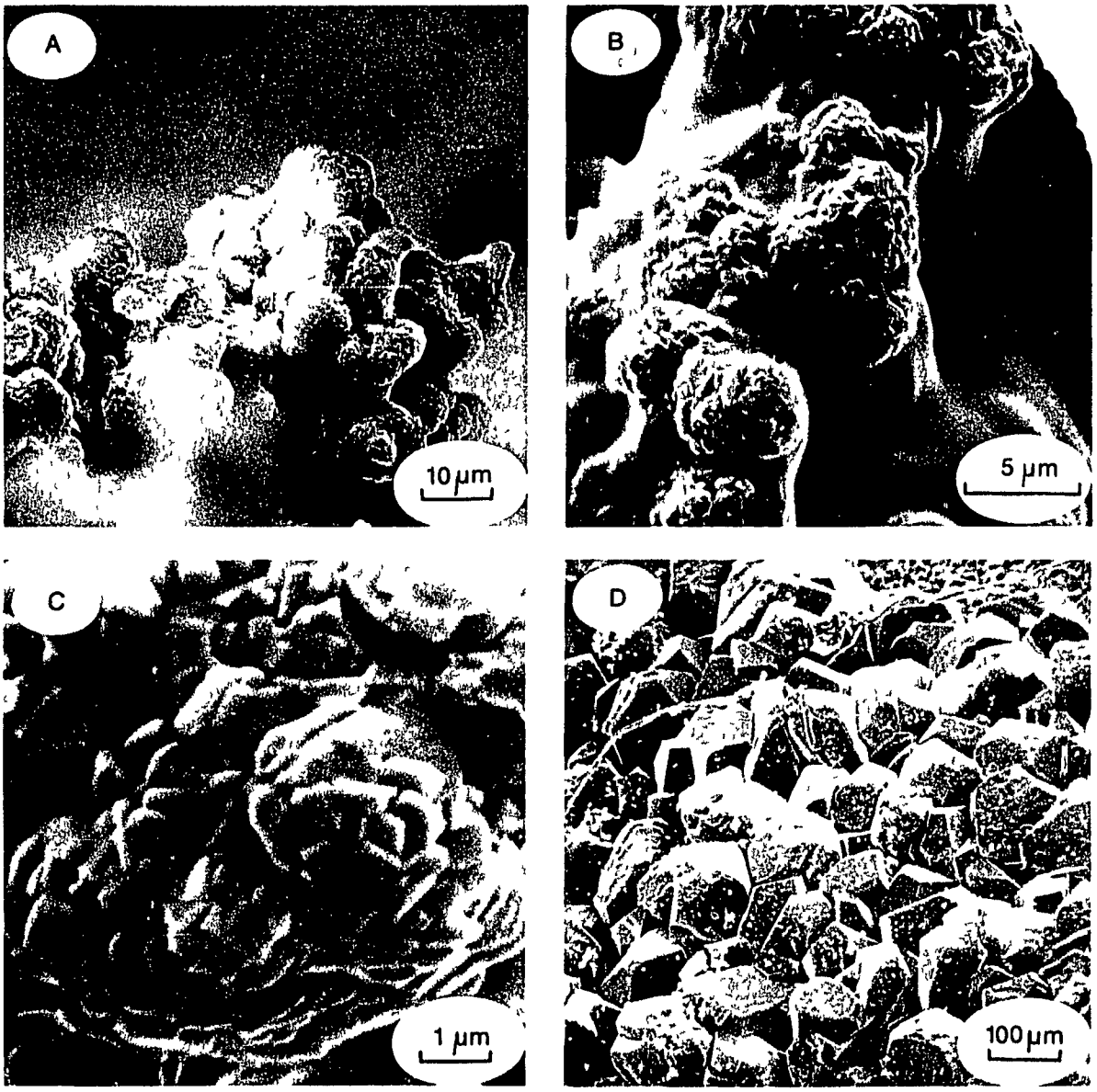

Figure 30. Characteristic Features of Carbonated Wetted β-C_2S and C_3S

A) C_3S 0.20 w/s, Carbonated 7 Days
B) C_3S 0.20 w/s, Carbonated 7 Days } Powders
C) C_3S 0.20 w/s, Carbonated 7 Days
D) β-C_2S Carbonated Under Water 21 Days (Pellet)

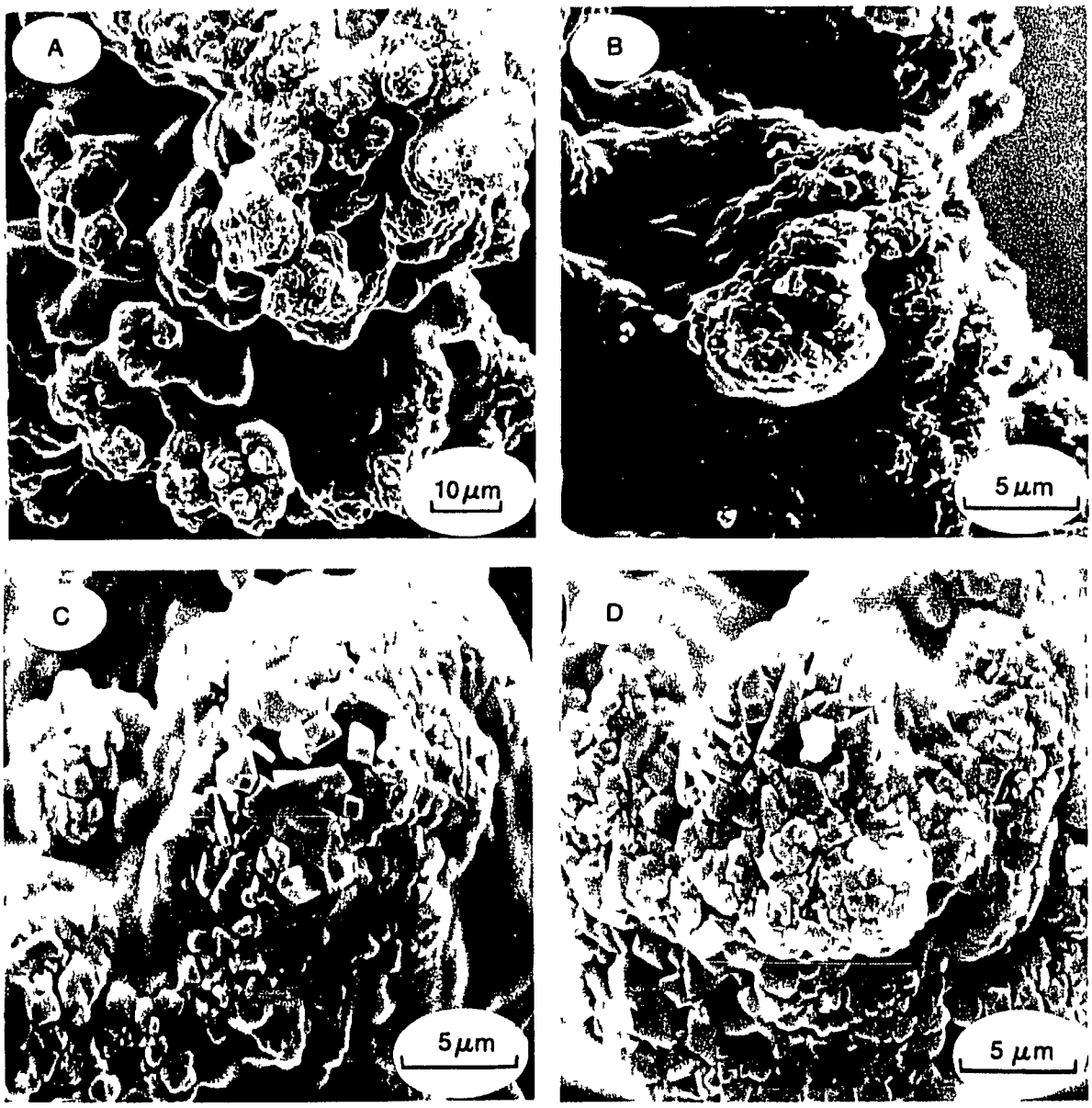

Figure 31. Similarity in Calcite and Aragonite Morphology Observed in Wetted Powders

A) β-C_2S 0.15 w/s, Carbonated 7 Days
B) C_3S 0.20 w/s, Carbonated 7 Days
C) β-C_2S 0.15 w/s, Carbonated 7 Days
D) C_3S 0.20 w/s, Carbonated 7 Days

Figure 32. Study of Carbonated Morphology Formed in Pellets Observed After Etching with HCl

A) β-C_2S Carbonated Unetched (Reacted 21 Days)
B) β-C_2S Carbonated Etched 3 Minutes 0.5 M HCl
C) β-C_2S Carbonated Etched 30 Minutes 0.5 M HCl
D) C_3S Carbonated Etched 30 Minutes 0.5 M HCl

residue. Figure 32B shows siliceous material around and possibly at the center of the grains. Figure 32C shows one large grain which was etched for 30 minutes and the siliceous residue has the same shape as the original grain. Finally, acid etching of carbonated C_3S revealed that the grains were not connected by a silica matrix, as was carbonated β-C_2S, but by a dissolvable carbonate matrix. Very thin silica shells, which are similar to those predicted in hydration theory of calcium silicates, were visible around each C_3S grain (Figure 32D).

D. Strength and Porosity

1. Specific Gravity

The specific gravities of the anhydrous calcium silicates were initially determined using water as the fluid. Calculated values were 3.260 ±0.011 g/cm^3 and 3.170 ±0.01 g/cm^3 for β-C_2S and C_3S, respectively, which compare favorably with data cited by Taylor, namely, 3.28 g/cm^3 and 3.15-3.25 g/cm^3 for β-C_2S and C_3S. A repeat determination using reagent grade benzene gave values of 3.20 and 3.10 g/cm^3 for β-C_2S and C_3S.

2. Strength Data

Figure 33a shows the compressive strength of calcium silicate pellets which were carbonated for 216 hours after being hydrated to 25% completion. The compressive strength on subsequent rehydration does not increase for the first 8-10 hours after which the strength increased 75-100 MPa (11-15 Ksi).

The compressive strength for hydrated calcium silicate pellets is shown in Figure 33b, as well as the time at which they attained 25 and 50% of complete hydration. C_3S reacted the fastest and β-C_2S the slowest while an

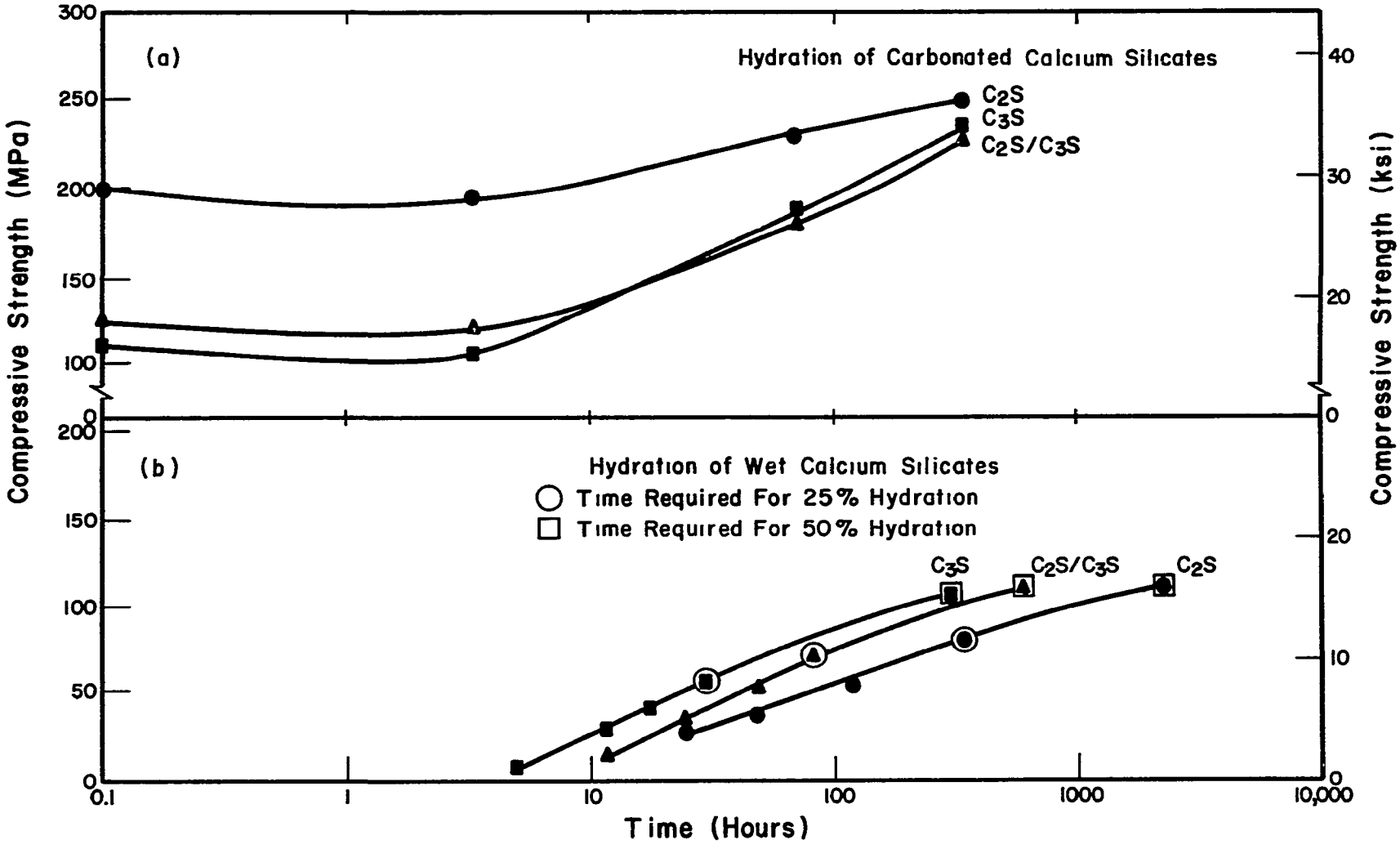

Figure 33(a). Compressive Strength of Carbonated Calcium Silicate Pellets Which Were Rehydrated

(b). Compressive Strength of Hydrating Calcium Silicate Pellets

equimolar mixture fell between the two extremes. The highest compressive strength was 110 MPa (16 Ksi) for all of the 50% hydrated silicates.

Figure 34 shows the compressive strength of calcium silicate pellets which have been subjected to varying degress of hydration ranging from 0-50% and then carbonated. In all cases the β-C_2S pellets were stronger than those of C_3S or the mixture and the apparent consistent trend in relative strength of the silicates was due to the relative porosities of the pellets. The 0% hydration pellets were reacted as dry pellets and had the highest initial porosity (49%) while the 50% hydrated samples had 36% porosity prior to carbonation. The rate of strength gain was quite rapid for the samples which had not been hydrated. The initial strength values for the pellets which had been hydrated 25 and 50% are the same data as those shown in Figure 33(b) for the hydrated samples. The strength gain for the hydrated samples was good (125-200 MPa) and the final compressive strengths were higher than the nonhydrated pellets. The maximum strength was 338 MPa (49 Ksi) for β-C_2S which was hydrated to 50% of completion and carbonated.

Figure 35a shows the diametral compression strength (split cylinder tension strength) for the calcium silicate samples which were hydrated after being carbonated. The relative strengths of all of the silicates when loaded in diametral compression were approximately 7-8 times lower than the straight compression values. The highest diametral strength was 50 MPa (7.3 Ksi) for β-C_2S.

The hydration strengths in the diametral mode were shown in Figure 35b and were consistent with the compressive strengths in Figure 34b. The highest diametral strength for the hydrated samples, 30 MPa (44 Ksi), occurred

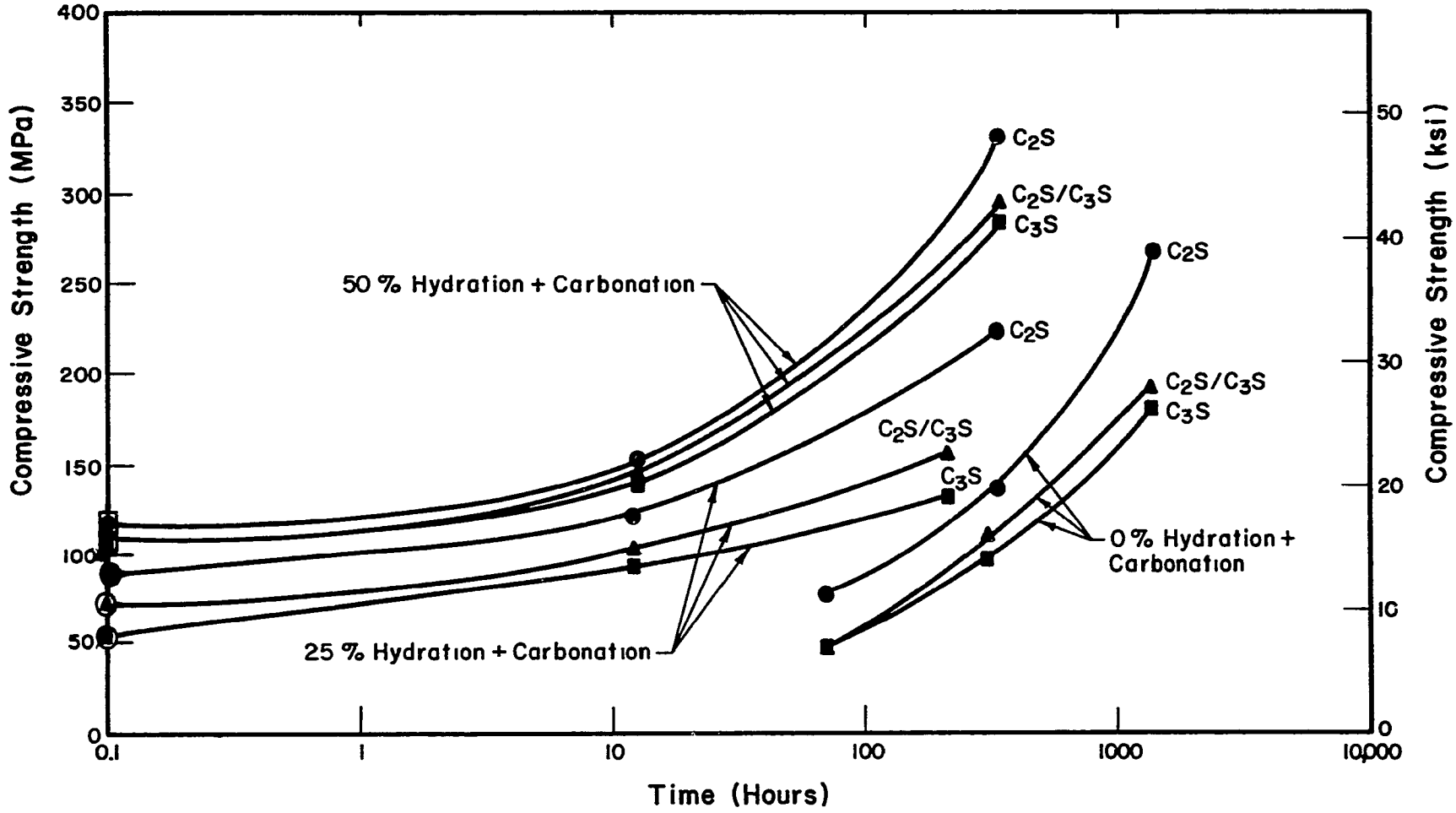

Figure 34. Effect of the Degree of Hydration on the Compressive Strength of Calcium Silicate Pellets

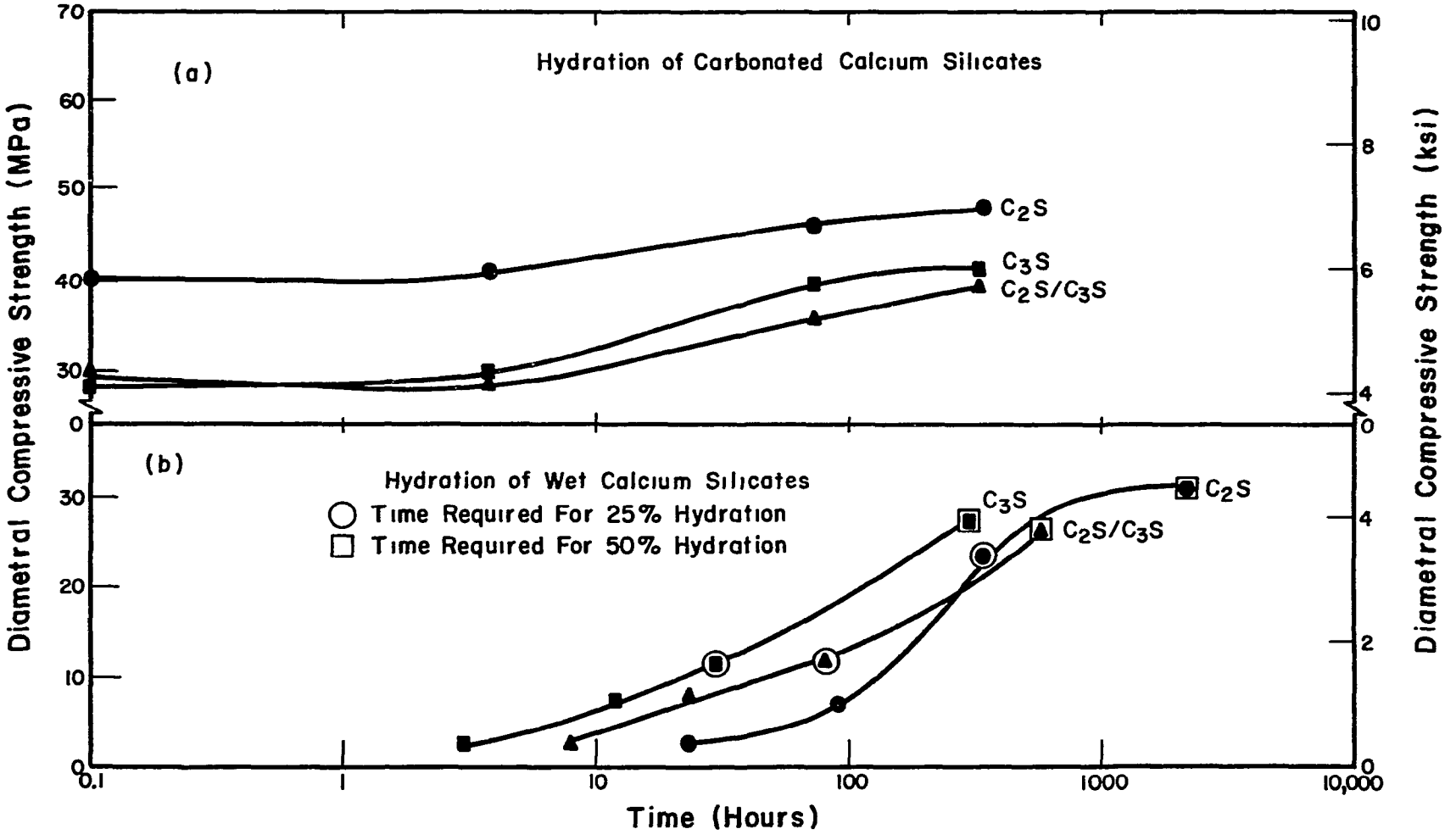

Figure 35(a). Diametral Compressive Strength of Carbonated Calcium Silicate Pellets Which Were Rehydrated
(b). Diametral Compressive Strength of Hydrating Calcium Silicate Pellets

for β-C_2S pellets which were hydrated 50%, then carbonated.

Figure 36 shows the diametral compressive strength for the three silicate systems discussed previously. The highest diametral strength occurred on 50% hydrated samples which had been carbonated and the value was 53 MPa (7.6 Ksi).

3. Porosity

Figure 37 shows the effect of porosity on the compressive strength of pressed calcium silicate pellets. The type of silicate or the reaction condition affect the final strength by controlling the manner in which the porosity is filled. An exponentially decreasing model for strength vs. porosity was curve fit and the regression coefficient was 0.98. At 0% porosity the theoretical strength was 566 MPa (83 Ksi).

The degree of reaction was found to have a linear dependency with porosity as is shown in Figure 38. The linear regression coefficient for the linear model was 0.86. The theoretical percent reacted for the carbonated calcium silicate predicted by this model was 92.4% reacted at 0% porosity. Both hydrated and carbonated samples were plotted on this figure and the porosity of the calcium silicate was a major factor in compressive strength. Figures 39a&b show the effect of porosity and degree of reaction on the diametral strength of hydrated samples and carbonated samples. The trends were the same as for the compression specimens, but the exponential dependency of diametral compression had different curve fitting constants. The same was true for the linear dependency of the degree of reaction vs. porosity for the diametral compression specimens.

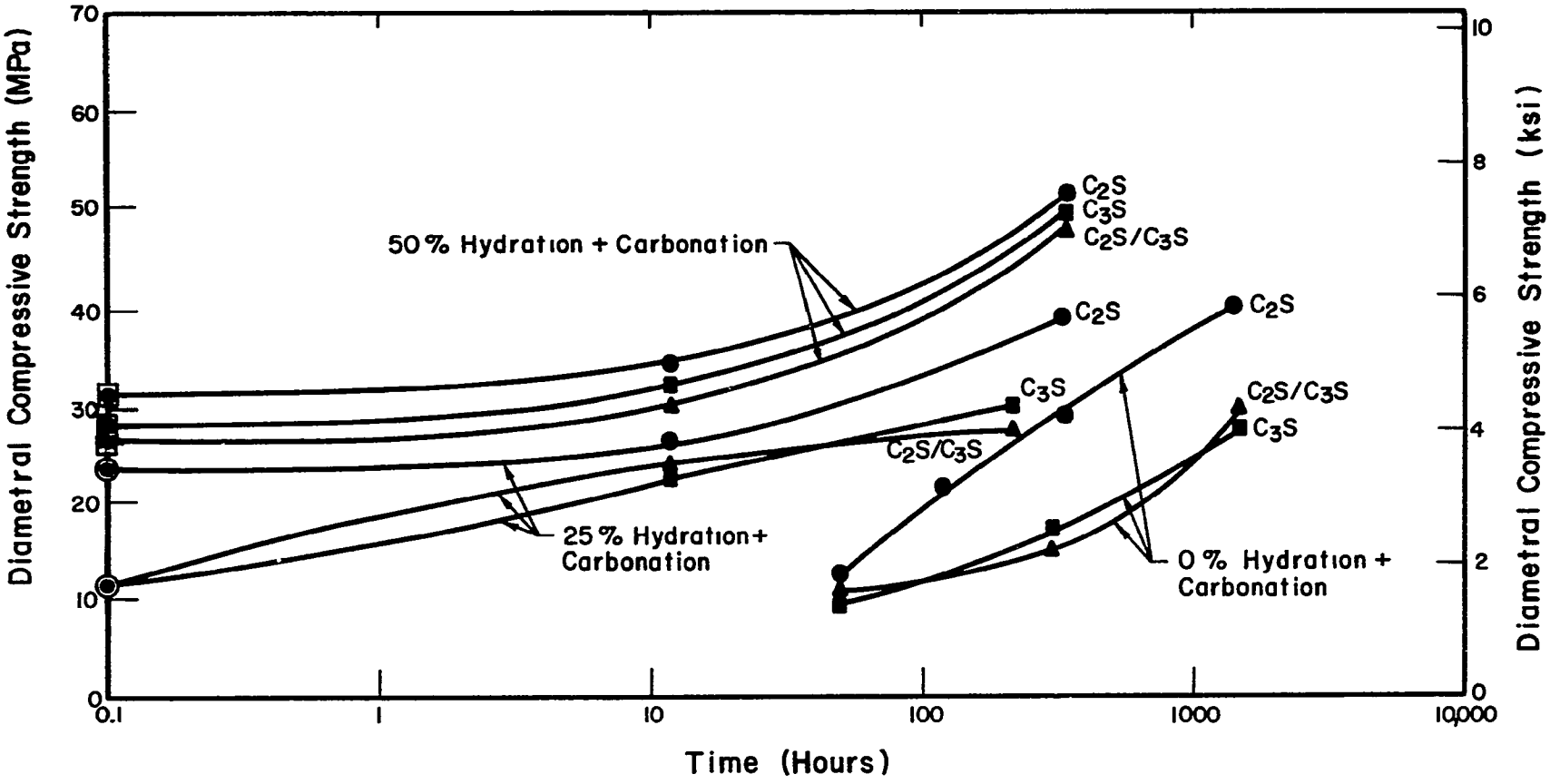

Figure 36. Effect of Degree of Hydration on the Compressive Strength of Carbonated Calcium Silicate Pellets

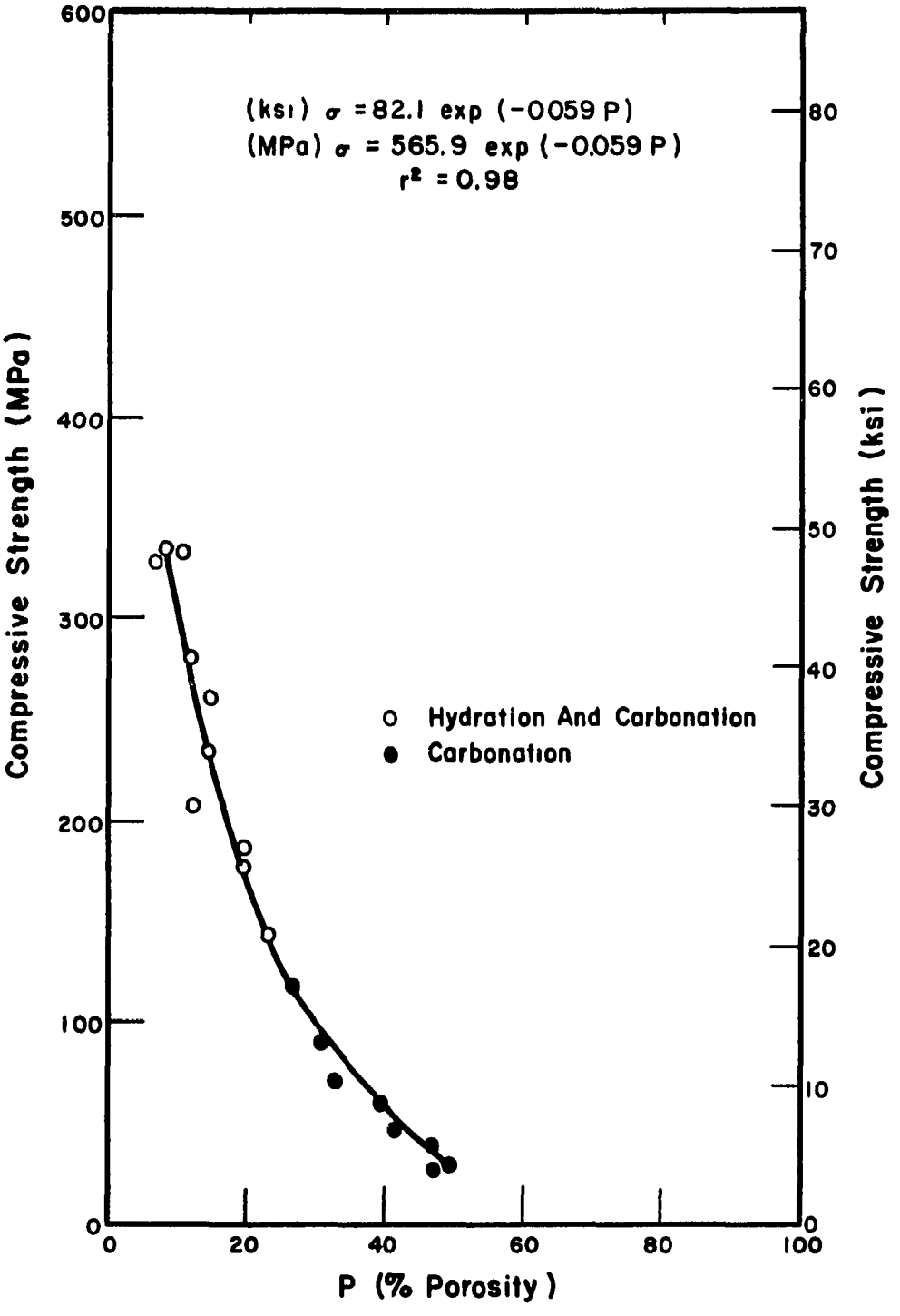

Figure 37. Effect of Porosity on Compressive Strength of Carbonated Calcium Silicate Pellets

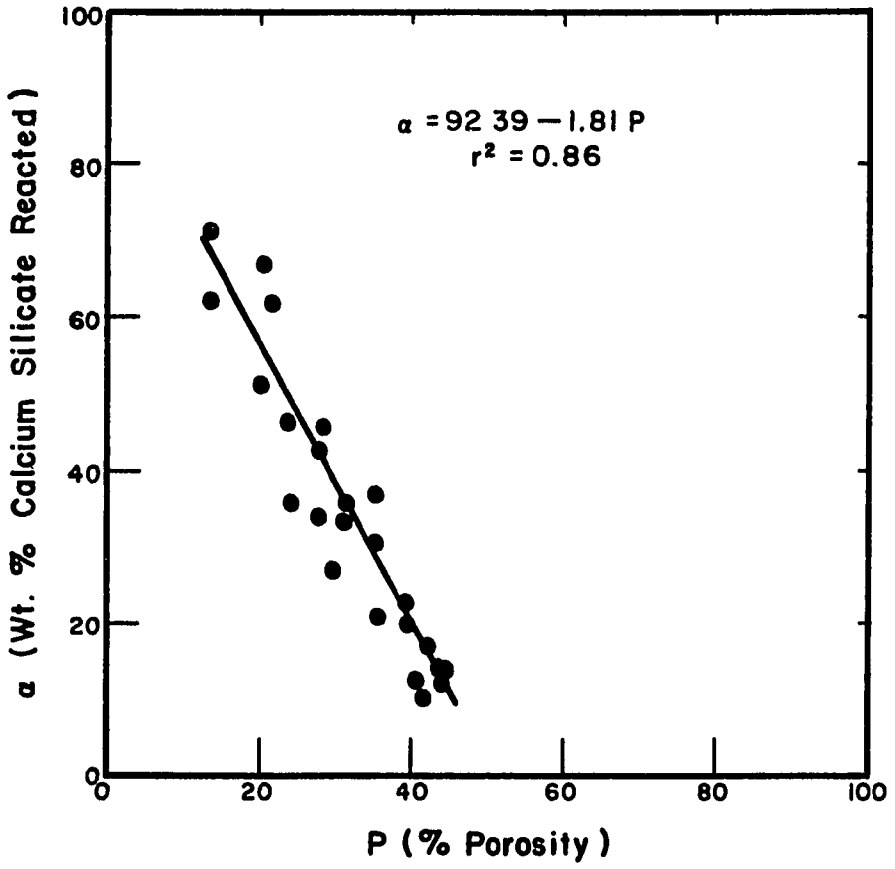

Figure 38. Effect of Degree of Reaction on Porosity of Carbonated Calcium Silicate Pellets

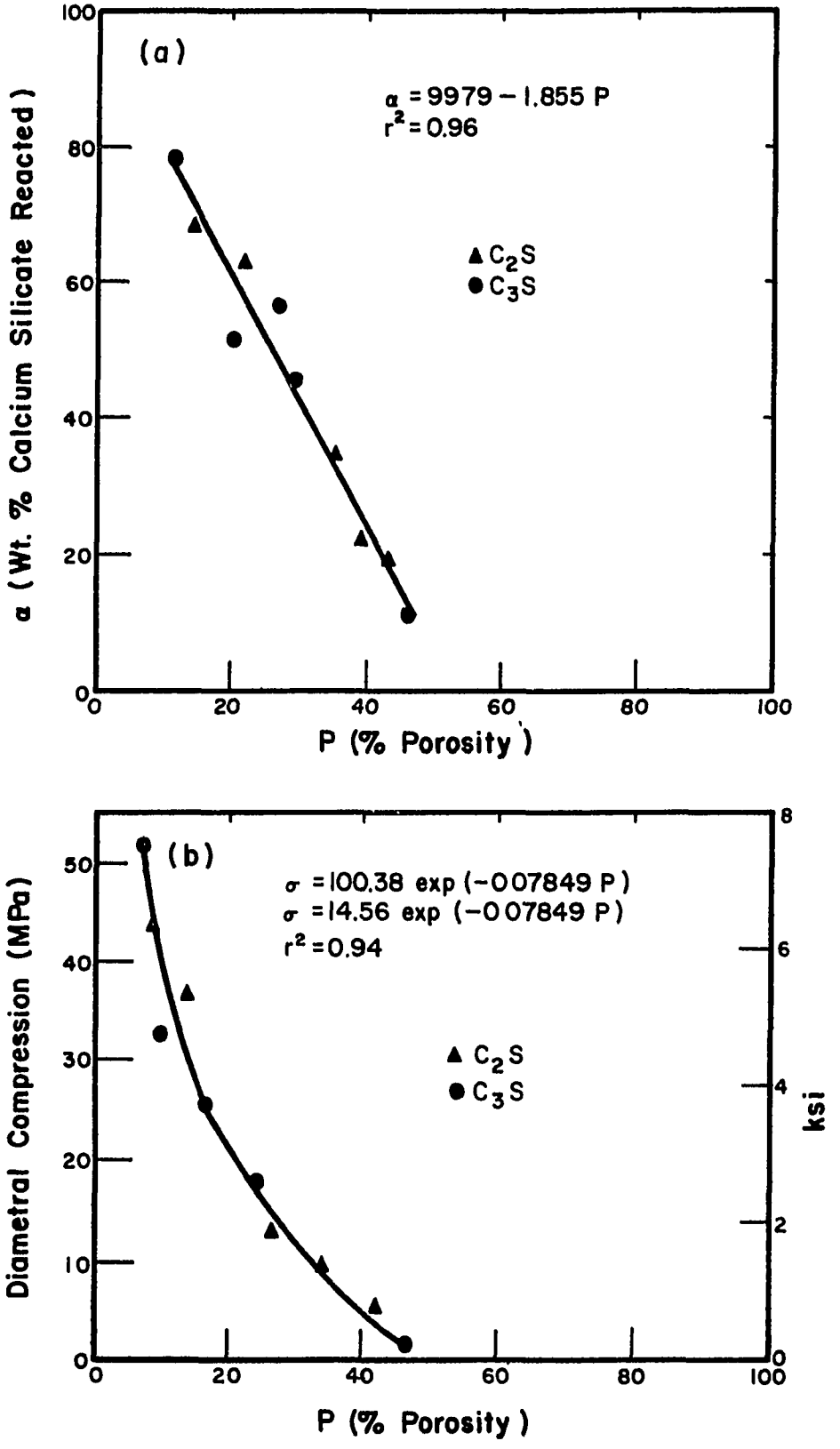

Figure 39(a). Effect of Porosity on Diametral Compressive Strength of Carbonated Calcium Silicate Pellets

(b). Effect of Degree of Reaction on Porosity of Carbonated Calcium Silicate Pellets

IV. DISCUSSION OF RESULTS

A. Experimental Methods

1. QXDA Methods

QXDA is the central analytical technique for determining the degree of carbonation of calcium silicates and the internal and external standard methods are compared in the following discussion.

a. QXDA Internal Standard Method

The amount of unreacted β-C_2S or C_3S and the amount of calcium carbonate formed during the carbonation process, were determined using TiO_2 (anatase) as an internal standard for the QXDA method. Anatase has a strong diffraction peak at 3.51 Å and that peak does not interfere with the major silicate or carbonate peaks, with the exception of vaterite, which was not detected in the reacted calcium silicates. The greatest problems in using an internal standard were determining the proper amount of standard and assuring thorough mixing of the standard and the dried, ground reacted calcium silicates. The QXDA runs were conducted using the highest intensity Cu K_α tube available during the period of this research which was a fine focus tube capable of operating at 36 Kv, 14 ma. The average area under each diffraction peak corresponded to 20,000-32,000 counts per peak which allowed a precision of 1.5-2.0% due strictly to counting statistics.[92,93] The comparison of the ratio of the area of the silicate peak to the carbonate peak also involved errors in setting integration limits and rejecting slight overlapping of nearby peaks so that the total precision of the QXDA method was no better than ±2.5 wt.%

The very early degrees of reaction were directly checked against unreacted

calcium silicates with anatase added since the ratio of the silicate and the carbonate peaks was relatively insensitive at low reaction times. Additionally, the early stages of carbonation form amorphous material (C-S-H gel, carbonate, and S-H gel) which cannot be detected by the QXDA method due to their poor crystallinity. The internal standard method worked the best for degrees of reaction ranging from 10-90 wt.% calcium silicate.

b. QXDA External Standard Method

The calibration curves for the external standard method were derived from the internal calibration runs. Both calcium silicate and carbonate were mixed with a constant amount of anatase and the relative areas of the silicate and the carbonate form a ratio which was related to the weight % calcium silicate remaining in the carbonated sample. This method is accurate from 15-75 wt.% of the reacted silicate because the silicate/carbonate ratio is quite sensitive to the degree of reaction. At low degrees of reaction the ratio changes very little while at high degrees of reaction the ratio changes very rapidly. Consequently, the precision of the external standard method is lower than the internal standard method. Again early reactions were compared directly to standard calcium silicates to determine the degree of reaction and the final stages of carbonation were determined by comparing the external standard data to the amount of carbonate formed which was directly related to the degree of calcium silicate reaction. The external standard method allowed samples to be studied while they were carbonating without destroying the surface morphology and allowed the examination of the crystalline phases and the determination of their relative amounts as a function of position for carbonated powders and pellets. The relative precision for the external standard QXDA method was ±5 wt.% and the

smallest area which could be examined was a spot 1 mm in diameter.

2. Mass Spectrometer-Thermogravimetric Analysis (MS-TGA)

The MS-TGA runs determined the identity and the relative amounts of materials which were evolved during heating carbonated or hydrated calcium silicates. Figure 22a shows the MS results which indicate that the water content decreased during continued carbonation and that the water evolved by hydration products would interfere with carbonate decomposition products. The $\overline{C}$ peaks increased in area and shifted to higher temperatures as the degree of carbonation increased. The shift to higher temperatures was a direct result of increased crystallinity which was verified by decreased surface area for the carbonate and increased crystal size as observed by SEM analysis. The TGA data (Figure 22b) indicated the relative weight losses with temperature and the weight losses due to water or carbon dioxide when used with the MS data.

B. Kinetics and Mechanisms of Carbonation

1. Dry Calcium Silicate Powders

a. Kinetic Model for Dry Carbonation

The degree of reaction data shown in Figures 6-9 were plotted as $\log \left[1-(1-\alpha)^{1/3}\right]^2$ versus log t according to eq. 12 and are presented in Figure 40. The plot shows a family of curves which are linear and have slopes of approximately 1.0. A slope of 1.0 would give a perfect fit to the kinetic model described in eq. 12 and the actual slopes ranged from 0.965 - 1.024. The carbonation model describes a reaction which is controlled by the rate at which volume is diminished and the reaction rate is controlled by a diffusion zone thus giving the model an exponential dependency of 3/2 with respect to

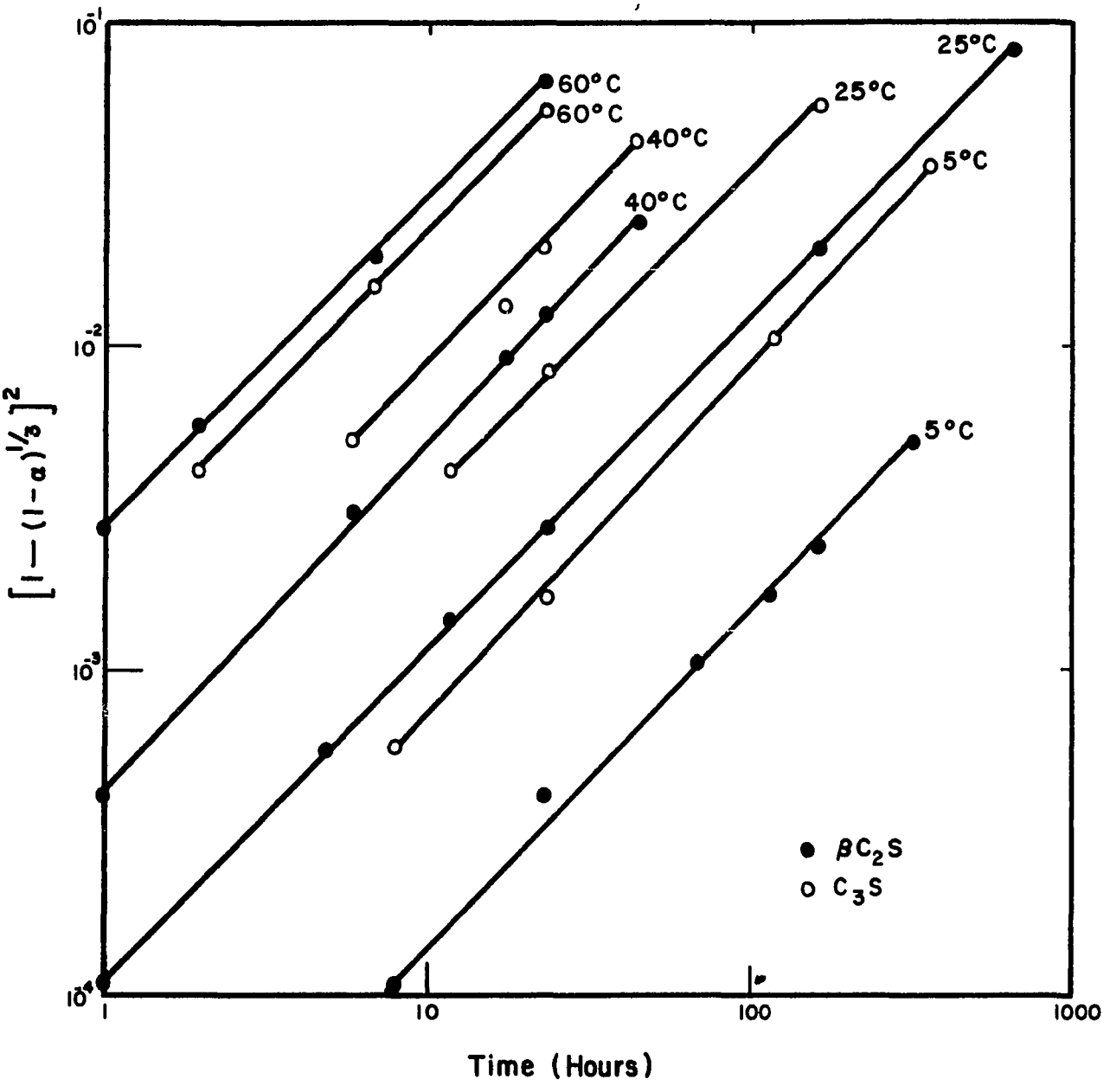

Figure 40. Diffusion Controlled-Decreasing Volume Kinetic Model for Carbonated Anhydrous β-C_2S and C_3S Powders

the degree of reaction (α). The slopes of the lines in Figure 40 equal the apparent rate constant (K_T') which equals KD/r_o^2. The true rate constant (K) and the diffusion coefficient (D) cannot be separated from K_T', and r_o^2 only affects K_T' as a constant for each fineness of the calcium silicate which was carbonated.

An Arrhenius plot (log K_T' versus 1/T(°K)) was plotted for each silicate to obtain the carbonation activation energy for β-C_2S (Figure 41) and C_3S (Figure 42) for a series of powder finenesses. Figure 41 is a family of parallel lines which give activation energies of 16.9 Kcal/mole for carbonation of dry β-C_2S powder. All of the finenesses tested had the same activation energy within the experimental accuracy of the determination. The higher surface area material 6300 cm^2/g reacted faster than the coarser powdered β-C_2S. Figure 42 shows similar results for C_3S except that C_3S reacted faster than β-C_2S and the K_T' values were higher for C_3S for corresponding finenesses and temperatures. The activation energy for the carbonation of dry powdered C_3S was 9.8 Kcal/mole.

The effect of surface area of the dry powdered calcium silicates is shown in Figures 43 and 44 which demonstrate the functionality of the apparent rate constant (K_T') and surface area (A). Both β-C_2S and C_3S showed that K_T' was a function of A^2 which was not unexpected. The following derivation shows the A^2 dependency of K_T'.

$$K_T' = KD/r_o^2 \tag{43}$$

$$\frac{V_o = 4/3\pi r_o^3}{A_o = 4\pi r_o^2} = \frac{r_o}{3} \tag{44}$$

$$\left(\frac{V_o}{A_o}\right)^2 = \frac{r_o^2}{9} \tag{45}$$

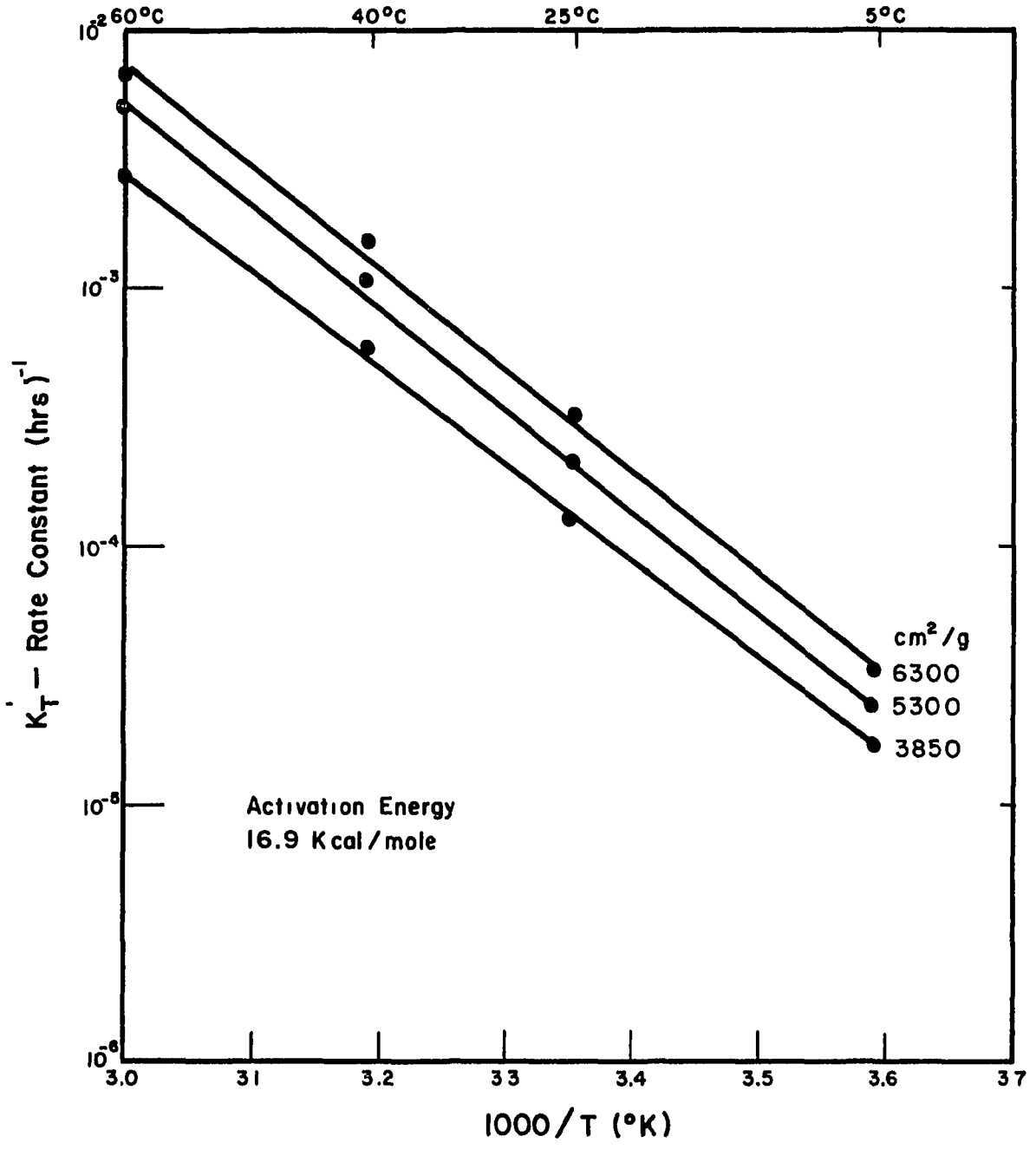

Figure 41. Arrhenius Plot for Carbonated Anhydrous β-C_2S Powders

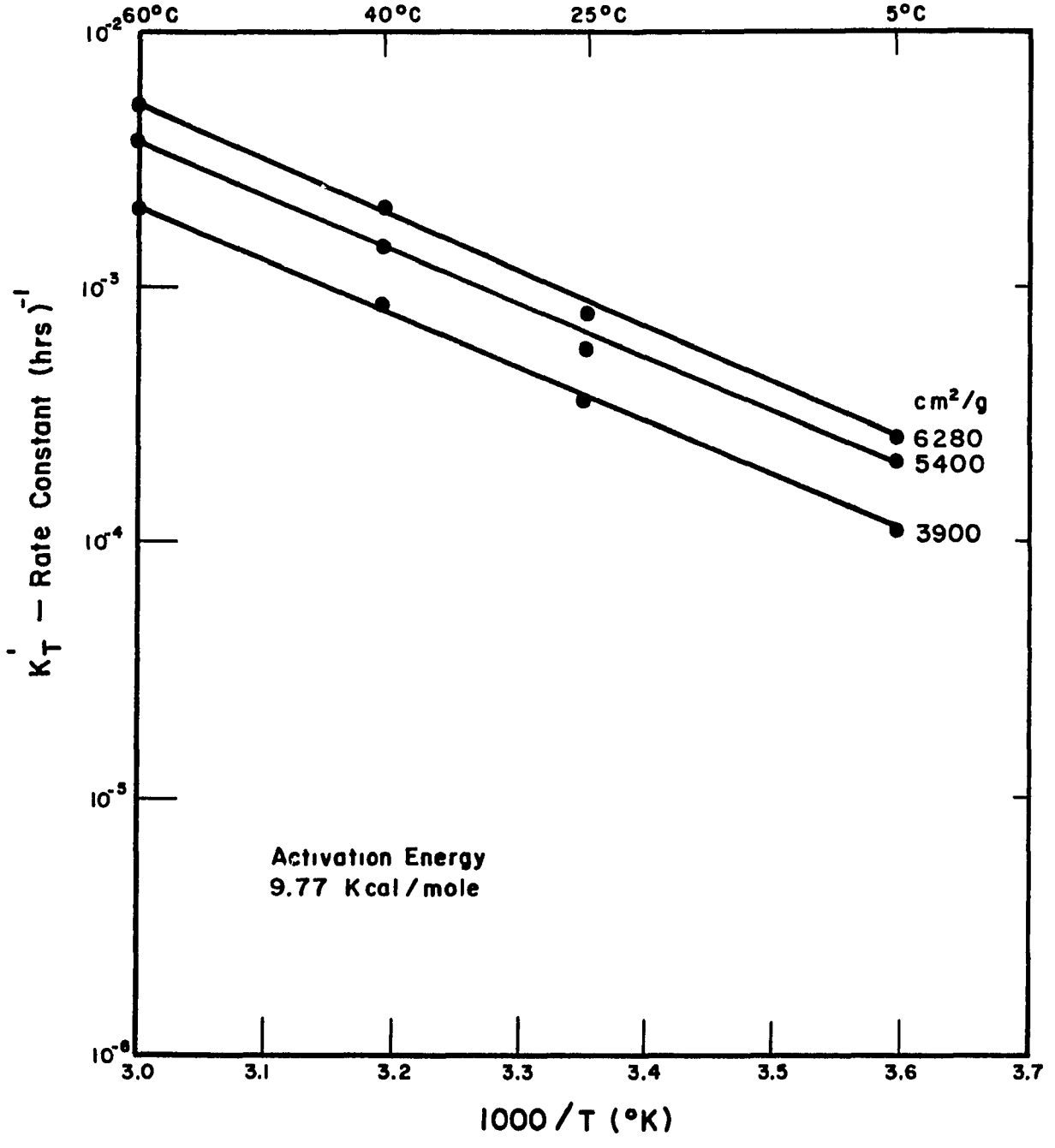

Figure 42. Arrhenius Plot for Carbonated Anhydrous C_3S Powders

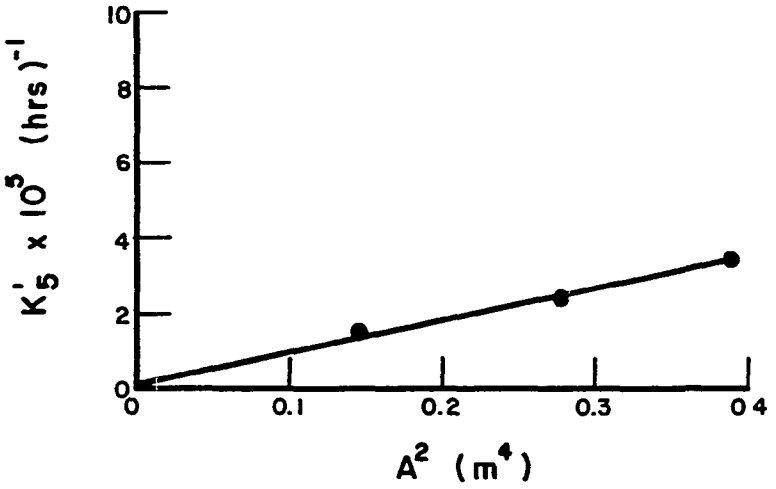

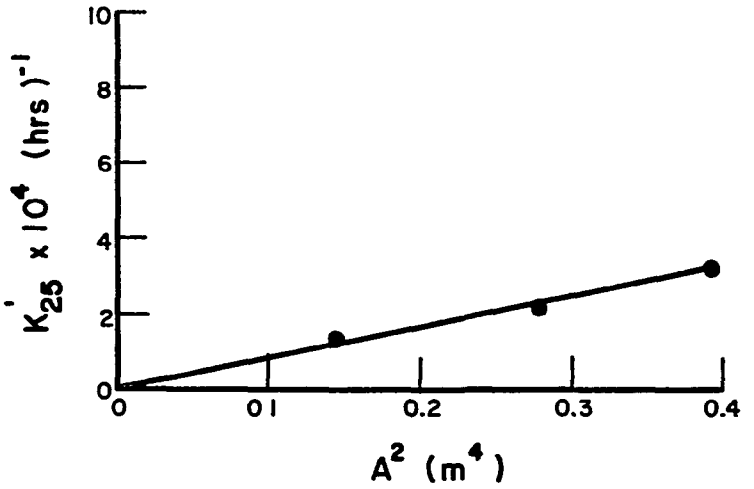

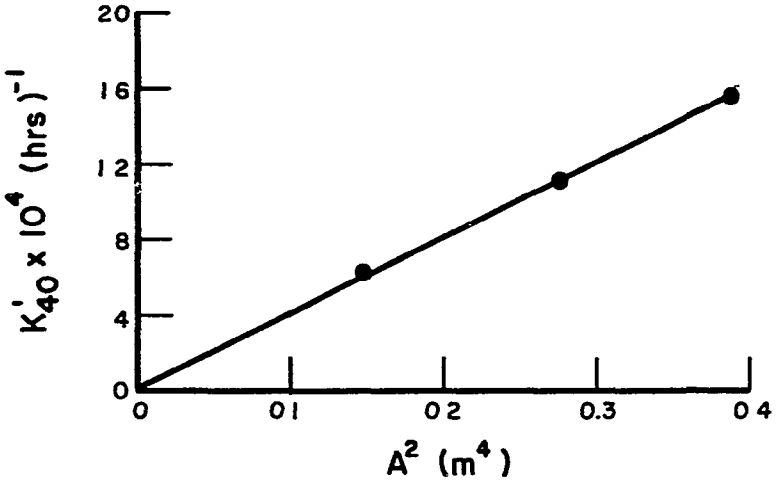

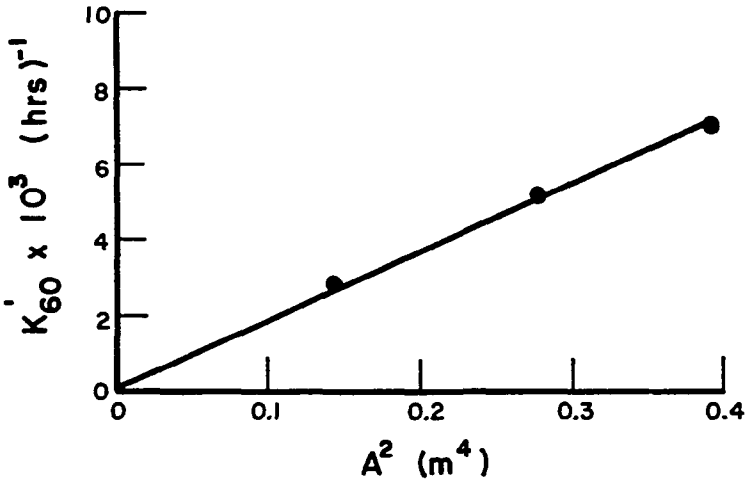

Figure 43. Effect of Surface Area on Carbonation Rate Constants for Powdered β-C_2S

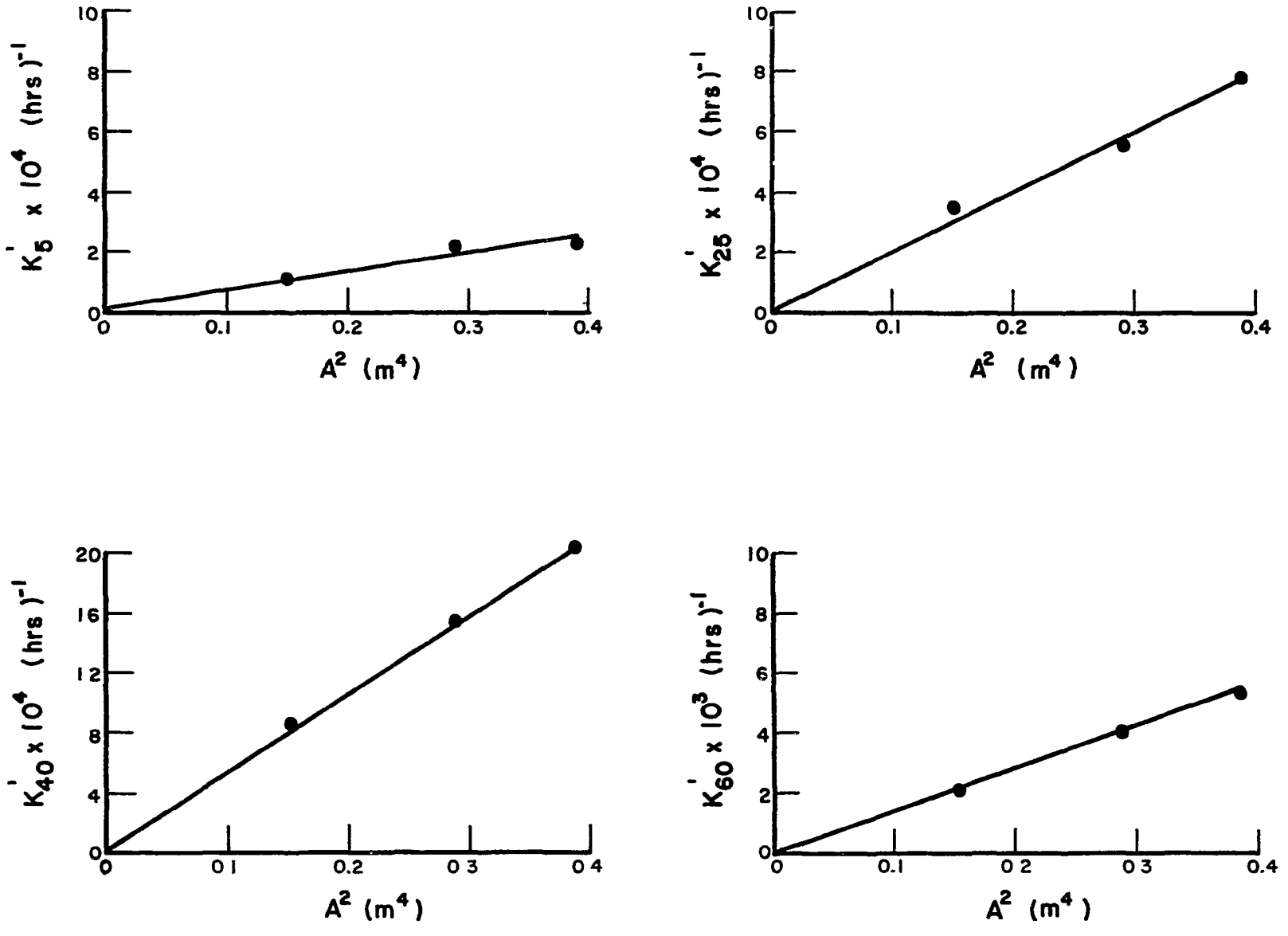

Figure 44. Effect of Surface Area on Carbonation Rate Constants for Powdered C_3S

Inverting and setting $V_o = 1$ since the volume of the particles is conserved:

$$K_T' = \frac{A^2 KD}{9} \tag{46}$$

The term KD/9 is a constant for the calcium silicate which is reacting. The pre-exponential term, K_o, and K_T' can be determined by calculation from equation 47.

$$K_o = \frac{K_T' \text{ (experimental)}}{\exp(-E_a/RT)} \tag{47}$$

Then the K_T' value can be determined for temperatures of interest by substituting K_o into equation 48 (the Arrhenius equation).

$$K_T' = K_o \exp(-E_a/RT) \tag{48}$$

also

$$K_o' = K_o/A_o^2 \tag{49}$$

where A_o = standard specific surface area.

Thus eq. 12 can be recast to contain K_o, E_a, A and T:

$$\alpha = 1 - \left[1 - \sqrt{K_o' \exp(-E_a/RT) A^2 t}\right]^3 \tag{50}$$

where R = 1.987 cal/mole°K

T = temperature (°K)

t = time (hours)

K_o' = 2.389×10^9 (β-C_2S) and 3.439×10^4 (C_3S)

E_a = 16.9 Kcal/mole (β-C_2S) and 9.8 Kcal/mole (C_3S)

A^2 = surface area (m^2/g)

α = wt.% calcium silicate reacted.

With eq. 50 the degree of reaction can be determined by evaluating K_o and E_a then introducing reaction times (t). The calculated degrees of reaction were within 3 wt.% of the experimental values for β-C_2S and C_3S powders. E_a is the energy needed to start the carbonation reaction while ΔH_f° is the energy difference from the initial to the final state. The rate constant for the carbonation reaction can be expressed by:

$$K_T' = \frac{kT}{h} \exp\ (\Delta S^\ddagger/R)\ \exp\ (-\Delta H^\ddagger/RT) \tag{51}$$

where $k = 1.38 \times 10^{-23}$ J/°K (Boltzmann's constant)

T = temperature (°K)

$h = 6.63 \times 10^{-34}$ J-sec (Planck's constant)

$\Delta S^\ddagger$ = activation entropy (cal/mole-°K)

$R = 1.987$ cal/mole-°K

E_a = activation energy (cal/mole)

$K_T' = \text{sec}^{-1}$

Equation 51 has the same form as eq. 48 except that

$$K_o = \frac{kT}{h} \exp\ (\Delta S^\ddagger/R) \tag{52}$$

K_o is known from eq. 47 and $\Delta S^\ddagger$ can be calculated.

$$\Delta S^\ddagger = R \ln\left(\frac{K_T' h}{kT}\right) + \frac{\Delta H^\ddagger}{T} \tag{53}$$

Assuming constant temperature and pressure

$$E_a = \Delta H^\ddagger + RT \tag{54}$$

$$\Delta G^\ddagger = \Delta H^\ddagger - T\Delta S^\ddagger \tag{55}$$

Therefore $\Delta G^{\ddagger}$, Gibbs Free energy of activation, can also be calculated

$$\Delta G^{\ddagger} = \Delta E_a - T\Delta S^{\ddagger} - RT \tag{56}$$

The enthalpy of formation (ΔH_f) for the carbonate reaction was calculated to be -44 and -83 Kcal/mole for β-C_2S and C_3S, respectively, while E_a was experimentally determined to be 16.9 and 9.8 Kcal/mole for β-C_2S and C_3S. The ΔH_f's for carbonation of β-C_2S and C_3S were calculated from thermodynamic tables using the following equations:

$$\Delta H_{f\beta\text{-}C_2S} = \Delta H_f(S\text{-}H) + 2\Delta H_f(C\bar{C}) - \Delta H_f(C_2S) - 2\Delta H_f(\bar{C}) - \Delta H_f(H) \tag{57}$$

$$\Delta H_{fC_3S} = \Delta H_f(S\text{-}H) + 3\Delta H_f(C\bar{C}) - \Delta H_f(C_3S) - 3\Delta H_f(\bar{C}) - \Delta H_f(H) \tag{58}$$

E_a was determined from the slopes of Figures 41 and 42 using the following equation:

$$E_a = (2.303)(1.987 \text{ cal/mole}) \frac{\Delta \log K_T'}{\Delta\, 1/T} \tag{59}$$

b. Effect of RH and $P_{\bar{C}}$ on Anhydrous Calcium Silicates

The relative humidity (RH) of the gas above the carbonating dry calcium silicates affects the degree of carbonation because the water vapor in the air is the sole source of water. Most of the data evolved during this study on dry silicates was taken from samples which were subjected to 100% RH. A separate study showed that the degree of reaction decreased as the %RH was lowered and that the relationship was approximately linear over specific RH ranges as shown by Figure 20. The behavior of the dry silicates was fitted to linear equations described by equation 60 and the pertinent coefficients are listed in Table 5.

$$\alpha_{RH} = (\underset{\text{from eq. 43}}{\alpha})((M \times \%RH) + C) \qquad (60)$$

Table 5

The Effect of RH on the Degree of Reaction of Anhydrous Calcium Silicates

	M	C	Range of RH
C_2S	2.6×10^{-3}	0	(0-100)
C_3S	3.63×10^{-3}	0	(0-80)
	0	0.29	(80-100)

Equation 60 describes the degree of reaction of anhydrous calcium silicate powders which were reacted at less than 100% RH. The C_3S required two straight line segments to describe the effect of RH. This may be due to the high affinity of the C_3S for water vapor and the tendency of the C_3S to form thin water films at RH values of (80-100%). An alternative explanation is that C_3S powder is more sensitive to surface phases (liquid water or reaction products) than β-C_2S and gel formation on the surface of the grains of C_3S lowers the degree of reaction of water with the underlying silicate. Surface contamination of C_3S with liquid water and reaction products thus flattens the (α vs %RH) curves for RH values greater than 55%.

The effect of $P_{\overline{C}}$ on α is shown by equation 61 and the curve fitting coefficients are listed in Table 6.

$$\alpha_{P_{\overline{C}}} = (\underset{\text{from eq. 43}}{\alpha})((M \times P_{\overline{C}}) + C) \qquad (61)$$

The anhydrous carbonated powders of β-C_2S and C_3S showed decreased reactivity as the $P_{\overline{C}}$ was decreased toward 0 atm. There was also a rapid drop in the rate of carbonation below a $P_{\overline{C}}$ value of 0.12 atm. (Figure 21).

Table 6

The Effect of $P_{\overline{C}}$ on the Degree of Reaction of Anhydrous Calcium Silicates

	M	C	Range of $P_{\overline{C}}$ (atm.)
C_2S	0.18	0.10	(0.12-1.0)
	1.43	-0.06	(0.05-0.12)
C_3S	0.125	0.16	(0.12-1.0)
	1.263	-0.20	(0.025-0.12)

The steep portions of the curves for β-C_2S and C_3S from 0.025-0.12 atm. carbon dioxide are caused by decreased pH in the water film surrounding each silicate grain. The $\overline{C}$ initially enters the water in low concentrations and cannot precipitate the calcium in solution. As the concentration of $\overline{C}$ increases, the various carbonates precipitate. Local concentrations of carbon dioxide can explain the threshold value, the break point in the curves and the polymorph of carbonate which forms, although $P_{\overline{C}}$ does not completely control the formation of specific carbonate species. All of the $P_{\overline{C}}$ studies were conducted at 24 hours and the degree of reaction could be accurately determined. If atmospheric concentrations of carbon dioxide were used in a similar study, the degree of reaction would not have been detectable. Long term studies of carbonated concretes and mortars with

atmospheric $\overline{C}$ (0.0003 atm.) have induction periods, as do the samples in this study, although the induction period and the time for complete carbonation with atmospheric $\overline{C}$ may take years.

The approximately linear effects of RH and $P_{\overline{C}}$ on the degree of reaction of anhydrous calcium silicate powders is mainly due to the fact that the water and carbon dioxide are carried to the reaction zone as gases, which is a rapid process, and the H and $\overline{C}$ react rapidly to precipitate carbonate with minimal gel formation.

c. Carbonation Mechanism for Anhydrous Calcium Silicate Powders

Equation 42 is a good approximation of the carbonation reaction for dry β-C_2S and C_3S powders

$$C_nS + n\overline{C} + H = nC\overline{C} + S\text{-}H \qquad (42)$$

C-S-H gel formation is minimal as is shown in Figure 16. Since both the water and $\overline{C}$ react as gases, the reaction is rapid and the rate of water adsorption is controlled by the RH and the exothermic reaction, which vaporizes water which would normally condense on the silicates. The temperature rise associated with anhydrous powders was monitored directly with a thermocouple and ranged from 7-14°C above the initial reaction temperature. The temperature rise persisted for only 30-60 minutes after which the reaction proceeded at a slow rate and the temperature was approximately constant.

As eq. 42 indicates, the carbonation reaction for dry silicate powders can go to completion without forming C-S-H gel while normal hydration, eqs. 4 & 5, forms gel and requires a multistep reaction mechanism which is slower than carbonation and which has different final reaction products. Normal hydration forms a gel with approximately 1.5 C/S and H/S ratios and

and some CH while complete carbonation forms dispersed silica gel and carbonate in varying crystal habits and sizes.

2. Wet Calcium Silicate Powders

a. Kinetic Models for Wet Carbonation

Wetted carbonated calcium silicate powders followed kinetic models similar to normal hydration except that the time scale was drastically compressed for the carbonated samples. Equation 12 with n = 1 described the first few minutes of carbonation and substitution of n = 2 described the major portion of carbonation (up to 90% reaction). The value of n ranged from 1.7-2.2 for most of the carbonation runs but the variation was not easily controlled due to the difficulty in monitoring the water content in in the samples of wetted powder during the entire reaction process.

If Figure 15, for the normal hydration of calcium silicates, were replotted as % hydration versus log time (not time), the resulting graph would be very similar to the plots for carbonated wet silicate powders (Figures 10-13), which show an initial rapid reaction period followed by a slower reaction rate at longer reaction times. The multiple stage carbonation mechanism will be discussed later. The wetted β-C_2S and C_3S powders fitted a kinetic model generally described by eq. 62. This equation was the most accurate for the later portion (> 20 minutes) of the carbonation reaction.

$$\alpha = K_T' \log t \qquad (62)$$

Not enough data were obtained on the wetted powders to determine a kinetic model comparable to eq. 50 for the dry reacted silicates.

The time needed to attain comparable degrees of reaction by hydration are quite different due to the nature of the two reactions. The hydration

reaction occurs throughout the wetted mass of the powder while the carbonation reaction proceeds from the surface of the powder toward the center of the mass. The free energy change for the two processes is also quite different as is indicat d by Table 7 which shows the relative thermodynamic data for the hydration and carbonation of wetted powders.

Table 7
Thermodynamic Properties for Carbonated and Hydrated Calcium Silicates at 298°K

	Ea	RT	$\Delta S^{\ddagger}$	$\Delta G^{\ddagger}$	ΔH_f	ΔS_f	ΔG_f
	Kcal/mole	Kcal/mole	Kcal/mole-°K	Kcal/mole	Kcal/mole	Kcal/mole-°K	Kcal/mole
Carbonation							
β-C_2S	16.9	0.592	-35.9	27.0	-44	-0.1233	- 7.24
C_3S	9.8	0.592	-57.8	27.0	-83	-0.1522	-37.62
Hydration (Ref. 94)							
β-C_2S	10-18	--	--	--	- 4.2	--	--
C_3S	2- 9	--	--	--	-22.4	--	--

The free energy values indicate that the carbonate is more negative, i.e., more thermodynamically stable, at the reaction temperatures in this study and thus is more likely to form than C-S-H gel or CH. The main reason for the carbonate formation is the large exotherm associated with carbonate formation which is sufficient to overcome the activation energy for carbonation and thus drive the reaction.

b. Effect of w/s on Wetted Calcium Silicates

The effect of w/s ratio can be seen in Figure 19 where definite maxima are observed at 0.12 and 0.16 w/s for β-C_2S and C_3S, respectively. The placement of the maxima corresponds to optimum liquid water content which allowed gaseous $\overline{C}$ and water vapor to enter the reaction zone of the wetted powder. Higher w/s ratios cause water to form in the pore space and liquid water blocks gaseous diffusion of $\overline{C}$ and H. Lower than optimum values of w/s depress the degree of reaction by starving the reaction zone of needed water. Decreased w/s causes a more rapid decrease in degree of reaction than high w/s ratios.

When the wetted calcium silicate powders were kept wet throughout the carbonation period and the reaction conditions held at 25°C with 100% RH and 100% $\overline{C}$ (0.15 w/s β-C_2S and 0.20 w/s C_3S), the samples completely reacted in 96 and 68 hours, respectively. At higher reaction temperatures the time for complete reaction would be reduced.

c. Effect of RH and $P_{\overline{C}}$ on Wetted Calcium Silicates

The RH affects the degree and rate of carbonation by controlling the rate at which water evaporates from the reacting silicate powders. Figures (10-13) show the effect of RH on the degree and the rate of carbonation of wetted powders (with 0 w/s plotted on Figures 10 and 11 for reference). β-C_2S and C_3S behave similarly, although the C_3S reacts more rapidly and to a greater extent for similar times of reaction. Figure 20 shows a cross plot of the wet carbonation data at 24 hours with the $P_{\overline{C}}$ fixed at 100% CO_2. From 0-55% RH the degree of reaction increased rapidly in a linear manner and from 55-100% RH the effect of RH was almost negligible. Equation 60 can be used to describe the behavior of the degree of reaction due to changes in RH but

now Table 8 must be used to supply the proper coefficients. As before, α is calculated from eq. 50 or measured experimentally.

Table 8

Effect of RH on the Degree of Reaction of Wetted Calcium Silicates

	M	C	Range of RH
C_2S	1.4555	0	(0-55)
	-0.111	0.80	(55-100)
C_3S	1.364	0	(0-55)
	-0.111	0.80	(55-100)

The effect of $P_{\overline{C}}$ can similarly be calculated using eq. 50, eq. 61 and Table 9.

Table 9

Effect of $P_{\overline{C}}$ on the Degree of Reaction of Wetted Calcium Silicates

	M	C	Range of $P_{\overline{C}}$
C_2S	0.447	0.27	(0.15-1.0)
	3.3	-0.14	(0.05-0.15)
C_3S	0.376	0.43	(0.15-1.0)
	4.7	-0.235	(0.05-0.15)

The major difference in the wet reacted powders is the higher rate and degree of reaction. Even initial w/s ratios of 0.05 supply the calcium

silicate powders with water and keep the carbonation reaction going. The maximum temperature rise measured in a sample of wetted calcium silicate powder reacted according to the conditions of Figure 11 was 8-10°C which was slightly lower than the dry powders. The liquid water carries heat away from the reaction zone and the measured temperature is quite low. Visual studies of wetted powders have noted that the water inside the powder vaporized at the surface of the powders after 2-5 minutes of carbonation and the local temperature at the reaction zone is considerably higher than the measured temperature. The fact that the surface may actually steam indicates local temperatures approaching 100°C. Temperature rises of over 15°C were not recorded because the reaction zone moved rapidly past the thermocouple and the water vapor migrating toward the surface of the powders cools the reaction zone and the unreacted mass of powder.

d. Carbonation Mechanisms for Wetted Calcium Silicate Powders

The carbonation mechanism for wet calcium silicates is considerably different than dry powders, although the overall reaction for the equation is the same. The proposed mechanism for carbonation of wet powders is a multi-step process described by equations 63-65.

$$C_nS + \overline{C} + H \text{ ----- } C\text{-}S\text{-}H + C\overline{C} \quad (63)$$

$$C\text{-}S\text{-}H + \overline{C} + H \text{ ----- } C'\text{-}S\text{-}H' + C\overline{C} \quad (64)$$

$$C'\text{-}S\text{-}H' + \overline{C} + H \text{ ----- } S\text{-}H + C\overline{C} \quad (65)$$

$$C_nS + n\overline{C} + H \text{ ----- } S\text{-}H + nC\overline{C} \quad (42)$$

Initial formation of gel and carbonate (eq. 63) is followed by carbonation of the gel (eqs. 64, 65). This model is supported by carbonate formation data (Figure 17 and 18) and C/S and H/S ratio data (Figures 23 and 24).

Figure 17 shows the amount of gel formed by the wet carbonated β-C_2S as a function of initial w/s ratio. As the w/s ratio was increased, the deviation from the formation of theoretical carbonate (according to eq. 42) increased and the amount of gel increased. As the w/s ratio approached 0, gel formation became minimal. The bulges in the curves (in Figure 17) are limited to the first 1-8 hours of carbonation after which the theoretical carbonate limit is closely followed.

The carbonation of the gel is a continuous process once it is initiated, and eq. 64 could be omitted; but the concept of a multi-step reaction mechanism is necessary. Additionally, the wet carbonation reaction will go to completion forming the same products as the dry carbonated samples. β-C_2S forms more C-S-H gel by weight than comparably treated C_3S and this is consistent with hydration eqs. 17 and 18 and Figure 18.

3. Calcium Silicate Pellets

The determination of reaction profiles and the phase analysis of diametral sections of fractured pellets were successfully accomplished. The dry pellets had a buildup of carbonate (predominantly aragonite) on the surfaces of the pellets and a very steep reaction gradient just beneath the surface of the samples as seen in Figure 14. The reaction gradients in the center of the dry samples were relatively flat and the degree of reaction uniformly increased with longer reaction periods. One surface point and six equally spaced points across a fractured and polished diameter of the pellets were examined by point QXDA and regular X-ray diffraction (XRD). The pellet was then ground into powder and the average composition determined and compared to the seven measured points across the diameter of the specimen. All of the analyses balanced out to within 5 wt.% silicate and carbonate. The use

of the x-ray diffractometer as a x-ray macroprobe was useful in determining point composition and quantity of phases, but required slow scanning speeds (1/2 or 1/4°2θ/min) to obtain sufficient counting statistics.

Similar studies were conducted on wetted pellets but the reaction profiles were considerably different (Figure 14). The surface was covered with carbonate as in the case of the dry samples, but the degree of reaction just below the surface was much higher for the wetted pellets. The rate of reaction was approximately 120-150 times greater than for the dry pellets. The center for the wetted pellets reacts more slowly than the outer surfaces, the reason being that the central portion becomes water starved as the exothermic carbonation reaction proceeds. This was observed previously by Berger, Young and Breese.[73] Eventually, the center carbonates and the reaction gradients level out. Steam curing with $\overline{C}$ is even more effective for rapid carbonation because the reactants move to the reaction zone in the vapor state and the pores in the pellets are not normally clogged with liquid water as is the case, at times, with wetted pellets.[24,33-35]

C. Properties of the Reaction Products

1. Stoichiometry of Carbonation Products

a. Carbonate Formation

Determination of the carbonate content was accomplished by QXDA and constant temperature pyrolysis. Both methods were more accurate at high degrees of reaction (50-90 wt.%). The QXDA method determined carbonate directly, while the pyrolysis method determined the weight loss attributed to combined $\overline{C}$ and the carbonate fraction was calculated. The dry silicate powders and pellets formed calcium carbonate directly as the silicate reacted according to

eq. 42. The theoretical carbonate line in Figure 16 shows the limit of carbonate formation for various degrees of reaction calculated from eq. 42. All of the dry silicates closely followed the theoretical line, and therefore the formation of gel was minimal since the calcia was immediately precipiated as carbonate.

Figures 17 and 18 show the deviation of wetted calcium silicates from the theoretical carbonation limit. The bulge of the curves indicates that the carbonate reaction causes the silicate to react rapidly initially forming not only calcium carbonate but also a substantial amount of C-S-H gel which carbonates later. This behavior was confirmed by both QXDA and pyrolysis techniques. The extent of deviation relies on accurate QXDA which was more difficult to obtain reproducibly for the wet reacted powders than for dry silicates. The family of curves in Figure 17 indicates that the theoretical carbonate formation limit was approached as the w/s ratio approached 0. Figure 18 shows the deviation of the wet β-C_2S and C_3S powders from theoretical carbonate formation. The maxima in the deviation occurs at 30-50% (1-2 hours of reaction) and the theoretical line is approached at 60-80% (1-12 hours) of carbonation. β-C_2S can form a higher weight fraction of C-S-H gel during hydration than C_3S can, as shown in eqs. (17 and 18).

b. Stoichiometry Calculations

The stoichiometry of the carbonated calcium silicates was determined by a material balance calculation. The silica from the reacted calcium silicate was assumed to form only C-S-H gel. The total calcia is divided between calcia in the gel, which was not measured directly, and calcia in the carbonate. The amount of carbon dioxide was determined from constant temperature pyrolysis as was the amount of water bound in the C-S-H gel. The

$\overline{C}$ was assumed to be completely associated with the calcia so that a specific amount of the calcia available from the reacted calcium silicate was tied up as carbonate. The calcia in the carbonate was subtracted from the reacted calcia and the remainder associated with the gel. The mass balance equations for C and S are given in equations 66 and 67.

$$C_{total} = C_{carbonate} + C_{gel} + C_{unreacted\ silicate} \quad (66)$$

$$S_{total} = S_{gel} + S_{unreacted\ silicate} \quad (67)$$

Finally, the calcia, silica and water in the gel were calculated on a molar basis and normalized to silica so that the C-S-H ratio was expressed as C_xSH_y where x was the C/S ratio and y was the H/S ratio. The amount of carbonate was determined by dividing the amount of carbonate by the anhydrous weight of the total calcium silicate sample.

The basic problem with this method is that small errors in the determination of the percentage of calcium silicate reacted yields large errors in the apparent stoichiometry of the gel. Both the wet and dry carbonated samples showed similar behavior during the course of the carbonation reaction. The dry calcium silicates showed a rapid drop in their C/S and H/S ratios with increased periods of carbonation (Figures 23-24). Berger[95] and Bukowski[75] observed the same type of behavior while carbonating non-hydraulic, γ-C_2S. While hydrated calcium silicates show a limit of 1.6-1.5 for C/S and H/S ratios of fully hydrated pastes, reacted carbonated samples show C/S and H/S ratios of 0.15-0.2 and 0.2-0.3 for β-C_2S and C_3S, respectively. Silicates which were carbonated wet showed a less drastic drop in their C/S and H/S ratios because more gel was formed and the carbonation of that gel took time (Figure 25). Carbonation does continue, however, and eventually the C-S-H

gel converts to S-H gel. C-S-H gel would be stable at room temperature if carbon dioxide were not present, but $\overline{C}$ forces $C\overline{C}$ to form and causes a -44 to -83 kcal/mole exotherm which drives the carbonation reaction to completion. The driving force for the hydration reaction is -4 to -22 kcal/mole and gel is stable under these conditions. Generally, C_3S carbonates faster than β-C_2S but the relative differences in rates of carbonation are much less pronounced than for the relative rates of hydration of C_3S and β-C_2S (Figure 15).

2. Surface Area

Both the C-S-H gel and the carbonates were formed with high surface areas and appreciably coarsened at longer carbonation periods. The C-S-H gel has the greatest surface area which is between 100-400 m^2/g, with the rate of surface area decrease generally following the degree of reaction. The carbonates which were formed initially also had high surface areas but not as high as C-S-H gel; the values ranged from 4-20 m^2/g. However, these determinations were made after the carbonates appeared on QXDA traces which implied crystalline carbonates. TEM analysis of the initial carbonation products showed carbonates intimately mixed with the gel and the surface area was comparable to the coarser gel.[77,78] The carbonates nucleate very early in the carbonation reaction and grow throughout the reaction, while the C-S-H gel partially converts to carbonate and silica gel.

3. Morphologies of Carbonated Calcium Silicates

The unreacted calcium silicates shown in Figure 26 were typical for the powders and pellets. The powder grains were equiaxed and not contaminated with water or carbon dioxide. No second phase was detected by x-ray analysis.

The pictures of the fractured pellets in Figure 26C&D show the lack of reaction products and the uniform morphology. Figure 27 shows the highly reacted surfaces of dry powdered and pelletized calcium silicates which contained aragonite. The aragonite commonly grew in orthorhombic shapes (either blocks or laths) which are indicative of this form of calcium carbonate. Figure 28 shows more aragonite morphologies on dry carbonated samples. Note the fractured grain in Figure 28A and the carbonate growing radially from the surface. Other uncommon carbonate morphologies are shown in Figures 28C&D; the hairlike material in those plates was proved to be a carbonate by energy dispersive x-ray analysis using SEM, and by acid etching, but positive phase identification was not possible.

Figures 29 and 30 show various morphologies found on carbonated calcium silicate (powders and pellets) which were reacted wet. Calcite was the predominate phase formed as long as the silicates were kept wet, but upon drying, aragonite grew as thin laths. Figure 31 shows similar morphologies for carbonated silicates with aragonite and calcite or pure calcite as the reaction product. Generally, the crystallites growing on the wet reacted powders were small (1 μm) but with long reaction periods when liquid water was present on the surfaces of dense pellets, larger crystals (10-15 μm) form (Figure 29). Carbonation under saturated water yielded 100 μm calcite crystals (Figure 30D).

The carbonation reaction also forms C-S-H gel in addition to calcium carbonate and this is partially resistant to HCl acid etching. The influence of the gel on the final structure can be seen in Figure 32. β-C_2S has a nearly continuous gel matrix which holds the pellet together after acid etching, while the C_3S has gel around each grain but has a carbonate matrix which was

dissolved by the acid. The differences in the bonding matrix should have some effect on the strength behavior, though none was detected in the compression or diametral compression data. Possibly creep or long term strength degradation[57] would be affected by the matrix morphology. The size or shape of the carbonate crystallites was not a significant factor in the strength of the pellets although the crystallites tended to grow into the pore space and strengthened the pellets by filling the voids.

D. Strength and the Effect of Porosity

1. Specific Gravity

The specific gravity of the unreacted calcium silicates was within the reported limits for the materials.[4,85] The 2% lower specific gravity values obtained using benzene instead of water as a suspending liquid were caused by a nonwetting problem with the benzene. The values obtained using water also decreased with time because the silicates hydrated and the reaction products had lower density than the unreacted grains of silicate.

2. Strength Data

The compressive and diametral compressive strength data was obtained on three types of calcium silicate pellets (β-C_2S, C_3S, and a 50:50 molar mixture of β-C_2S and C_3S). The 50:50 mixture of silicates was tested to simulate portland cement composition. The pellets were treated by two special reaction conditions (carbonated then hydrated and hydrated then carbonated). The carbonated-hydrated samples are shown in Figures 33a and 35a. The carbonation treatment gives roughly twice the strength of portland cement and the pellet was carbonated only 216 hours. Hydration of the carbonated material caused the strength to increase more rapidly than normal hydration

because only a small amount of porosity needs to be filled to effect large changes in compressive strength at low porosities.

Hydrated pellets (25 and 50% reacted) were tested for strength as shown in Figures 33b and 35b. Some pellets were subjected to carbonation for varying time periods. The relatively high values for the compressive strength of the hydrated pellets were due to the high initial density of the pressed pellets, which was up to 70% theoretical density for the silicates tested. Figure 34 shows the relation of the degree of hydration to the strengthening of the calcium silicates by carbonation. The unhydrated pellets gained strength more slowly than the hydrated samples on carbonation because there was more pore space to fill in the unhydrated samples. All of the variation within each test group was due to internal porosity variation caused by different particle size for each group. The pressing efficiencies listed in decreasing order were β-C_2S, β-C_2S/C_3S and C_3S. The maximum strength (350 MPa, 49 Ksi) attained in this study was below the theoretical compressive strength which is approximately 800 MPa (120 Ksi) as determined by Roy and Gouda[83] (Figure 45).

The diametral compression (split cylinder tensile) tests were run to determine the tensile strength of the carbonated calcium silicate (Figure 36). The trends observed for the compression testing were also seen in the diametral samples but the strength values were 6-8 times lower than normal compression which commonly occurs in brittle materials.[81,96] The scatter in the diametral compression specimens (40% and 25%) and the stress values are probably slightly high due to the small size of the specimens. The specimens were placed on their side and loaded. The platen can either crush the bearing surface giving low readings or hold the cylinder together since the

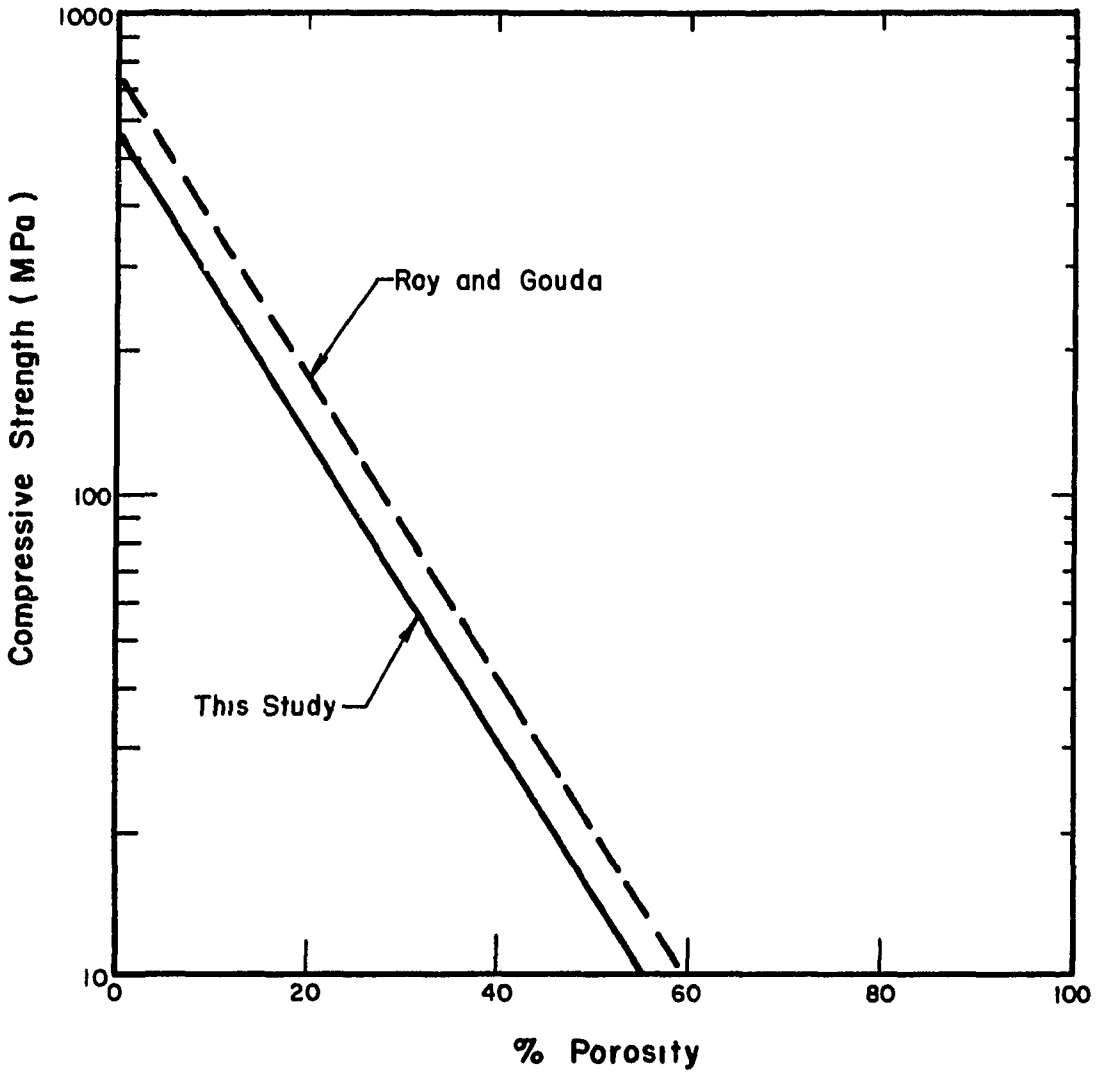

Figure 45. Effect of Porosity on the Compressive Strength of Pelletized Calcium Silicates

the loading area compresses and a lateral force is needed to separate the halves of a fractured pellet in addition to the tensile forces developed within the sample.[96] The crushing effect was lessened by placing 0.13 mm thick copper foil above and below the loading points. The copper shims did not alleviate the shear force problem which would only be solved by using larger samples.[96]

3. Effect of Porosity on Strength

Both the diametral compression and the regular compression strengths depend on the porosity of the pellet when it was tested. The composition of the pellet and the reacting conditions per se have little effect on the strength. The reaction parameters did affect the rate at which the porosity was filled, but the important material parameter was porosity which is strongly influenced by initial pressing. The strength decreased in an exponential fashion with increased porosity (Figures 37 & 39b) while the degree of reaction showed a linear dependency on the porosity (Figures 38 & 39a). These relations held for the compression and diametral compression samples. The regression coefficients for the exponential porosity models shown in Figures 37 and 39b were 0.98 and 0.93 for the compression and "tensile" strengths, respectively. The regression coefficient for the relation of percent calcium silicate (α) reacted to the porosity were 0.86 and 0.96 for compression and tension (Figures 38 and 39a).

An equation can be written to calculate the compressive or tensile strength of pressed β-C_2S, C_3S or C_2S/C_3S as functions of porosity and degree of reaction.

$$\alpha = A - B(P) \tag{68}$$

$$P = \frac{A - \alpha}{B} \qquad \text{Figures (38 \& 39a)} \tag{69}$$

$$\sigma = C \exp(-D(P)) \qquad \text{Figures (37 \& 39b)} \tag{70}$$

$$\sigma = C \exp\left[-D\left(\frac{A - \alpha}{B}\right)\right] \tag{71}$$

Most of the carbonated strength specimens were less than 100% reacted so the majority of the load was carried by a thin carbonated shell surrounding the pellet. The stress was determined using the entire loading area so the actual failure stress in the thin carbonate shell was much higher than the reported value. Strict evaluation of the strength of the carbonated pellets would require the use of complex composite strength theory which was beyond the scope of this investigation.

V. CONCLUSIONS

1. The reaction of anhydrous β-C_2S and C_3S powders followed a decreasing volume kinetic model with the rate controlled by diffusion. The general form of the kinetic rate equation was:

$$\left[1 - (1-\alpha)^{1/3}\right]^2 = K_T' \, t$$

where α = degree of carbonation

K_T' = apparent rate constant

t = time

2. The activation energies for carbonation of anhydrous β-C_2S and C_3S powders were experimentally determined to be 16.4 and 9.8 Kcal/mole, respectively. No comparable data were obtained for wetted calcium silicate powders which were carbonated.

3. The kinetic model for wetted β-C_2S and C_3S powders was generally described by:

$$\alpha = K_T' \log t + C$$

where C = a constant

The logarithmic model did not fit the wetted silicate powders reaction rate as well as the model for dry powders. The reaction rate for the wetted silicates depended on the amount and distribution of water and the agglomeration of the wetted silicate particles.

4. Both the anhydrous and wetted calcium silicate powders showed a dependency on relative humidity, partial pressure of CO_2, initial water/solids

ratio, particle fineness, reaction time and reaction temperature. Generally, an increase in any of these parameters increased the rate of carbonation.

5. Carbonated anhydrous β-C_2S and C_3S powders formed only aragonite while the wetted powders first formed calcite then formed aragonite as the exothermic carbonation reaction dried the samples. The wetted C_3S powders initially formed more calcite than aragonite but the opposite was true for wet carbonated β-C_3S samples.

6. Calcite formation was favored when distilled water was used while aragonite formation was preferred when silicates were reacted dry or when deionized water was used to form wetted samples.

7. The strength of pelletized β-C_2S, C_3S and a 50:50 molar mixture increased exponentially as the porosity decreased. The porosity of the pellets decreased approximately linearly with the degree of carbonation. The maximum tensile and compressive stresses recorded during this study were 47 MPa (7.5 Ksi) and 330 MPa (49 (Ksi), respectively. The compressive strength of the compacts was considerably lower than theoretical value of 750-900 MPa or 109-131 Ksi.

LIST OF REFERENCES

1. Dapples, E. C., Basic Geology for Science and Engineering, John Wiley and Sons, Inc., New York, N. Y. (1959).

2. Bogue, R. H., The Chemistry of Portland Cement, Reinhold Publishing Co., New York, N. Y. (1959).

3. Lea, F. M., The Chemistry of Cement and Concrete, Chemical Publishing Co., New York, N. Y. (1971).

4. Taylor, H.F.W., The Chemistry of Cements, Vol. 1, Academic Press Inc., New York, N. Y. (1972).

5. Rowland, J. L., "Improvement in the Manufacture of Artificial Stone," U.S. Patent No.109, 669 (Nov. 29, 1870).

6. Rowland, J. L., "Improvement in Hardening Artificial Stone Walls, Concrete, Etc.," U.S. Patent No. 128,980 (July 16, 1872).

7. Rowland, J. L., "Manufacture of Artificial Stone," U.S. Patent No. 137,322 (April 1, 1873).

8. Rowland, J. L., "Manufacture of Artificial Stone," U.S. Patent No. 149,682 (April 14, 1874).

9. Rowland, J. L., "Manufacture of Artificial Stone," U.S. Patent No. 153,020 (July 14, 1874).

10. Von Pittler, W., "Artificial Lithographic Stone," U.S. Patent No. 326,254 (Sept. 15, 1885).

11. Sprogle, D. M., "Processes of Making Artificial Stone," U.S. Patent No. 139,274 (May 27, 1873.

12. Sprogle, D. M., "Apparatus for Hardening Stone Artificially," U.S. Patent No. 147,522 (Feb. 17, 1874).

13. Heinzerling, C., "Artificial Stone," U.S. Patent No. 591,168 (Oct. 5, 1897).

14. Owen, W., "Process of Manufacturing Artificial Stone," U.S. Patent No. 731,608 (June 23, 1903).

15. Lukens, H. S., "Composition of Matter and Method of Making the Same," U.S. Patent No. 1,561,473 (Nov. 17, 1925).

16. Lukens, H. S., "Dolomitic Articles and Method of Making Same," U.S. Patent No. 1,597,811 (Aug. 31, 1926).

17. Parkhurst, L. M., "Gypsum Product and Method of Producing the Same," U.S. Patent No. 1,620,915 (Marc. 15, 1927).

18. Joosten, H., "Process of Solidifying Permeable Rock, Loosely Spread Masses or Building Structures," U.S. Patent No. 1,827,238 (Oct. 13, 1931).

19. Bradly, F. L., "Modifications of the Physical Properties of Cement Produced by Carbonation," Cement 4, 10 (1931).

20. Platzman, C. R., "Physical Changes in Cement Mortar Produced by Carbon Dioxide Reaction," Zement 21, 26 (1932).

21. Bessey, G. E., "Effect of Carbon Dioxide on Cement and Lime Mortars," Jour. Soc. Chem. Ind. 52 (1933).

22. Schless, S., "Process for the Manufacture of Artificial Stone from Lime," U.S. Patent No. 1,907,369 (May 2, 1933).

23. Jones, P. W., "Stone-like Structural Material," U.S. Patent No. 1,992,488 (Feb. 26, 1935).

24. Meyers, S. L., "Effect of Carbon Dioxide on Hydrated Cement and Concrete," Rock Products (Jan. 1949).

25. McMillian, E. C., "Effect of Carbon Dioxide on Fresh Concrete," Jour. Amer. Concr. Inst. 53, 225 (Aug. 1956).

26. Leber, I. and Blakely, F. A., "Some Effects of Carbon Dioxide on Mortars and Concrete," Jour. Amer. Concr. Inst. 53, 295-308 (Sept. 1956).

27. Verbeck, G., "Carbonation of Hydrated Portland Cement," ASTM Spec. Tech. Report No. 205 (1958).

28. Cole, W. F. and Kroone, B., "Carbonate Minerals in Hydrated Portland Cement," Nature 184, 57 (Sept. 5, 1959).

29. Alexander, K. M. and Wardlaw, J., "A Possible Mechanism for Carbonation Shrinkage and Crazing, Based on the Study of Thin Layers of Hydrated Cement," Jour. Res. NBS Physics and Chemistry (Dec. 1959).

30. Kroone, B. and Blakely, F. A., "Reaction Between Carbon Dioxide and Gas Mortar," Jour. Amer. Concr. Inst. 56 (Dec. 1959).

31. Staley, R. W., "Method of Curing Cement - Type Cold Molding Compositions," U.S. Patent No. 2,496,895 (Feb. 7, 1950).

32. Moore, W. H. et al., "Process for Improved Silicate Bonded Molds and Cores," U.S. Patent No. 2,883,723 (April 28, 1959).

33. Huhta, R. S., "Carbonation of Concrete Block: A Look at Two Plants," Concrete Products (Jan. 1960).

34. Toennies, H. T., "Artificial Carbonation of Concrete Masonry Units," Jour. Amer. Concr. Inst. (Feb. 1960).

35. Toennies, H. T. and Shideler, J. J., "Plant Drying and Carbonation of Concrete Block - NCMA-PCA Cooperative Program," Jour. Amer. Concr. Inst. (May 1963).

36. Zelmanoff, H., "Process for the Manufacture of Artificial Stone Articles," U.S. Patent No. 3,149,986 (Sept. 22, 1964).

37. Bierlich, K. G., "Manufacture of Portland Cement Products," U.S. Patent No. 3,468,993 (Sept. 23, 1969).

38. Cole, W. F. and Kroone, B., "Carbon Dioxide in Hydrated Portland Cement," Jour. Amer. Concr. Inst. (June 1960).

39. Cole, W. F. and Kroone, B., "Carbon Dioxide in Hydrated Portland Cement," Jour. Amer. Concr. Inst. 56, 1584-1586 (Dec. 1960).

40. Powers, T. C., "A Hypothesis on Carbonation Shrinkage," Jour. PCA Res. and Devel. Lab. 40-50 (May 1962).

41. Hunt, C. M. and Tomes, L. A., "Reaction of Hardened Portland Cement Paste with Carbon Dioxide," Jour. Res. NBS-Physics and Chemistry 66 (Nov. 1962).

42. Guinier, A. and Regourd, M., "Structure of Portland Cement Minerals," Proceedings of the Fifth International Symposium on the Chemistry of Cement, Tokyo, Parts 2 & 3 (1968).

43. Kondo, R. et al., "Mechanisms and Kinetics on Carbonation of Hardened Cement," Proceedings of the Fifth International Symposium on the Chemistry of Cement, Tokyo, Part 2, 402-409 (1968).

44. Hamada, M., "Neutralization (Carbonation) of Concrete and Corrosion of Reinforcing Steel," Proceedings of the Fifth International Symposium on the Chemistry of Cement, Tokyo, Part 2, 343-369 (1968).

45. Smolczyk, H. G. (Written discussion of Ref. 43), Part 2, 369-384 (1968).

46. Manns, W. and Wesche, K., "Variation in Strength of Mortars Made of Different Cements Due to Carbonation," Proceedings of the Fifth International Symposium on the Chemistry of Cement, Tokyo, Part 3, 385-393 (1968).

47. Meyer, A., "Investigations on the Carbonation of Concrete," Proceedings of the Fifth International Symposium on the Chemistry of Cement, Tokyo, Part 3, 394-401 (1968).

48. Shideler, J. J., "Carbonation Shrinkage of Concrete Masonry Units," Jour. PCA Res. and Devel. Lab. 36-50 (Sept. 1963).

49. Kroone, B., "Effect of Gaseous Carbon Dioxide on Concrete," Indian Concrete Journal, 379 (Oct. 1963).

50. Kamimura, K. et al., "Changes in Weight and Dimensions in the Carbonation of Portland Cement Mortars," Mag. Concr. Res. 17, No. 50 (March 1965).

51. Pihlajavaara, S. E., "Some Results of the Effect of Carbonation on the Porosity and Pore Size Distribution of Cement Paste," Materiaux et Constructions 1, No. 6 (1968).

52. Lentz, C. W., "Effect of Carbon Dioxide on Silicate Structures in Portland Cement Paste," XXXVI Congres International de Chimie Industrielle, Compte Rendu II, Gr. VII, p. 17-445, Bruxelles (Sept. 1966).

53. Swenson, E. G. and Sereda, P. J., "Mechanism of the Carbonation Shrinkage of Lime and Hydrated Cement," Jour. Appl. Chem. 18, 111-117 (April 1968).

54. Imperato, L. G., "Methods and Compositions for the Manufacture of Portland Cement," U.S. Patent No. 3,607,327 (Sept. 21, 1971).

55. Matsuda, O. and Yamada, H., "Investigation of the Manufacture of Building Materials by Carbonation Hardening of Slaked Lime," Sekko to Sekkai, 125 (1973).

56. Uschmann, W., "Production of Compact Construction Elements from Lime and Admixture by Treatment with Carbon Dioxide Gas," Doctor rerum naturalium, Building Academy of GDR, Institute of Building Materials, Weimar (Feb. 1974).

57. Sakaeda, O., Fukihara, M., and Imai, K., "Changes in Properties of Products Hardened by Carbonation with Slaked Lime as Basic Material," Gypsum and Lime, 133 (1974).

58. Moorehead, D. R. and Morand, P. J., "Some Observations of the Carbonation of Portlandite $Ca(OH)_2$ and its Relationship to the Carbonation Hardening of Lime Products," 3rd Symposium on Science and Research in Silicate Chemistry, Brno, Czechoslovakia (1975).

59. Sauman, Z., "Carbonation of Porous Concrete and its Main Binding Components," Cem. Concr. Res. 1, 645-662 (1972).

60. Sauman, Z., "Effect of CO_2 on Porous Concrete," Cem. Concr. Res. 2, 541-549 (1972).

61. Sauman, Z., "Long-term Carbonation of the Phases $3CaO \cdot Al_2O_3 \cdot 6H_2O$ and $3CaO \cdot Al_2O_3 \cdot SiO_2 \cdot 4H_2O$," Cem. Concr. Res. 2 (1972).

62. Diamon, M. et al., "Through Pore Size Distribution and the Kinetics of the Carbonation Reaction of Portland Cement Mortars," Jour. Amer. Cer. Soc. 54, No. 9 (Sept. 1971).

63. Pihlajavaara, S. E. and Pilhmam, E., "Effect of Carbonation on Microstructural Properties of Cement Stone," Cem. Concr. Res. 4, 149-154 (1974).

64. Maycock, J. N. and Skalny, J., "Carbonation of Hydrated Calcium Silicates," Cem. Concr. Res. 4, 69-76 (1974).

65. Slegers, P. A. and Rouxhet, P. G., "Carbonation of the Hydration Products of Tricalcium Silicate," Cem. Concr. Res. 6, 381-388 (1976).

66. LaRosa, P. J. et al., "Carbonate Bonding of Taconite Tailings," EPA-670/2-74-001, 1-53 (Jan. 1974).

67. Stuart, E. B., "Method for Producing a Hard Paving or Surface Material," U.S. Patent No. 3,526,172 (Sept. 1, 1970).

68. Simunic, B., "Process for Accelerating the Initial Hardening of Elements Formed of a Mixture of Cement or Other Lime-Containing Hydraulic Binder and Organic or Inorganic Aggregates Therefor," U.S. Patent No. 3,492,385 (Jan. 27, 1970).

69. Klemm, W. A. and Berger, R. L., "Accelerated Curing of Cementitious Systems by Carbon Dioxide, Part I; Portland Cement," Cem. Conr. Res. 2, 5 (1972).

70. Berger, R. L. and Klemm, W. A., "Accelerated Curing of Cementitious Systems by Carbon Dioxide; Part II: Hydraulic Calcium Silicates and Aluminates," Cem. Conr. Res. 2, 6 (1972).

71. Berger, R. L., Young, J. F., and Leung, K., "Acceleration of Hydration of Calcium Silicates by Carbon Dioxide Treatment," Nature, Phy. Sci. 240, 97 (1972).

72. Klemm, W. A. and Berger, R. L., "Calcination and Cementing Properties of $CaCO_3$-SiO_2 Mixtures," Jour. Amer. Cer. Soc. 55, 10 (1972).

73. Young, J. F., Berger, R. L., and Breese, J., "Accelerated Curing of Compacted Calcium Silicate Mortars on Exposure to CO_2," Jour. Amer. Cer. Soc. 57, 9 (1974).

74. Berger, R. L. and Bukowski, J. M. (Unpublished) "Reaction of Naturally Occurring Calcium Silicate and Calcium Alumino-Silicate Minerals with CO_2," (1975).

75. Bukowski, J. M., "Reaction of Gamma Dicalcium Silicate and Pseudowollastonite with Carbon Dioxide and Water," M.S. Thesis, University of Illinois (1976).

76. Kondo, R. and Ueda, S., "Kinetics of Hydration of Cements," Cem. Concr. Res. Part II, 203-248 (1972).

77. De Carvalho, A. A., "The Hydration of Evaporated Thin Films of Calcium Silicates," M.S. Thesis, University of Illinois (July 1971).

78. Tiegs, T. N., "Investigation of Ion Thinned Tricalcium Silicate by Transmission Electron Microscopy," M.S. Thesis, University of Illinois (1975).

79. Grudemo, A., "The Microstructure of Hardened Cement Paste," Proc. Fourth Intern. Symp. on the Chemistry of Cement, Washington, D.C., National Bureau of Standards Monograph 43, Vol. II, 615-647 (1960).

80. Lawrence, F. V. and Young, J. F., "Hydration of Tricalcium Silicate Pastes: I, Cem. Concr. Res. 3, 2,149-61 (1973).

81. Kingery, W. D., Introduction to Ceramics, John Wiley & Sons, Inc., New York, N. Y., pp. 335-341 (1960).

82. Campbell, L. E., "Some Orthosilicates and Their Hydrates," Ph.D. Thesis, Purdue University (1967).

83. Roy, D. M. and Gouda, G. R., "High Strength Generation in Cement Pastes," Cem. Concr. Res. 3, No. 6, 807 (1973).

84. Handbook of Chemistry and Physics, 51st Edition, ed. R. C. Weast, The Chemical Rubber Co., Cleveland, Ohio (1970-1971).

85. ASTM Powder Diffraction File, Cards 4-0477, 5-0453, 5-0586, 9-351, 9-352, 13-192, Am. Soc. Test. Mat. Publ. No. PDIS-171, Philadelphia, PA (1977).

86. Murray, J. W., "The Deposition of Calcite and Aragonite in Caves," Jour. Geology 62, 481-492 (1960).

87. Wray, J. L. and Daniels, F., "Precipitation of Calcite and Aragonite," Jour. Am. Chem. Soc. 79, 2031-2034 (1957).

88. Zeller, E. J. and Wray, J. L., "Factors Influencing the Artificial Precipitation of Calcium Carbonate," Bull. Geol. Soc. Amer. 65, 1329-1330 (1954).

89. Brooks, W. L. et al., "Calcium Carbonate and Its Hydrates," Royal Society of London Phil. Trans. 18, 689-693 (1950).

90. Lodding, W., Gas Effluent Analysis, Marcel Dekker, Inc., New York, N. Y., 50-70 (1967).

91. 1958 Book of ASTM Standards, "Surface Area by Air Permeability (Blaine Method)," C-204-55.

92. Azaroff, L. V., Elements of X-ray Crystallography, McGraw-Hill Book Co., New York, N. Y., p. 517 (1968).

93. Van Olpen, H. and Parrish, W., X-ray and Electron Methods of Analysis, Plenum Press, New York, N. Y., Vol. 1 (1968).

94. Copeland, L. E. and Kantro, D. L., "Hydration of Portland Cement," Proceedings of the Fifth International Symposium on the Chemistry of Cement, Tokyo, Parts 2 & 3, 387-391 (1968).

95. Berger, R. L., "Carbonation of γ-C_2S," unpublished work.

96. Rudnick, A. et al., The Evaluation and Interpretation of Mechanical Properties of Brittle Materials, AFML-TR-67-316, DCIC 68-3, pp. 135-145, Battelle Memorial Institute (1968).

VITA

Chris Joe Goodbrake was born December 23, 1946 in Vandalia, Illinois, where he was raised and educated. He completed his secondary education in 1965.

He attended the University of Illinois at Urbana-Champaign and graduated with a B.S. degree in ceramic engineering in 1970.

Upon graduation he accepted a position as a materials and processes engineer with McDonnell Douglas Astronautics Company-East in St. Louis, Missouri. His area of specialization was ceramic materials and high temperature technology.

In 1974 he returned to the University of Illinois where he taught electron microscopy and earned a M.S. degree in ceramic engineering in 1975 with a thesis topic, "The Use of Coal Bottom Ash as a Ceramic Raw Material."

Patents:

U.S. Patent 3,935,060, "Fibrous Insulation and Processes for Making Same," Jan. 27, 1976 (with J. C. Blome, M. W. Vance and M. E. O'Brian).